

20

# A TRIDENT SCHOLAR PROJECT REPORT

NO. 224

"The Neutralization of Surf Region Mines"



19950929 003

UNITED STATES NAVAL ACADEMY  
ANNAPOLIS, MARYLAND

This document has been approved for public  
release and sale; its distribution is unlimited.

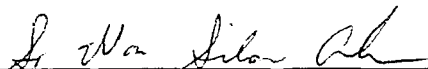
DTIC QUALITY INSPECTED 3

REPORT DOCUMENTATION PAGE			Form Approved OMB no. 0704-0188	
<small>Public reporting burden for this collection of information is estimated to average 1 hour of response, including the time for reviewing instructions, searching existing data sources, gathering and maintaining the data needed, and completing and reviewing the collection of information. Send comments regarding this burden estimate or any other aspects of this collection of information, including suggestions for reducing this burden, to Washington Headquarters Services, Directorate for Information Operations and Reports, 1215 Jefferson Davis Highway, Suite 1204, Arlington, VA 22202-4302, and to the Office of Management and Budget, Paperwork Reduction Project (0704-0188), Washington DC 20503.</small>				
1. AGENCY USE ONLY (Leave blank)		2. REPORT DATE 9 May 1995		3. REPORT TYPE AND DATES COVERED
4. TITLE AND SUBTITLE The neutralization of surf region mines				5. FUNDING NUMBERS
6. AUTHOR(S) So Won Silas Ahn				
7. PERFORMING ORGANIZATIONS NAME(S) AND ADDRESS(ES) U.S. Naval Academy, Annapolis, MD				8. PERFORMING ORGANIZATION REPORT NUMBER USNA Trident report; no. 224 (1995)
9. SPONSORING/MONITORING AGENCY NAME(S) AND ADDRESS(ES)				10. SPONSORING/MONITORING AGENCY REPORT NUMBER
11. SUPPLEMENTARY NOTES Accepted by the U.S. Trident Scholar Committee				
12a. DISTRIBUTION/AVAILABILITY STATEMENT This document has been approved for public release; its distribution is UNLIMITED.				12b. DISTRIBUTION CODE
13. ABSTRACT (Maximum 200 words) There is significant military interest in the dynamic behavior of a net array of circular cylinders traveling through a fluid medium. Although research has been conducted on a towed single line configuration in water, there is little information regarding the dynamic behavior of a towed net configuration. This investigation examined the effect that physical geometry, tow velocity, and tow angle-of-attack had on the lift and drag acting on a net towed in water. The measurements indicate a significant relationship between these factors and the stability of the net, and also provide normalized polynomial equations which will be useful in predicting the aero-ballistics of the net.				
14. SUBJECT TERMS towed net array; towed net configuration; fluid dynamics; net aero-ballistics; net stability; tow angle-of-attack; tow velocity				15. NUMBER OF PAGES
				16. PRICE CODE
17. SECURITY CLASSIFICATION OF REPORT UNCLASSIFIED		18. SECURITY CLASSIFICATION OF THIS PAGE UNCLASSIFIED		19. SECURITY CLASSIFICATION OF ABSTRACT UNCLASSIFIED
				20. LIMITATION OF ABSTRACT UNCLASSIFIED

**"The Neutralization of Surf Region Mines"**

by

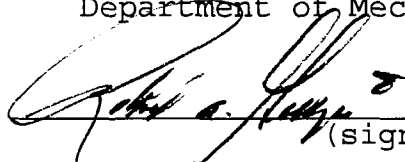
Midshipman So Won Silas Ahn, Class of 1995  
United States Naval Academy  
Annapolis, Maryland



(signature)

**Certification of Adviser Approval**

Professor Robert A. Granger  
Department of Mechanical Engineering



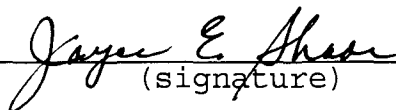
(signature)

9 MAY 1995

(date)

**Acceptance for the Trident Scholar Committee**

Associate Professor Joyce E. Shade  
Chair, Trident Scholar Committee



(signature)

9 May 95

(date)

Accession For	
NTIS GRA&I	<input checked="" type="checkbox"/>
DTIC TAB	<input type="checkbox"/>
Unannounced	<input type="checkbox"/>
Justification	
By	
Distribution/	
Availability Codes	
Dist	Avail and/or Special
A	

USNA-1531-2

## Acknowledgments

This project could not have been completed without the able assistance of Mr. Steve Enzinger and Mr. Don Bunker, whose unparalleled professionalism and knowledge of the USNA Tow Tank System were invaluable throughout the tow test runs. I am also deeply indebted to Mr. Carl Owen, whose enthusiasm and expertise as the Rickover Hall TSD Foreman helped to get this project off its feet and running. Finally, I would like to express my gratitude to Professor Robert Granger, whose guidance in this project has been both constructive and inspiring.

## Table of Contents

<u>Section</u>	<u>Page</u>
Abstract.....	1
1. Introduction.....	2
2. Facility and Equipment.....	6
3. Measurement Techniques.....	17
3.1: Experimental Procedure.....	20
4. The Measurements.....	23
4.1: NDP versus Angle-of-Attack.....	26
4.2: NLP versus Angle-of-Attack.....	40
5. A Resume of the Findings.....	67
6. References.....	71
Appendix A: Experimental Results and Method.....	72
Appendix B: Polynomial Fit.....	103
Appendix C: Alternative Method for Neutralizing Surf Region Mines.....	109

## List of Figures

<u>Figure</u>	<u>Page</u>
Figure 1: Mine Countermeasures in the Littoral Region...	4
Figure 2: USNA 380-Foot Towing Tank.....	7
Figure 3: Planar Motion Mechanism.....	8
Figure 4: Verniered Gear on Towing Carriage.....	8
Figure 5: PMM-to-Array Interface.....	10
Figure 6: Block Gauges with Extension Arm and Streamlined Surface.....	10
Figure 7: Two Block Gauges and a Cross-connecting Line.	11
Figure 8: Block Gauge Calibration Graph.....	12
Figure 9: Load Binder Assembly.....	14
Figure 10: Cylinders (3 Views).....	16
Figure 11: Portion of Net Array.....	16
Figure 12: Diagram of Struts and Leading Line Array.....	19
Figure 13: Conceptual Layout of HLS.....	21
Figure 14: Effect of Number of Arrays on NDP (Test Run at Low Tow Velocity/11 Cylinders/Low Pre-tension).....	27
Figure 15: Effect of Number of Arrays on NDP (Test Run at Low Tow Velocity/6 Cylinders/Low Pre-tension).....	29
Figure 16: Effect of Number of Cylinders on NDP (Test Run at High Tow Velocity/3 Arrays/Low Pre-tension).....	30
Figure 17: Effect of Number of Cylinders on NDP (Test Run at Low Tow Velocity/1 Array/Low Pre-tension).....	31
Figure 18: Effect of Number of Cylinders on NDP (Test Run at Low Tow Velocity/2 Arrays/Low Pre-tension).....	32
Figure 19: Effect of Tow Velocity on NDP (Test Run at 11 Cylinders/2 Arrays/Low Pre-tension).....	34
Figure 20: Effect of Tow Velocity on NDP (Test Run at 11 Cylinders/3 Arrays/Low Pre-tension).....	35
Figure 21: Effect of Tow Velocity on NDP (Test Run at 11 Cylinders/4 Arrays/Low Pre-tension).....	36
Figure 22: Effect of Tow Velocity on NDP (Test Run at 6 Cylinders/2 Arrays/Low Pre-tension).....	37
Figure 23: Effect of Tow Velocity on NDP (Test Run at 3 Cylinders/3 Arrays/Low Pre-tension).....	38
Figure 24: Effect of Pre-tension on NDP (Test Run at 11 Cylinders/2 Arrays/Low Tow Velocity).....	39
Figure 25: Effect of Pre-tension on NDP (Test Run at 11 Cylinders/3 Arrays/Low Tow Velocity).....	41
Figure 26: Effect of Pre-tension on NDP (Test Run at 6 Cylinders/2 Arrays/Low Tow Velocity).....	42
Figure 27: Effect of Number of Arrays on NLP (Test Run at Low Tow Velocity/11 Cylinders/Low Pre-tension).....	43

<u>Figure</u>	<u>Page</u>
Figure 28: Effect of Number of Arrays on NLP (Test Run at Low Tow Velocity/11 Cylinders/Low Pre-tension).....	45
Figure 29: Effect of Number of Arrays on NLP (Test Run at Low Tow Velocity/6 Cylinders/Low Pre-tension).....	46
Figure 30: Effect of Number of Arrays on NLP (Test Run at Low Tow Velocity/3 Cylinders/Low Pre-tension).....	47
Figure 31: Effect of Number of Arrays on NLP (Test Run at Low Tow Velocity/6 Cylinders/High Pre-tension).....	49
Figure 32: Effect of Number of Cylinders on NLP (Test Run at Low Tow Velocity/1 Array/Low Pre-tension).....	50
Figure 33: Effect of Number of Cylinders on NLP (Test Run at Low Tow Velocity/2 Arrays/Low Pre-tension).....	51
Figure 34: Effect of Number of Cylinders on NLP (Test Run at Low Tow Velocity/3 Arrays/Low Pre-tension).....	52
Figure 35: Effect of Number of Cylinders on NLP (Test Run at Low Tow Velocity/4 Arrays/Low Pre-tension).....	53
Figure 36: Effect of Number of Cylinders on NLP (Test Run at Low Tow Velocity/3 Arrays/High Pre-tension).....	55
Figure 37: Effect of Tow Velocity on NLP (Test Run at 11 Cylinders/1 Array/Low Pre-tension).....	56
Figure 38: Effect of Tow Velocity on NLP (Test Run at 6 Cylinders/2 Arrays/Low Pre-tension).....	57
Figure 39: Effect of Pre-tension on NLP (Test Run at 11 Cylinders/1 Array/Low Tow Velocity).....	59
Figure 40: Effect of Pre-tension on NLP (Test Run at 11 Cylinders/3 Arrays/Low Tow Velocity).....	60
Figure 41: Effect of Pre-tension on NLP (Test Run at 11 Cylinders/4 Arrays/Low Tow Velocity).....	61
Figure 42: Effect of Pre-tension on NLP (Test Run at 6 Cylinders/1 Array/Low Tow Velocity).....	62
Figure 43: Effect of Pre-tension on NLP (Test Run at 6 Cylinders/4 Arrays/Low Tow Velocity).....	63
Figure 44: Effect of Pre-tension on NLP (Test Run at 3 Cylinders/1 Array/Low Tow Velocity).....	64
Figure 45: Effect of Pre-tension on NLP (Test Run at 3 Cylinders/2 Arrays/Low Tow Velocity).....	65
Figure 46a: Deployed Weapon, Top View.....	110
Figure 46b: Deployed Weapon, Perspective View.....	111
Figure 47: Undeployed Weapon, Perspective View and Top View.....	112

## List of Tables

<u>Table</u>	<u>Page</u>
Table A.1: Portion of the Pre-test Matrix.....	74
Table A.2: Experimental Data.....	76
Table B.1: Polynomial Term Coefficients for Normalized Lift and Drag Equations.....	105



## Nomenclature

<u>Symbol</u>	<u>Meaning</u>	<u>Units</u>
$\alpha$ .....	angle-of-attack.....	degrees
D.....	drag force.....	lbf
L.....	lift force.....	lbf
NDP.....	normalized drag parameter.....	ft <sup>2</sup>
NLP.....	normalized lift parameter.....	ft <sup>2</sup>
$\rho$ .....	density of fluid medium..	lb/ft <sup>3</sup>
X1.....	x-component force on left strut.....	lbf
Y1.....	y-component force on left strut.....	lbf
X2.....	x-component force on right strut.....	lbf
Y2.....	y-component force on right strut.....	lbf
U <sub>∞</sub> .....	tow velocity.....	ft/sec

Besides these symbols, there are two terms in this report which may be unfamiliar to some readers, and therefore merit further explanation.

Littoral region refers to the ocean and land areas near the shore. Because future military threats will probably come from smaller countries or political groups who must by necessity fight closer to their own coastlines, the United States Navy has recognized a need to develop and enhance capabilities in this region.

Reynolds number (Re) is a measure of the ratio of the inertia force on an element of fluid to the viscous force on an element, and is represented by the following equation:

$$Re = \frac{\rho V l}{\mu} \quad (i)$$

where  $V$  and  $l$  are some characteristic velocity and length, respectively, and  $\mu$  is the fluid viscosity. Reynolds number is non-dimensional (Munson (1994)).

## Abstract

There is significant military interest in the dynamic behavior of a net array of circular cylinders traveling through a fluid medium. Although research has been conducted on a towed single line configuration in water, there is little information regarding the dynamic behavior of a towed net configuration. This investigation examined the effect that physical geometry, tow velocity, and tow angle-of-attack had on the lift and drag acting on a net towed in water. The measurements indicate a significant relationship between these factors and the stability of the net, and also provide normalized polynomial equations which will be useful in predicting the aero-ballistics of the net.

## 1. Introduction

In the aftermath of the Cold War, naval focus has been shifting from the open-ocean to littoral regions. As a result, future military threats are expected to come from smaller countries equipped with inexpensive but effective weapons. An example of this would be land mines placed close to the shore to hinder amphibious operations. In light of this, minesweeping capabilities have become a topic of special interest to the United States Navy. Because conventional minesweeping techniques are not tailored for shallow-water operations, they are not nearly as effective at clearing mines near the beach in what is referred to as the surf zone.

One possible solution currently under scrutiny is a portable, rocket-propelled "net" with explosive charges distributed evenly throughout the array. The lines of the net would be made of detonating cord or rope arranged in a grid-like pattern, and explosive charges would be placed at regular intervals along the lines of the net. The net would be connected to a line of high strength nylon webbing which would couple the rocket propulsion system to the explosive array (Granger (1994)). Prior to deployment, the net would be carried on board an air-cushion vehicle that would travel within range of the surf zone. The net would then be fired by the two rockets, spreading the net out before it impacted the surf. Upon impact, it would sink to the bottom and the

detonate, producing sympathetic explosions from submerged land mines within the effective area of the weapon. The resulting "cleared area" would allow safe passage for personnel and amphibious vehicles. The air-cushion vehicle near the center of Figure 1 illustrates the net being deployed.

Unfortunately, little is known at this time regarding the fluid behavior of a net array of fixed charges. Two recent inquiries in a related area were conducted by Granger (1993 and 1994). In these investigations, the behavior of a single line array of fixed charges was examined. The present study continues this earlier research, exploring the dynamic behavior of a net array of fixed charges. Of particular interest is the behavior of the prototype net as it is deployed from the launch platform and travels through the air. The aerodynamic characteristics of the net determine significant performance parameters like range and stability.

To determine the dynamic characteristics of the prototype net, a one-half scale model of the net was designed, built, and towed at a specific Reynolds number in various underwater configurations to obtain experimental values of the total lift and total drag on the system of charges as a function of angle-of-attack. The experimental results of lift and drag were then normalized with respect to the dynamic pressure so that a complete similitude could be achieved between the test model (traveling in water) and the prototype (traveling in

(Truver (1994))

air) (Munson (1994)). The following two equations illustrate the normalization of the drag and lift:

$$NDP = \frac{D}{\frac{1}{2}\rho U_{\infty}^2} \quad (1)$$

$$NLP = \frac{L}{\frac{1}{2}\rho U_{\infty}^2} \quad (2)$$

Note that the denominator in both equations is the dynamic pressure. This is the same nomenclature used by Granger (1994), and therefore facilitates a comparison of results. By matching the Reynolds number of the model and the prototype, the equivalent speed of the prototype could be determined. Then, by matching the drag and lift coefficients, the lift and drag forces for the prototype net moving through the air could be determined. The calculated results could also be expressed in regression polynomials to simplify aerodynamic analysis. Due to the time taken by the experimental portion of this investigation, a theoretical aerodynamic analysis was not conducted for this report. A theoretical study on the behavior of a single line array in water was conducted by Granger (1993).

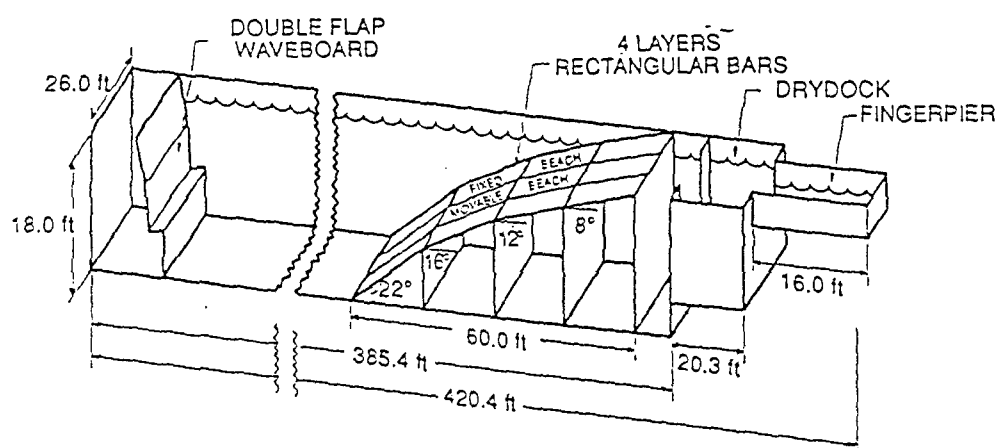
## 2. Facility and Equipment

The experiment was conducted in the 380-foot Tow Tank located in the basement of Rickover Hall at the United States Naval Academy. Constructed of steel and concrete, the facility consists of a tank with glass viewing windows, control room, waveboard, beach area, and both high-speed and low-speed towing carriages. A schematic of the Tow Tank facility is presented in Figure 2. Note that neither the beach area nor the waveboard were used during this investigation. The finger pier located at the right hand end of the tank in Figure 2 allowed easy transportation of the arrays from the shore to the carriage. The carriage could be moved along the rails above the surface of the water at a predetermined constant speed over approximately 300 feet of the tank length.

The Box Beam Support, a part of the PMM (Planar Motion Mechanism), is located on the underside of the carriage. Figure 3 shows a side view of the PMM. The PMM includes a verniered circular gear which allows the operator to rotate and set the PMM through 180 degrees in the horizontal plane. Figure 4 shows a picture of this verniered gear. In the experiments on a single line array conducted by Granger (1994), special struts and extensions were designed and fabricated to serve as the direct interface between the array and the PMM. This same equipment was used to connect the



# U.S. NAVAL ACADEMY HYDROMECHANICS LABORATORY 380 FT TOWING TANK



- Notes:
- (1) Not to scale
  - (2) All dimensions are inside measurements

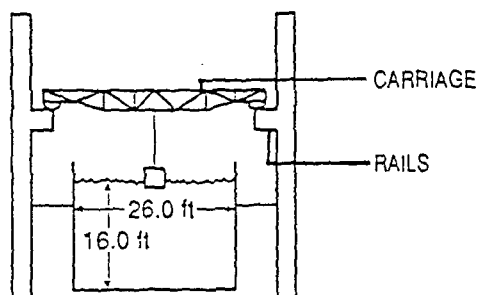


**Figure 2: USNA 380-Foot Towing Tank**



Figure 3: Planar Motion Mechanism

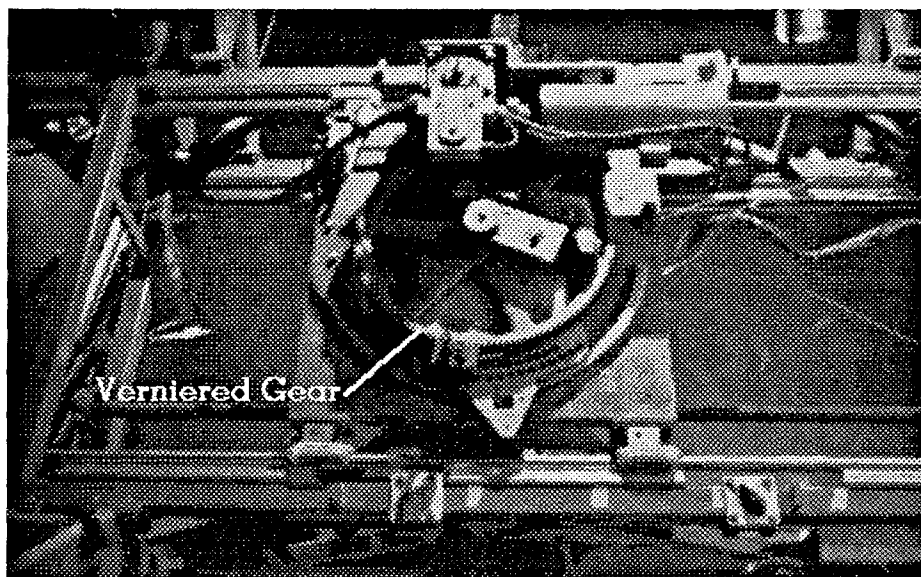


Figure 4: Verniered Gear on Towing Carriage

present net array to the PMM. Figure 5 presents the entire interface. The four principal sections of this assembly are described below.

The steel extension arm, located at the top right hand corner of Figure 5, joined the interface to the PMM. Figure 6 also illustrates this connection.

Near the top center of Figure 5 is the dual block gauge assembly. Figure 6 is an expanded picture of this section. The angle brackets positioned the two force block gauges that measured the forces acting on the net array. Figure 7 shows both of these block gauges. The gauge is a Hydronautics 4-inch modular block unit rated for a maximum load of 500 lbf. The load cell was excited using a 10 VDC power supply whose output was fed to a variable-gain data translation A/D board in the computer. Average voltage readings during towing were converted to pounds based on the initial calibration graph (See Figure 8).

In the center of Figure 5 is the streamlined strut assembly. A one-inch diameter solid stainless steel bar was fitted into a hollow one-inch<sup>2</sup> stainless steel rectangular bar, which was in turn fitted into a 1.42-inch diameter stainless steel pipe. This provided sufficient strength to withstand a 2000 ft-lbf moment. The reinforced bar was cantilevered to a block gauge, and a streamlined plate was fitted to the assembly to minimize the drag. Since the assembly was free to rotate, the streamline surface could

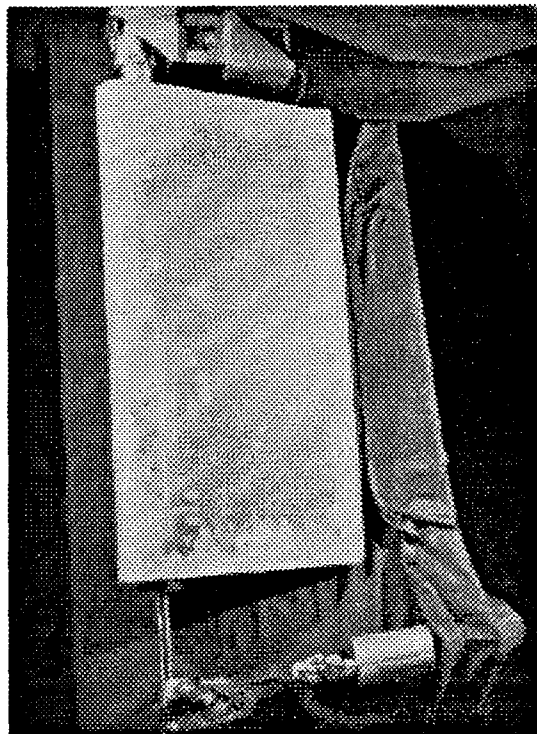


**Figure 5:** PMM-to-Array  
Interface

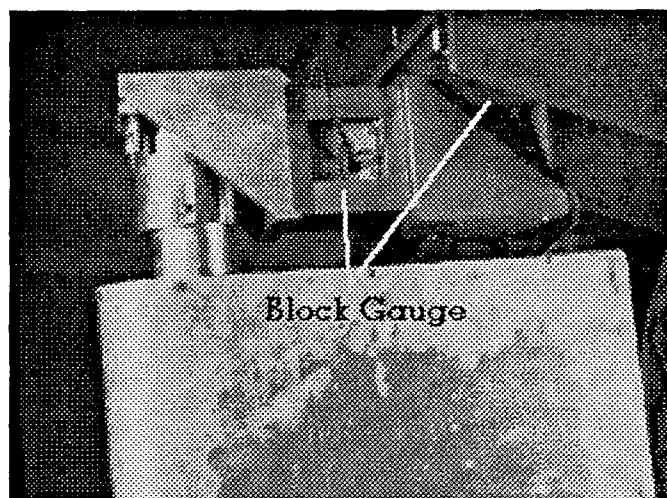


**Figure 6:** Block Gauges with  
Extension Arm and Streamlined  
Surface

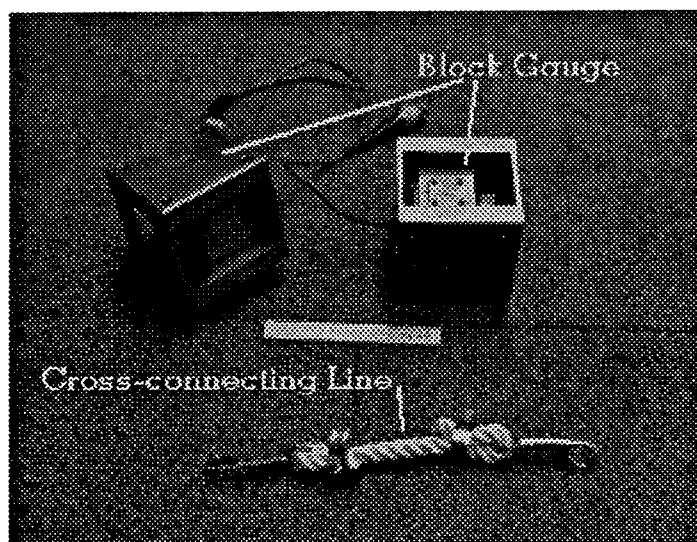


**Figure 7:** Two Block Gauges and a Cross-connecting Line

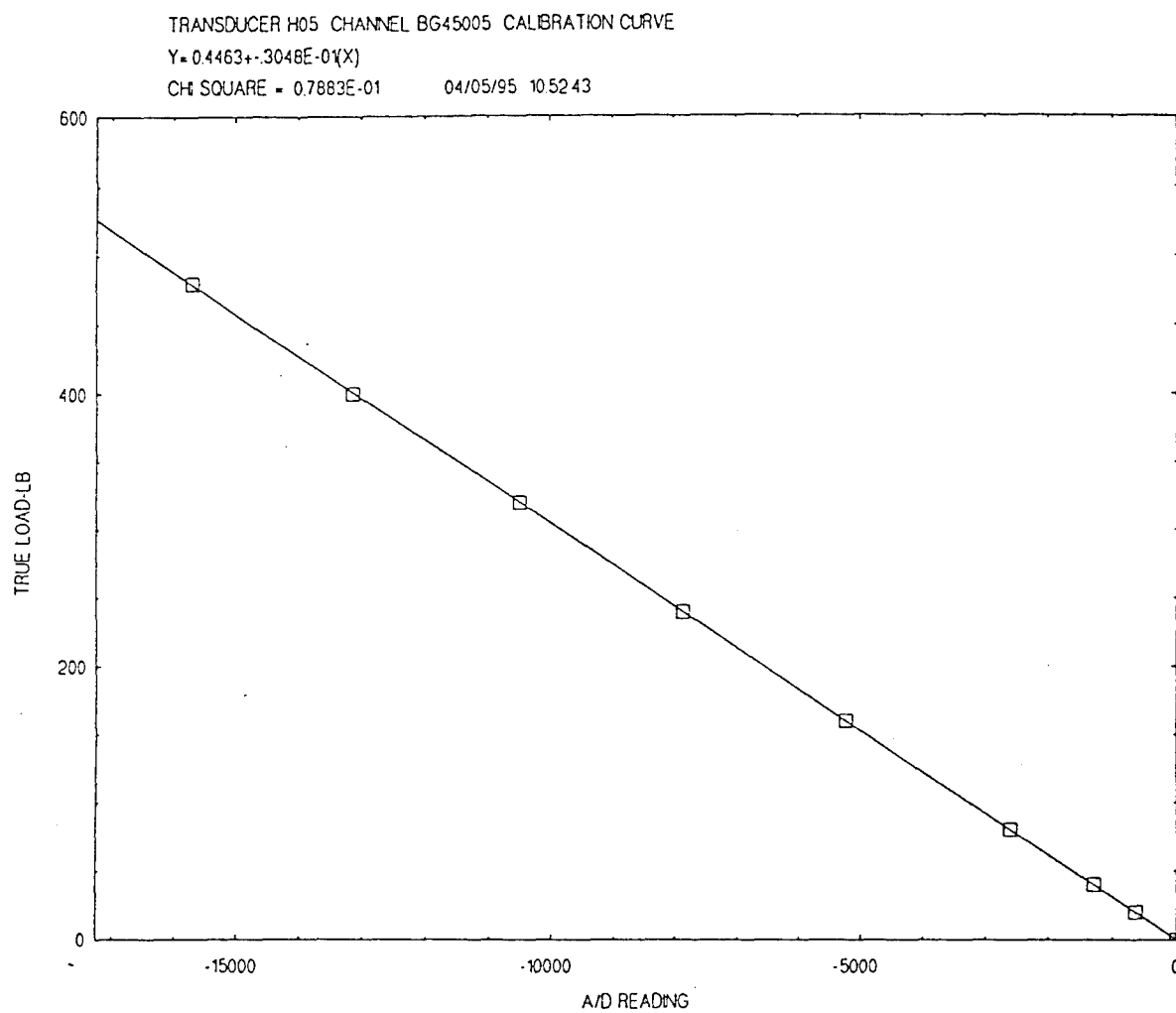


**Figure 8:** Block Gauge Calibration Graph

align itself with the fluid flow during a specific test, helping to reduce the total drag. When connected to the PMM, the strut assembly placed the net array four feet below the free-surface in order to reduce the effect of surface turbulence on the measurements.

The load binder assembly is seen to be located at the bottom of one of the streamlined strut assemblies in Figure 5. An expanded picture of the assembly is shown in Figure 9. The purpose of the load binder was to put tension on the leading line array. Since the leading line array could not be fed directly through the load binder, it was threaded through a steel ring and secured to itself using two large clamps. A length of webbing was also threaded through the steel ring, and the free ends of the webbing were fed into the load binder. The other end of the leading line array was looped and secured around the opposite strut. Tension was applied to the leading line array by ratcheting the load binder.

The net array of cylinders was constructed exclusively for this experiment. An important consideration in the design of the net array was the speed and ease with which it could be changed. The four major components of the net array are discussed below.

To simulate the explosive charges of the prototype net, circular cylinders were designed and fabricated. The cylinders were constructed of 3.5 inch OD schedule 40 aluminum 6061T6 pipe which had endplates made of 0.125 inch aluminum

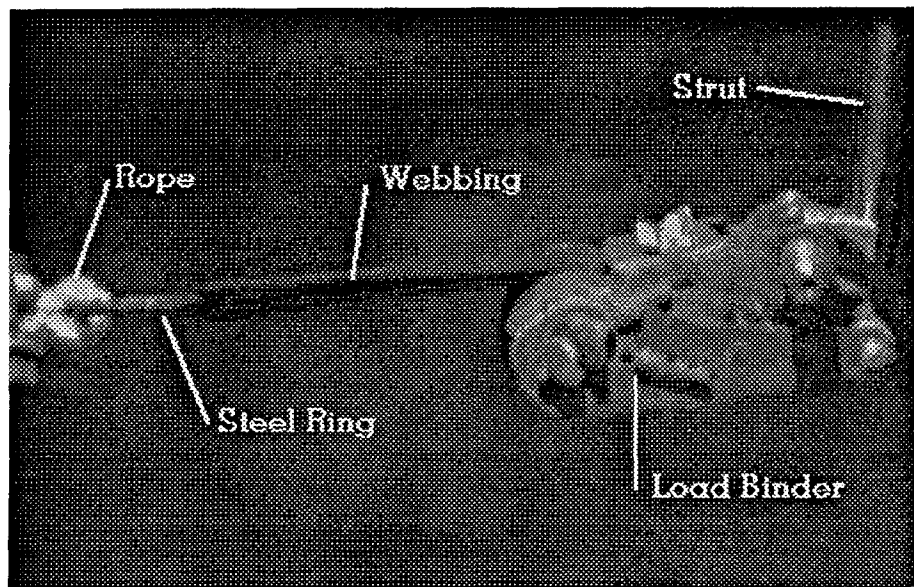


**Figure 9:** Load Binder Assembly



5052 sheet welded onto both ends. Figure 10 shows three different views of the cylinder. The completed cylinders were 6.125 inches in length. The single lines were threaded through the large central hole in the ends (diameter  $9/16$  inches), and water entered the cylinder via four smaller outer holes (diameter 0.125 inches) located on both ends of the cylinder. With the cylinders full of water, the cylinder-rope system had a slight negative buoyancy.

The primary structural component of the net array was the single line array. Each line array was made of half-inch diameter three strand nylon rope, and had a length of 15 feet. The ends were cut and shaped by a hot knife to prevent fraying, thereby making it easier to thread through each of the cylinders.

Consecutive single line arrays were attached to each other by cross-connecting lines as shown in Figure 11. These cross-connecting lines were one-foot in length, and consisted of two steel bolt snaps joined by a length of rope. The rope was looped through the ring at the bottom of the bolt snap and secured to itself with half-inch width steel hose clamps at both ends. One of these cross-connecting lines is located at the bottom of Figure 7. The "snapping" end of the bolt snap had a 0.75 inch diameter and was easily fastened around the line arrays. These were placed between consecutive cylinders to complete the "net" effect.

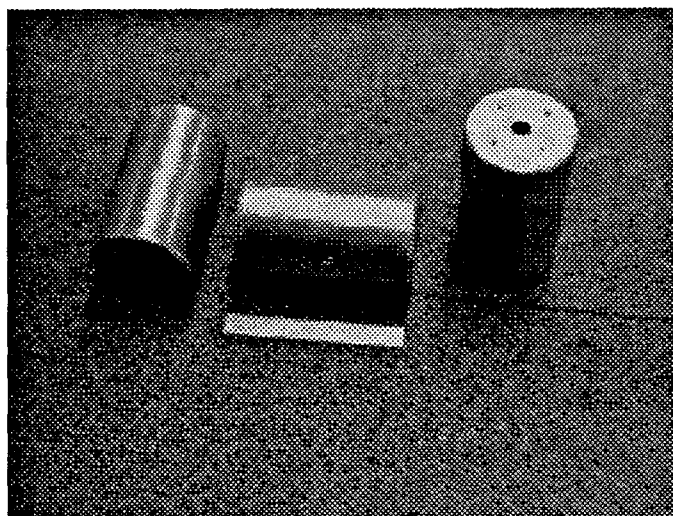


Figure 10: Cylinders (3 Views)

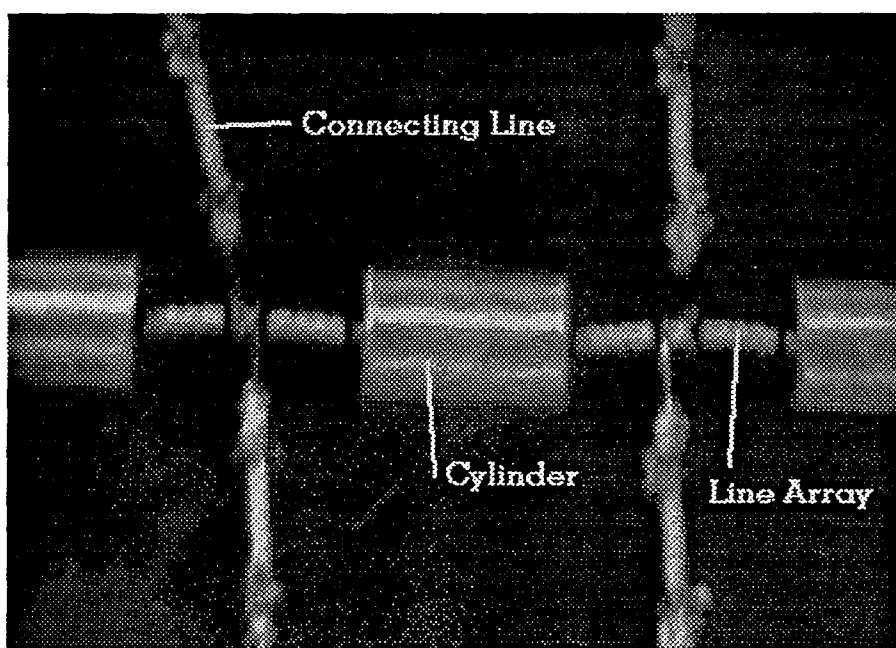


Figure 11: Portion of Net Array

To prevent the cylinders and connecting lines from slipping out of their original positions, rubber hose clamps served as "stops." When attached securely to a line, these hose clamps were immobile.

For real time observation of the underwater net array during carriage movement, a miniature video camera was placed underwater forward of the test rig and focused on the net array. The images captured by the camera of the net's stability were recorded onto video tape for subsequent observation and analysis.

### **3. Measurement Techniques**

The measurement technique used in this experiment was to tow the net array in various configurations and to record the effects of these modifications on the lift and drag forces acting on the net array. The five parameters altered in the experiment and their ranges are as follows:

- (a) Number of line arrays (1 through 8);
- (b) Number of cylinders per line array or relative cylinder spacing (3 cylinders/36 inches, 6 cylinders/24 inches, 11 cylinders/12 inch spacing);

- (c) Pre-tension\* of the first line array (low/high tension);
- (d) Angle-of-attack ( $\alpha$ ) of the net array with direction of motion (0, 6, 10, 16, 20, 26, 30, 40, 50, 60, 70, 80, 90 degrees for single line arrays, and 30, 40, 50, 60, 70, 80, 90 degrees for configurations with two or more arrays). See Figure 12;
- (e) Speed of towing carriage (3 knots/5.04 ft/sec, 6 knots/10.07 ft/sec).

Note that in (c), the two available tensions were named low and high. Due to the elastic properties of the rope, the tensioning equipment could not hold a constant value of tension. This was especially apparent during the low tension trials. The low tensions were maintained as close to 100 pounds as possible, and the high tensions were maintained as close to 200 pounds as possible.

Before any actual tow tests were run, a pre-test matrix was developed, enumerating the possible combinations of the five parameters outlined above. This was used as a guideline for the test runs. A representative portion of the pre-test matrix is depicted in Table A.1 in Appendix A.

The experimental measurements of the forces acting on each of the streamlined struts were collected by means of the

---

\*Pre-tension simulated the tension placed on the first array by the rocket delivery system.

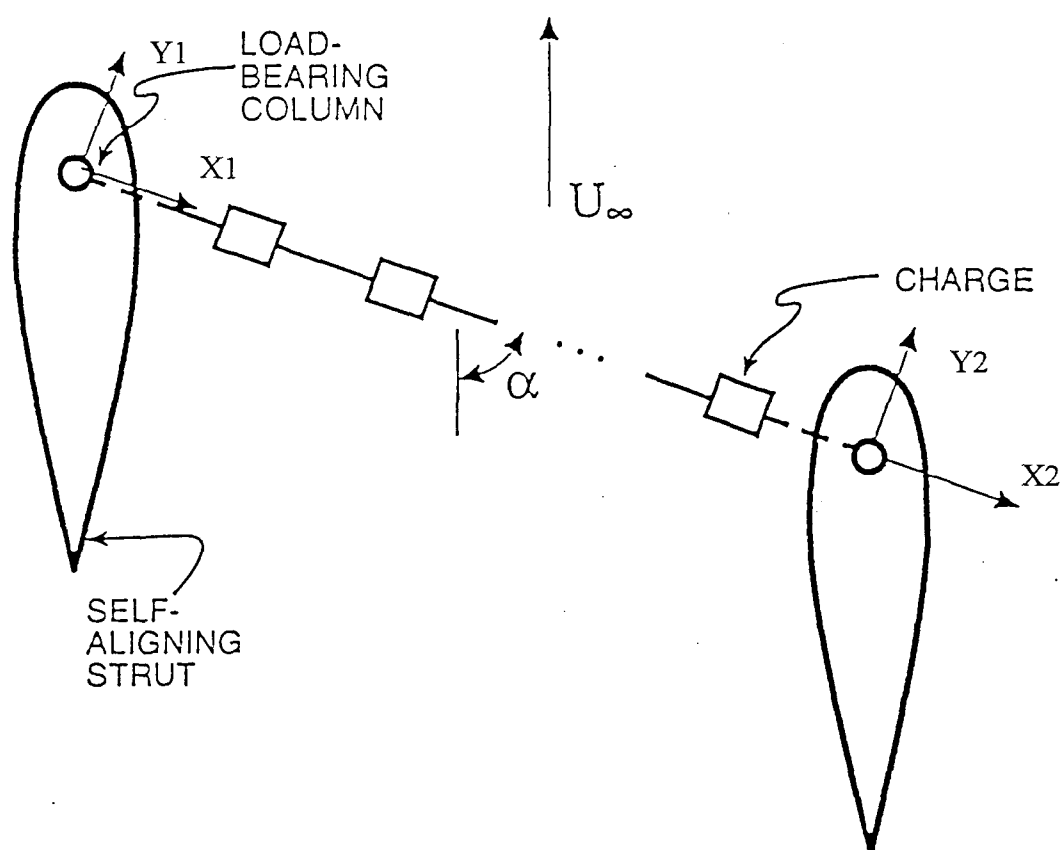


Figure 12: Diagram of Struts and Leading Line Array

Hydrodynamics Laboratory System (HLS) as described by Granger (1994). Figure 13 presents a conceptual layout of the HLS. It runs on an Ethernet Local Area Network featuring a fileserver, an application server and five workstations, all of which are fully implemented through a 486 computer system. The purpose of the HLS is to provide a flexible user-oriented program for control of data acquisition, analysis of acquired data, and the production of graphic and tabular output of the acquired data and analysis results.

### 3.1: Experimental Procedure

The procedure utilized to obtain the data is delineated below:

- ▶ STEP 1: Referring to the pre-test matrix (see Appendix A), the desired net array configuration was assembled ashore near the finger pier and transported to the carriage through the water by scuba divers. If tension needed to be adjusted, that was also taken care of by the divers.
- ▶ STEP 2: Angle-of-attack of the array and the pre-tension of the leading line array were set. Once the pre-tension was verified by the computer and recorded, the carriage quickly accelerated to the predetermined tow velocity. Data consisting of the x- and y- components of the forces acting on each streamlined strut (see Figure 12) were

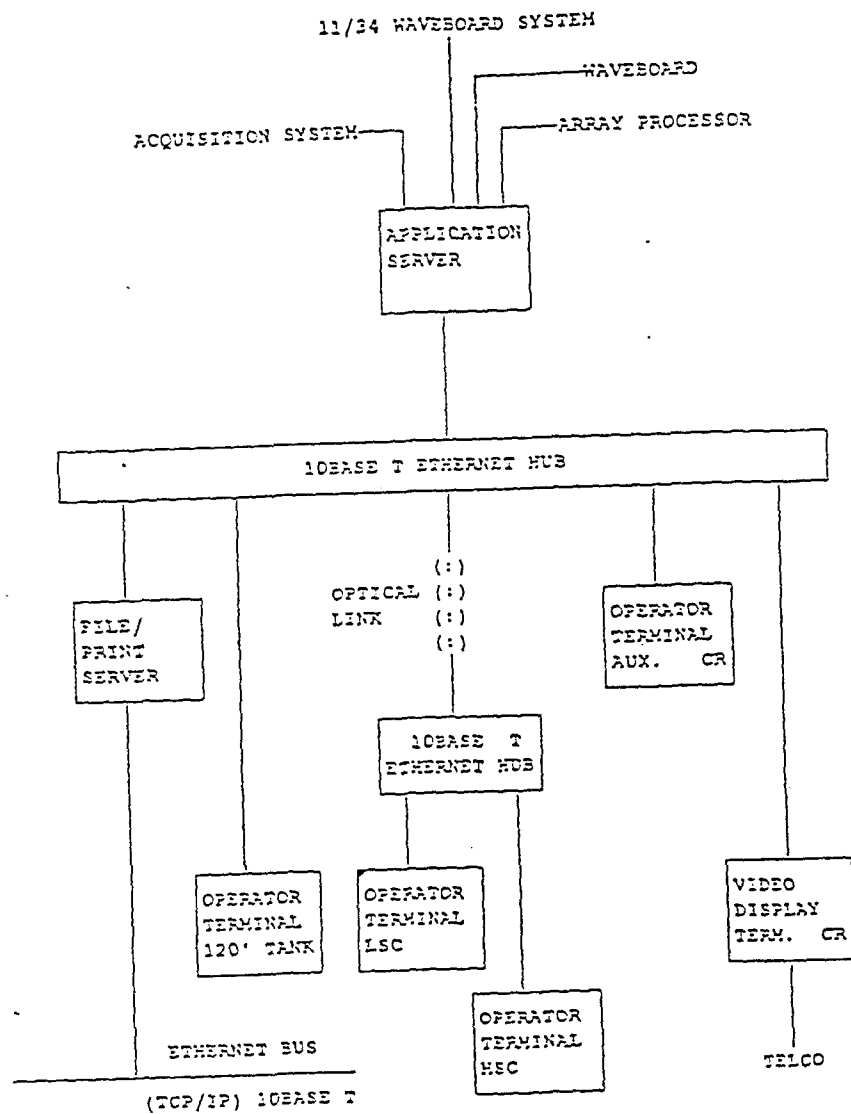


Figure 13: Conceptual Layout of HLS

taken while the carriage ran at constant speed. The carriage quickly decelerated before it could collide with the waveboard, and was then brought back to the initial position. The x- and y- forces on the net array were recorded by a sampling process (slowest sampling rate was 51.2 samples per second).

- ▶ STEP 3: The data were truncated, cutting out the acceleration at the beginning of the run and the deceleration at the end of the run. The remaining values were averaged and recorded. All these calculations were conducted while the carriage was returning to the initial position.
- ▶ STEP 4: Steps 1 through 3 were repeated, changing angles-of-attack, velocities, number of line arrays, number of cylinders per line array, and pre-tension in the leading line array (in that order). Modifications to the pre-test matrix occurred due to two reasons. First, the maximum moment that each streamlined strut could withstand was 2000 ft-lbf. Since each strut was four feet in length, the maximum force limitation was 500 lbs. Second, tow tank use for this experiment was limited to just under three weeks for data collection. Because of this, the pre-test matrix was abbreviated in order to run as many different net configurations as possible. Another consequence of the time constraint was that



measurements could not be repeated for an uncertainty analysis.

Table A.2 in Appendix A lists the collected and corrected data obtained from the measurements.

#### 4. The Measurements

The data in its raw form were collected as force components on each strut parallel to the first line array (x-component) and perpendicular to it (y-component). Figure 13 presents the nomenclature used to describe the geometry of the force components. Referring to Figure 13, one should note the following:

- $\alpha$ : Angle-of-attack (degrees);
- $\rho$ : Density of water (lbs/ft<sup>3</sup>);
- X1: Force parallel to leading line array on left strut (lbs);
- X2: Force parallel to leading line array on right strut (lbs);
- Y1: Force perpendicular to leading line array on left strut (lbs);
- Y2: Force perpendicular to leading line array on right strut (lbs);
- $U_{\infty}$ : Tow Velocity (ft/sec).

The forces obtained were then corrected by subtracting the x- and y- components of the tare readings for the struts and the pre-tension on the leading line array, which acts solely in the x-direction.

Using the corrected force values, the actual drag and lift forces can be expressed by the following equations:

$$D = \left( \frac{X1 + X2}{2} \right) \cos \alpha - \left( \frac{Y1 + Y2}{2} \right) \sin \alpha \quad (3)$$

$$L = \left( \frac{X1 + X2}{2} \right) \sin \alpha + \left( \frac{Y1 + Y2}{2} \right) \cos \alpha \quad (4)$$

Based on these equations, the drag and lift were represented in this experiment by the Normalized Drag Parameter (NDP) and the Normalized Lift Parameter (NLP), respectively. These were determined as follows:

$$NDP = \frac{(X1 + X2) \cos \alpha - (Y1 + Y2) \sin \alpha}{\rho U_{\infty}^2} \quad (5)$$

$$NLP = \frac{(X1 + X2) \sin \alpha + (Y1 + Y2) \cos \alpha}{\rho U_{\infty}^2} \quad (6)$$

Both of these parameters are in fact the coefficient of drag or lift multiplied by area. Since they are identical to the ones used by Granger (1994), it is easier to make a comparison of the results.

The NDP and NLP data for the various experimental runs were plotted against angle-of-attack in order to analyze the effect of modifying net array geometry, tow velocity, and angle-of-attack on the forces which acted on the net array. Polynomials were fit to the data and plotted through the data points and were grouped together in families of curves. Appendix B lists the polynomial equations calculated for each individual curve. These equations could be used in a similitude analysis to predict the behavior of the net array as it traveled in the air.

Each family of curves isolated and varied one of the net array configuration variables (number of arrays, number of cylinders per line array, velocity, or pre-tension), thereby illustrating its effect on the behavior of the array. The following sections discuss the experimental results. Note that the graphs containing curves for a single line array also have a dashed-line curve on them, with the exception of Figure 37, which has two dashed-line curves for two separate tow velocities. Each dashed-line curve represents the polynomial equations of NDP or NLP (as appropriate) with respect to angle-of-attack obtained by Granger (1994) for the single line array with two cylinders towed through water for the speed

indicated on the graph. It is important to point out two differences between the equipment used in the investigation outlined by Granger (1994) and the equipment used in the present investigation. First, Granger used two parallel strands of webbing to hold the cylinders to each other and to the struts instead of the single rope setup used in the present investigation. Second, although the cylinders in both experiments had the same diameter to length ratio, Granger's cylinders were two times as long as the cylinders used in the present study. The discrepancy in cylinder size was accounted for by Reynolds number matching.

#### 4.1: NDP versus Angle-of-Attack

(a) Each of the curves in Figure 14 demonstrate the general behavior of NDP with increasing angle-of-attack for the test runs. NDP is at its minimum value at low angle-of-attack, increasing gradually with angle-of-attack to peak at approximately  $75^\circ$ . Above this angle, NDP either remains constant or decreases slightly. The NDP for the single line array with two cylinders from Granger(1994) coincided almost exactly with the one array configuration with eleven cylinders. In the plots depicting NDP vs angle-of-attack (Figures 14-26), the data points at the  $40^\circ$  angle-of-attack are significantly lower than the curve drawn through the other points in the low velocity cases. Considering the consistent nature of this "anomaly" along with the fact that it does not

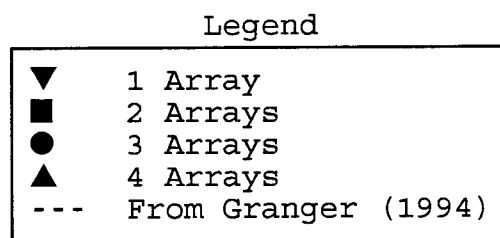
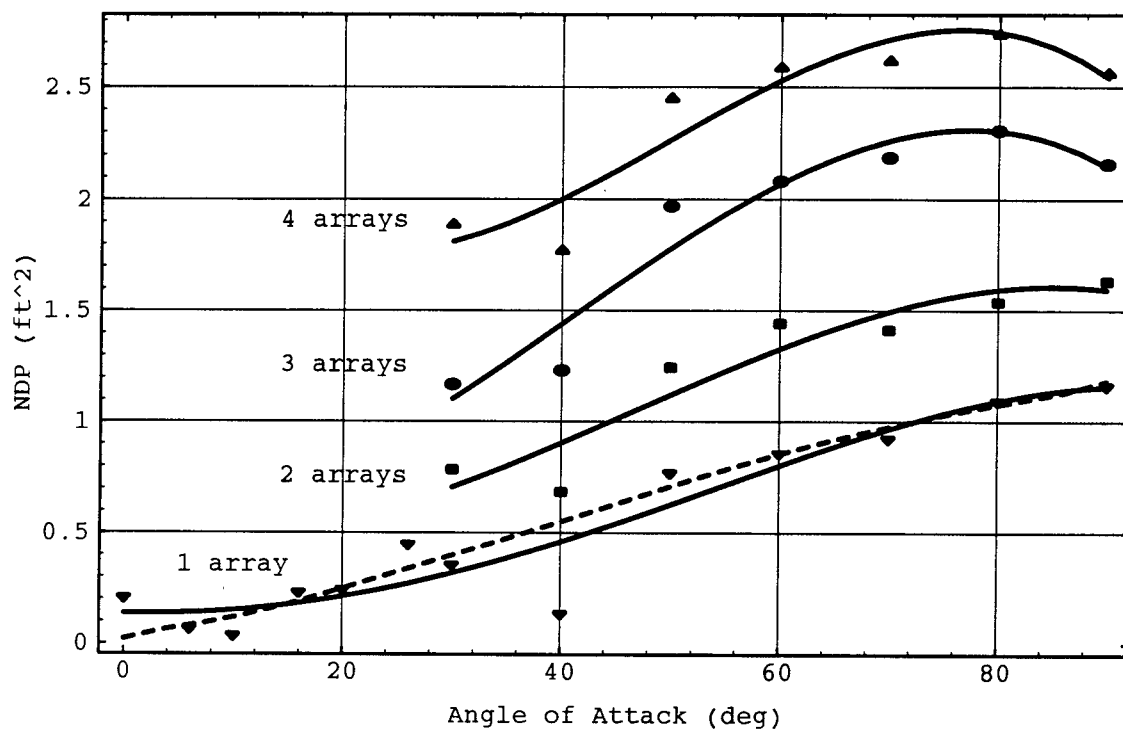


**Figure 14:** Effect of Number of Arrays on NDP  
(Test Run at Low Tow Velocity/11 Cylinders/Low Pre-tension)

occur in the high velocity cases, it is difficult to dismiss as experimental error. Indeed, the NDP drop-off seen between  $30^\circ$  and  $50^\circ$  seems to be an inherent characteristic of the net's behavior at low velocity.

(b) Effect of Number of Arrays on NDP: Figure 14 demonstrates the general effect of increasing the number of line arrays in the tow configuration. The addition of line arrays increases the amount of drag that the net produces. The only deviation from this trend is shown in Figure 15: from  $30^\circ$  to  $35^\circ$ , NDP for the two array case is slightly higher than that for the three array case. Note that by decreasing the number of cylinders from eleven to six, the NDP for the present one array case in Figure 15 is significantly lower than Granger's single line array.

(c) Effect of Number of Cylinders per Line Array on NDP: Generally, increasing the number of cylinders per line in the net increased NDP (see Figure 16). Deviations from this trend occurred in the nets portrayed in Figures 17 and 18. In Figure 17, the three cylinder per line case has a higher NDP than the six cylinder per line case from  $0^\circ$  to  $20^\circ$ . As shown in Figure 18, the six cylinder per line condition generates a higher NDP than the eleven cylinder per line condition between  $30^\circ$  and  $38^\circ$ .

(d) Effect of Tow Velocity on NDP: The net array was towed at two different velocities which are referred to in this section as low velocity (3 knots) and high velocity (6

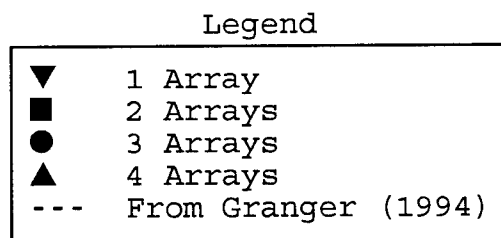
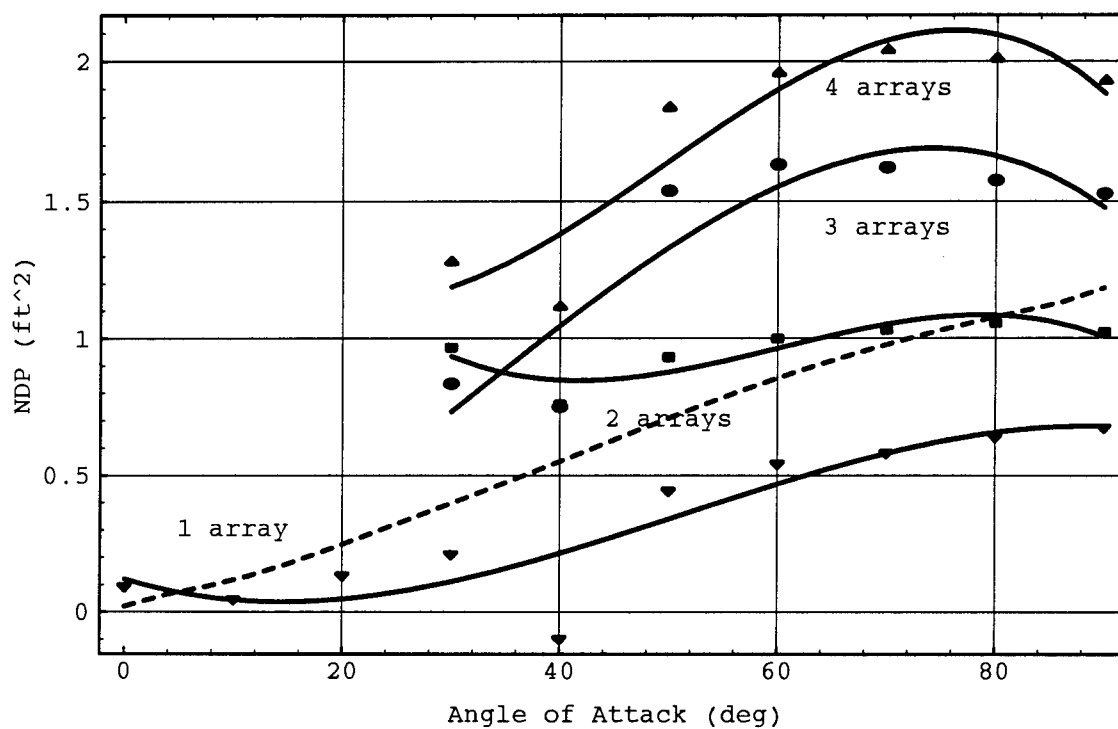


**Figure 15:** Effect of Number of Arrays on NDP  
(Test Run at Low Tow Velocity/6 Cylinders/Low Pre-tension)

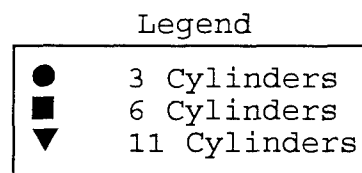
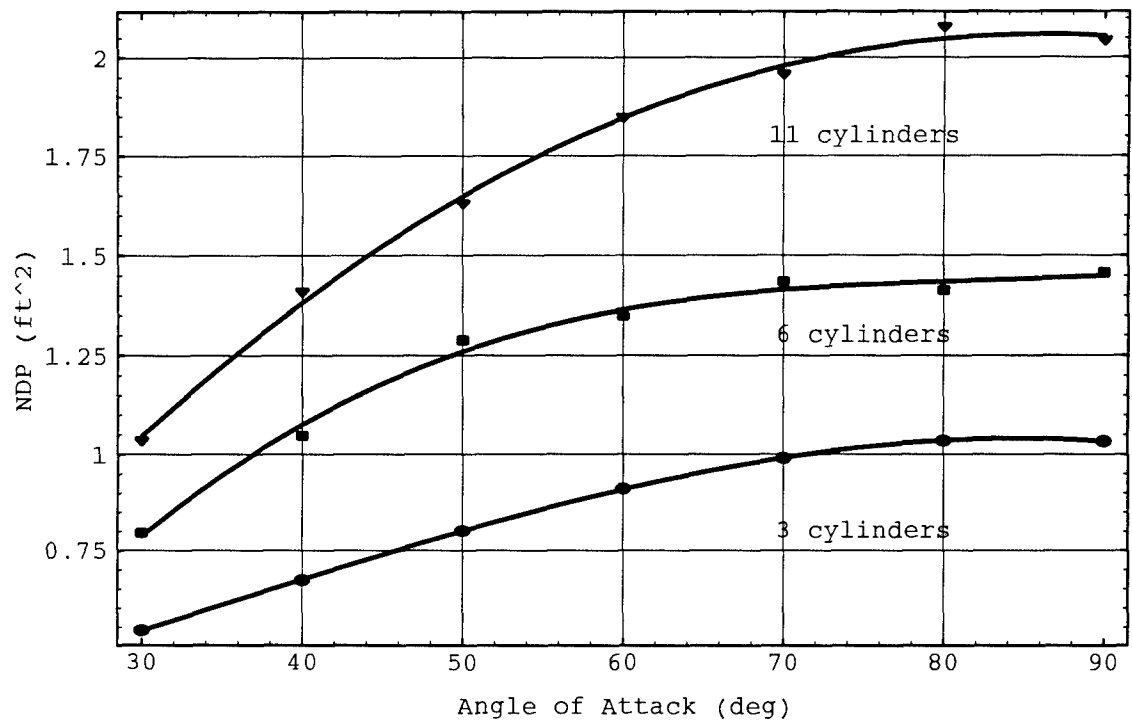
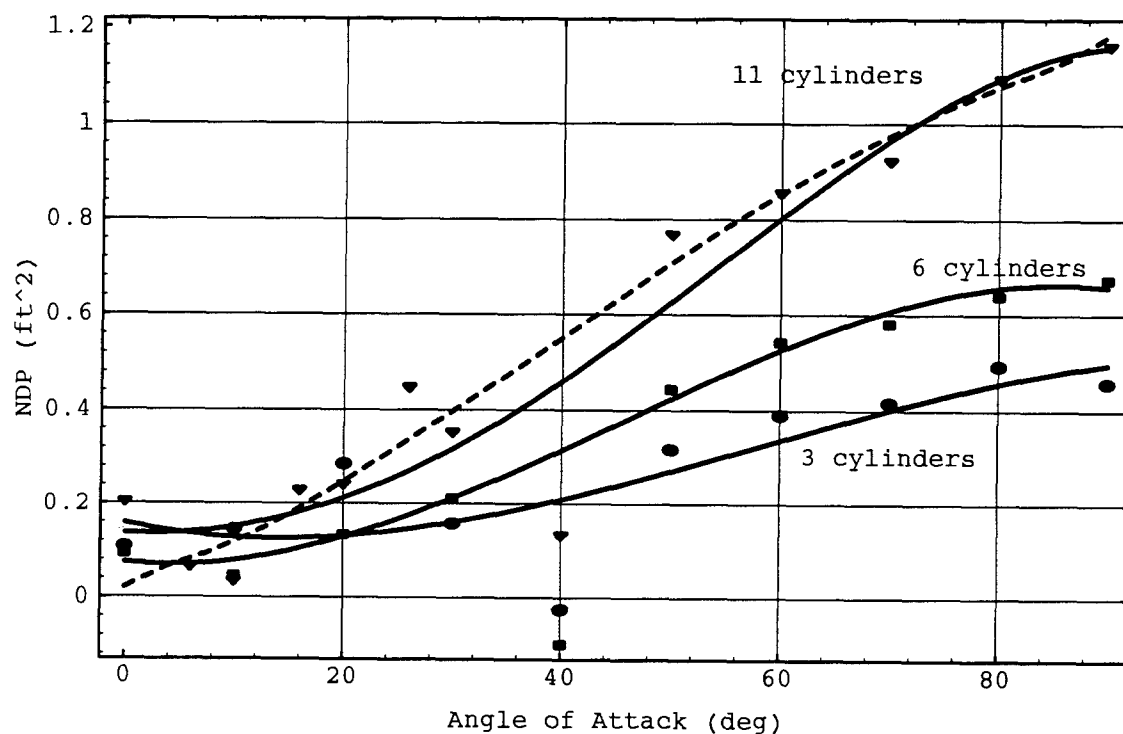


**Figure 16:** Effect of Number of Cylinders on NDP  
(Test Run at High Tow Velocity/3 Arrays/Low Pre-tension)

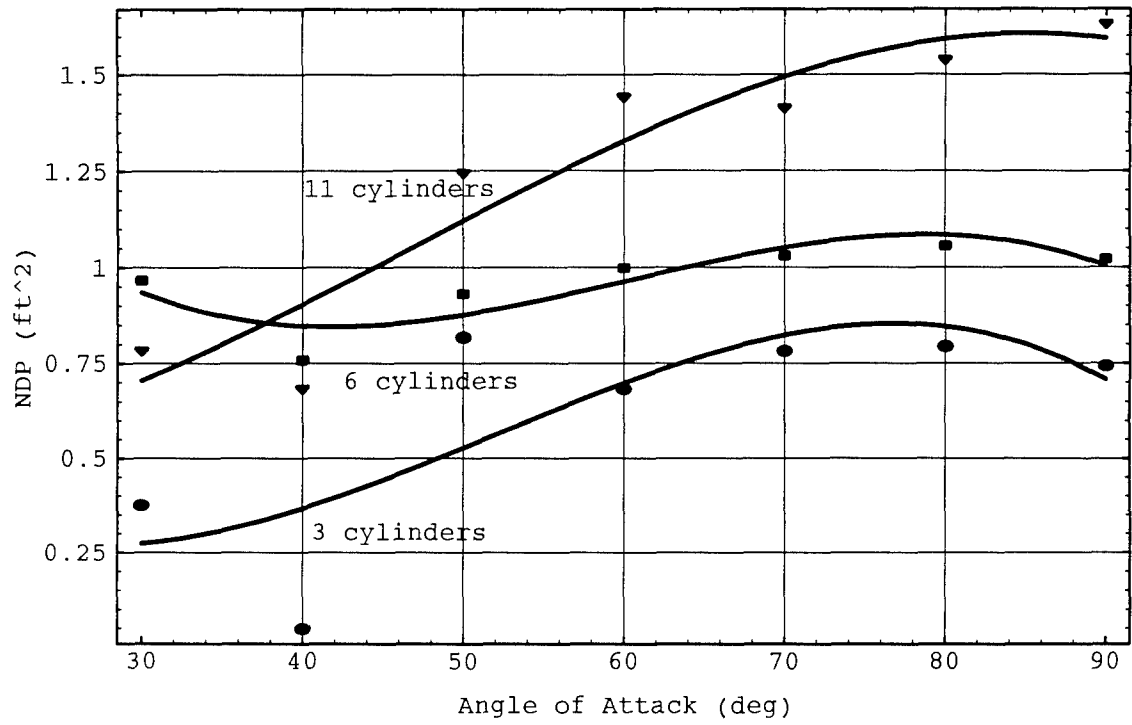




## Legend

●	3 Cylinders
■	6 Cylinders
▼	11 Cylinders
---	From Granger (1994)

**Figure 17:** Effect of Number of Cylinders on NDP  
(Test Run at Low Tow Velocity/1 Array/Low Pre-tension)



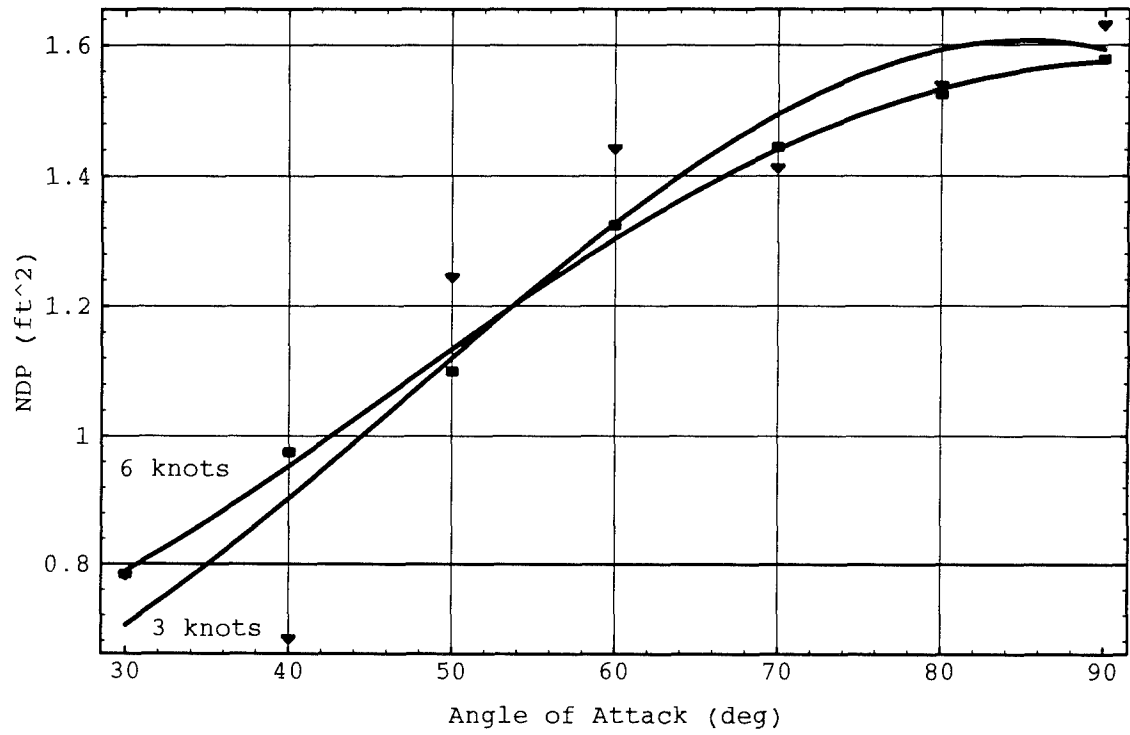
## Legend

●	3 Cylinders
■	6 Cylinders
▼	11 Cylinders

**Figure 18:** Effect of Number of Cylinders on NDP  
(Test Run at Low Tow Velocity/2 Arrays/Low Pre-tension)

knots). For the eleven cylinder per line net, increasing the tow velocity did not noticeably affect the NDP curves for the nets with one or two line arrays and eleven cylinders per line. Figure 19 illustrates this point for the two array, eleven cylinder per line case. With the addition of one more array, velocity begins to have a greater impact on the drag. In Figure 20, the low and high velocity curves are similar at low angles-of-attack. However, at low velocity, NDP increases at a greater rate than at high velocity between  $50^\circ$  and  $80^\circ$ , maxing out at approximately  $80^\circ$ . Figure 21 presents the four array, eleven cylinder per line case. Though similar to the results shown in Figure 20, the low and high velocity curves do not coincide at low angles-of-attack. Again, the low velocity curve increases at a greater rate from  $50^\circ$  to  $78^\circ$ , decreasing rapidly thereafter to approach the high velocity curve. Similar behavior was seen for the six cylinder per line cases with the exception of the low velocity curve on Figure 22. Unlike the other graphs, NDP is highly nonlinear, possessing a sine wave-like behavior with increasing angle-of-attack. The sequence of plots for the three cylinder per line nets also yield comparable trends. A representative plot of this behavior is presented in Figure 23.

(e) Effect of Pre-Tension on NDP: Figure 24 shows the typical effect of increasing the pre-tension on the leading line array. The NDP for the high tension case is higher than the NDP for the low tension case. Exceptions to this trend



Legend

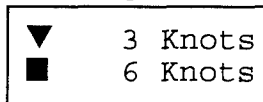
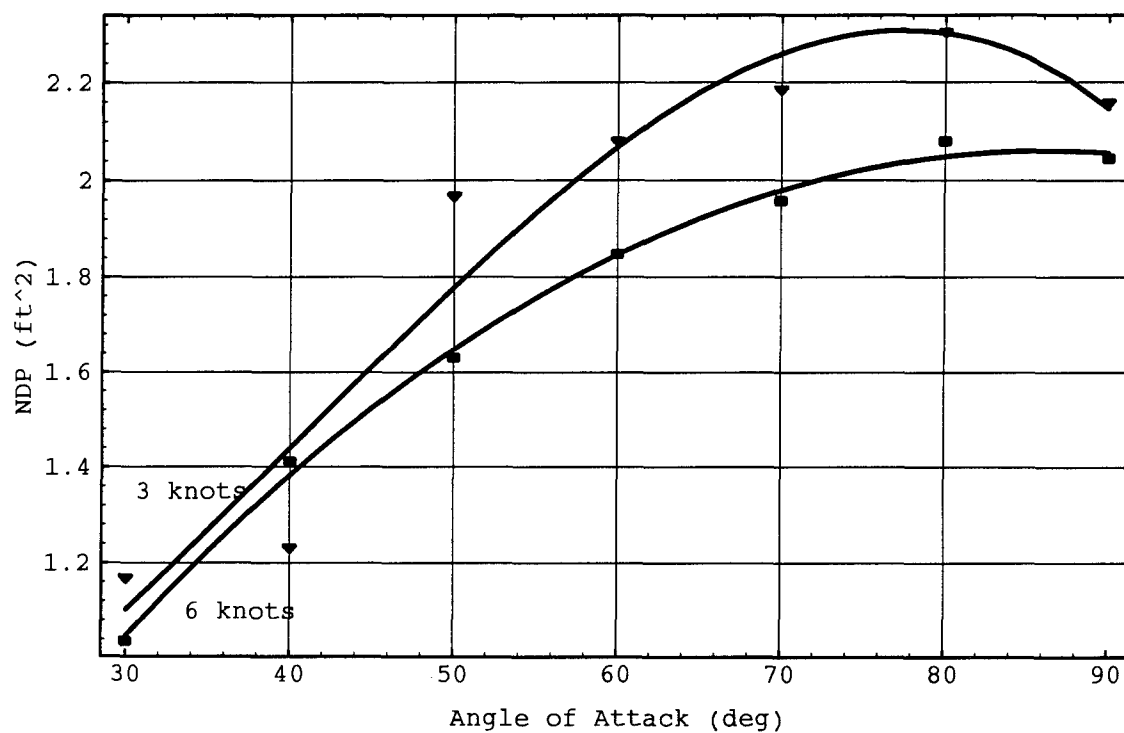


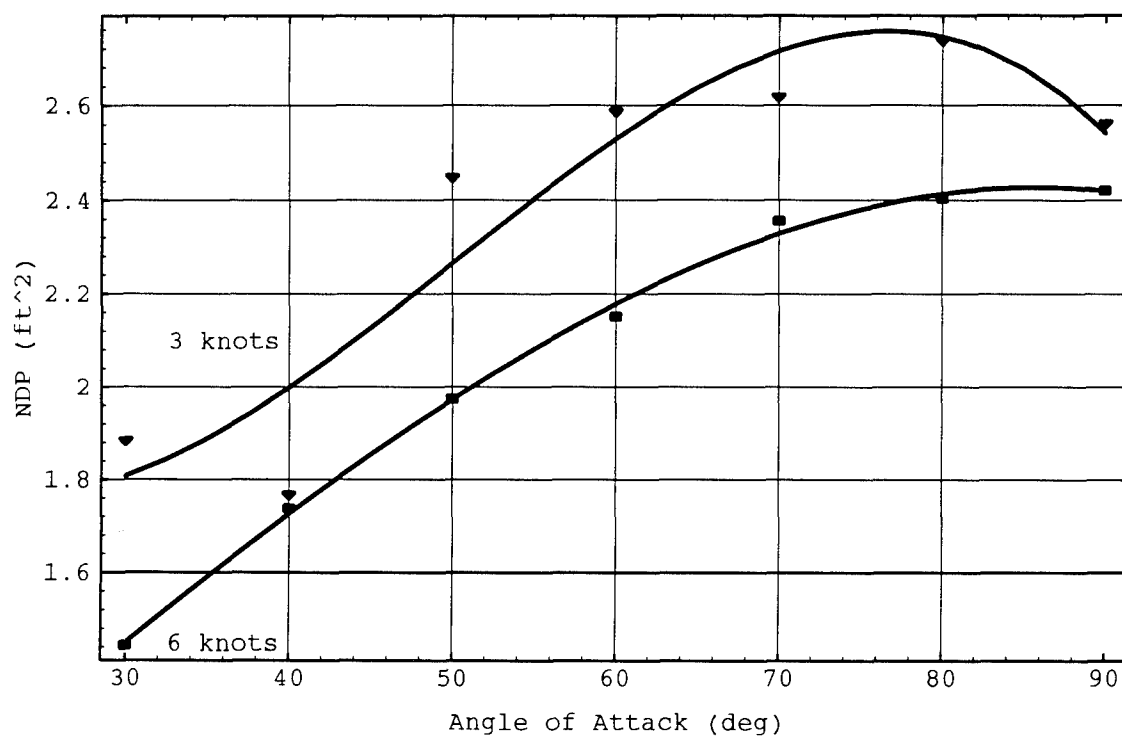
**Figure 19:** Effect of Tow Velocity on NDP  
(Test Run at 11 Cylinders/2 Arrays/Low Pre-tension)



## Legend

▼	3 Knots
■	6 Knots

**Figure 20: Effect of Tow Velocity on NDP**  
(Test Run at 11 Cylinders/3 Arrays/Low Pre-tension)



Legend

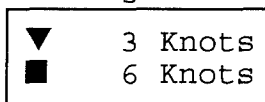
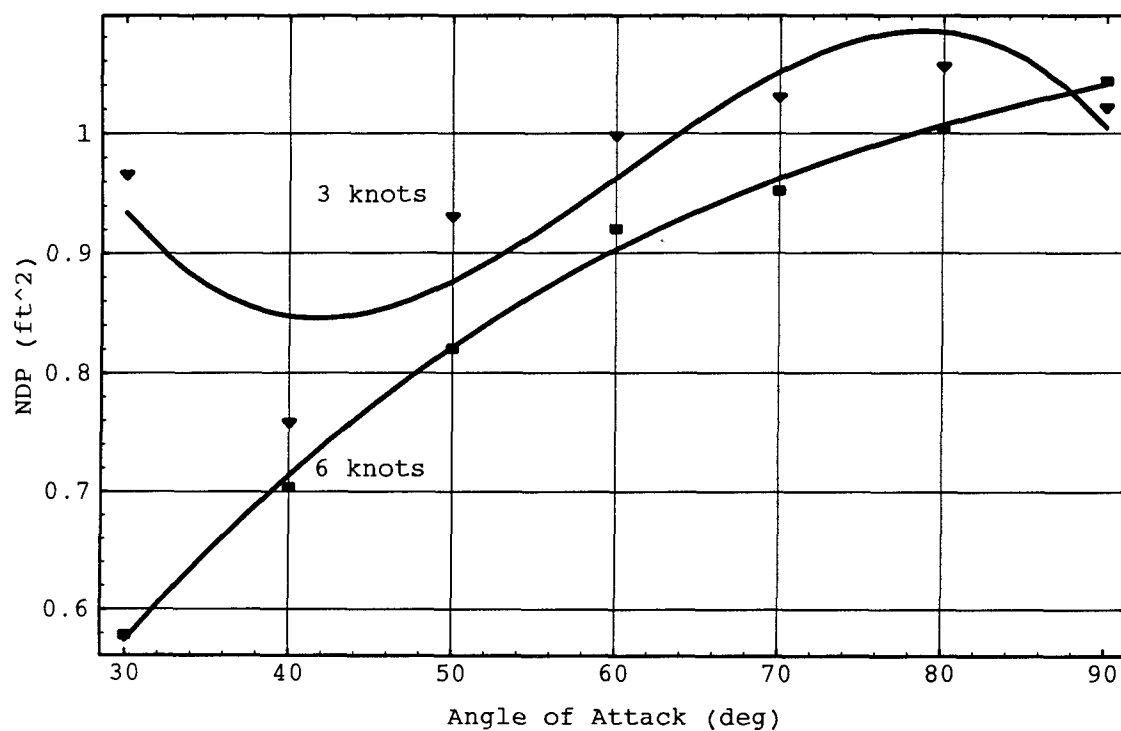


**Figure 21:** Effect of Tow Velocity on NDP  
(Test Run at 11 Cylinders/4 Arrays/Low Pre-tension)



## Legend

▼	3 Knots
■	6 Knots

**Figure 22:** Effect of Tow Velocity on NDP  
(Test Run at 6 Cylinders/2 Arrays/Low Pre-tension)

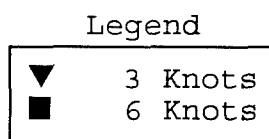
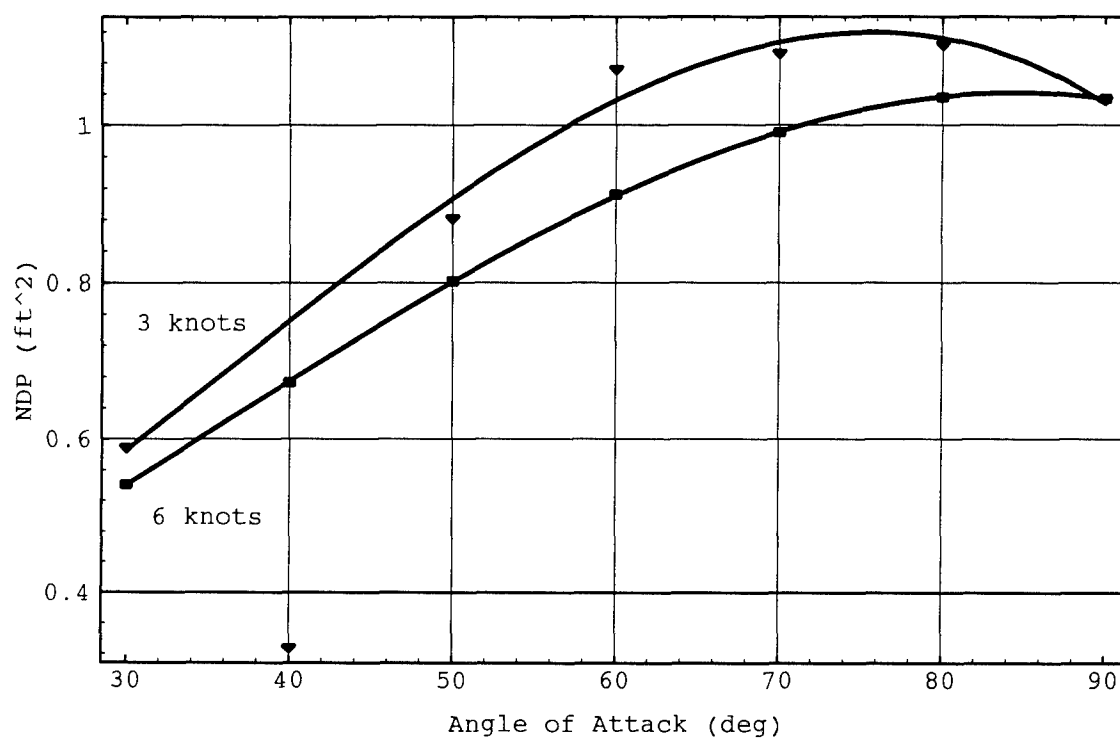
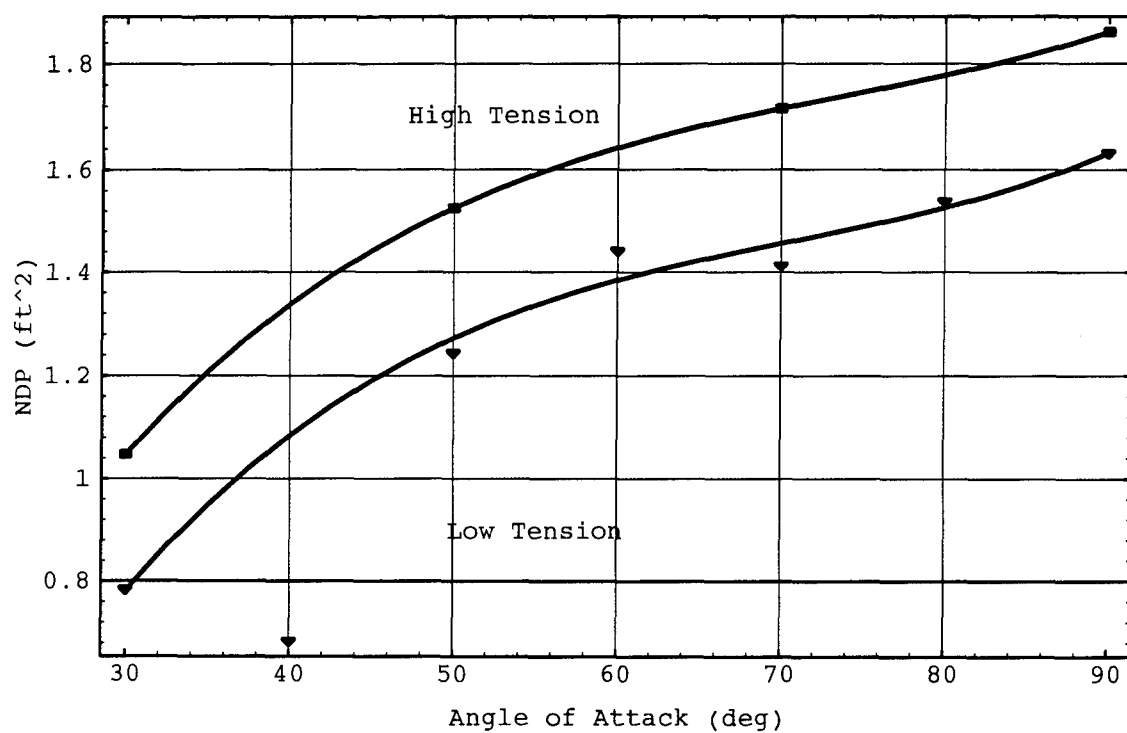


**Figure 23:** Effect of Tow Velocity on NDP  
(Test Run at 3 Cylinders/3 Arrays/Low Pre-tension)





## Legend

- |   |              |
|---|--------------|
| ▼ | Low Tension  |
| ■ | High Tension |

**Figure 24:** Effect of Pre-tension on NDP  
(Test Run at 11 Cylinders/2 Arrays/Low Tow Velocity)

were observed in Figures 25 and 26. In Figure 25, the low tension curve rises slightly above the high tension curve between  $64^\circ$  and  $82^\circ$ . In Figure 26, the low tension curve is slightly higher than the high tension curve between  $30^\circ$  to  $34^\circ$ . Thus, pre-tension of the leading line array appears to be a significant factor to consider in the behavior of the towed nets. This differs from the measured results of Granger (1994).

#### 4.2: NLP versus Angle-of-Attack

(a) In general, the normalized lift parameter (NLP) versus angle-of-attack plots reveal a downward concave curve at the early angles-of-attack ( $0^\circ$  to  $45^\circ$ ) before it settled out around the zero NLP region at higher angles-of-attack. This shows that there are well-defined regions of either maximum and/or minimum lift at specific angles-of-attack. An example of this is the single array curve on Figure 27. Of course, there were some exceptions to this trend, and these are discussed below. Note that on Figure 27, NLP for Granger(1994) single line array remained just under zero until  $80^\circ$ , and then jumped up to just above one  $\text{ft}^2$ .

(b) Effect of Number of Arrays on NLP: Figures 27 and 28 present the effect of number of arrays on NLP for the single array with eleven cylinders per line at low speed and low tension. In Figure 27, note that the one and two array curves are nearly coincident, with both showing lift values in the

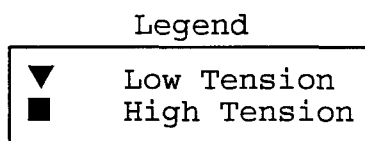
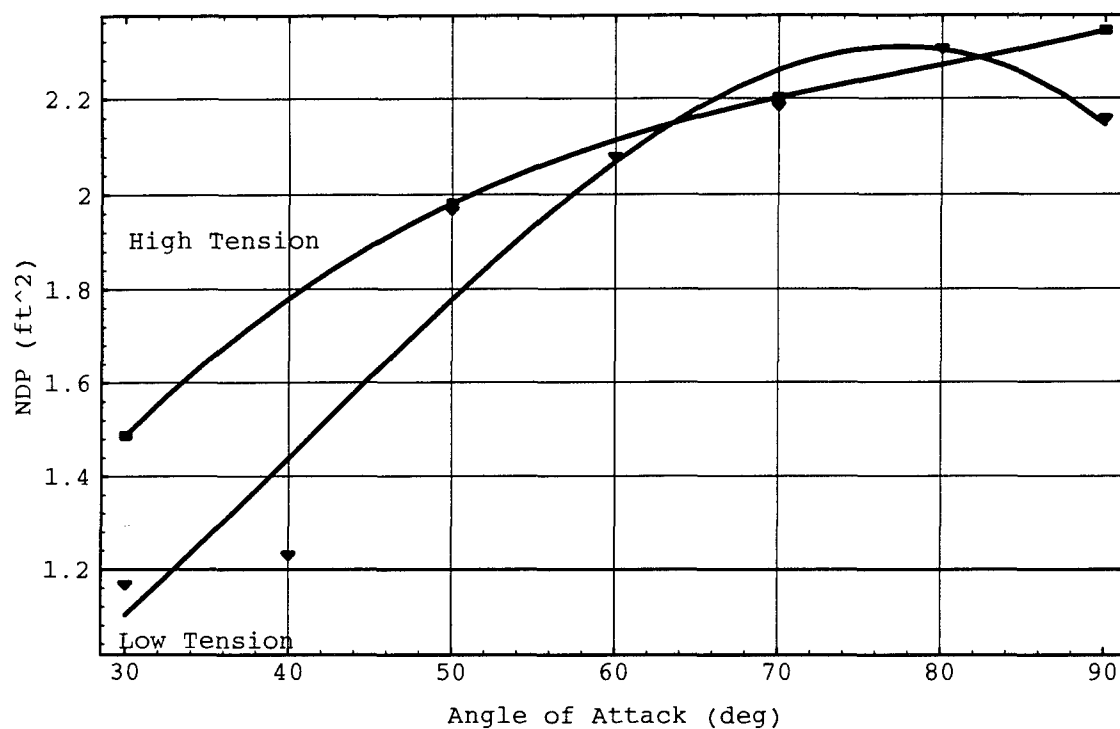
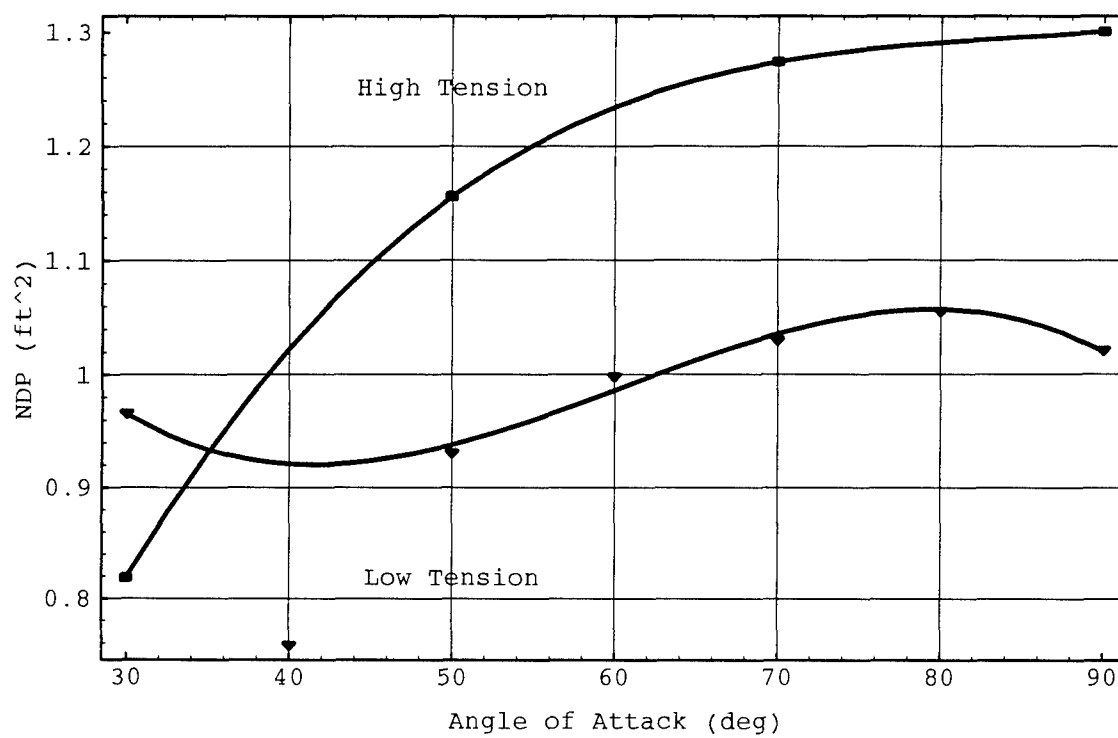


**Figure 25:** Effect of Pre-tension on NDP  
(Test Run at 11 Cylinders/3 Arrays/Low Tow Velocity)



Legend

▼	Low Tension
■	High Tension

**Figure 26:** Effect of Pre-tension on NDP  
(Test Run at 6 Cylinders/2 Arrays/Low Tow Velocity)

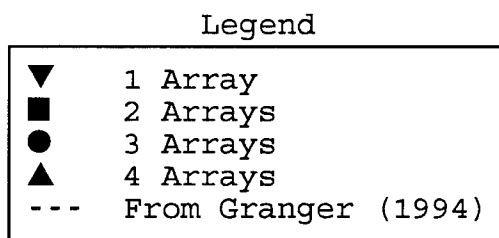
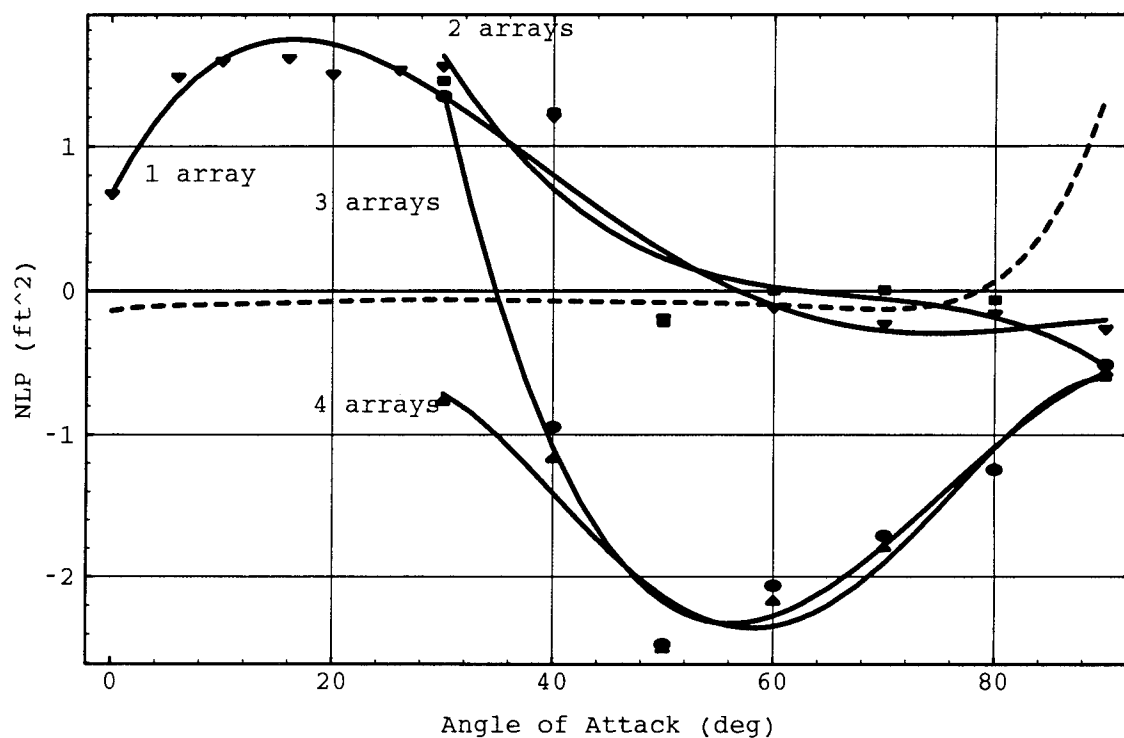
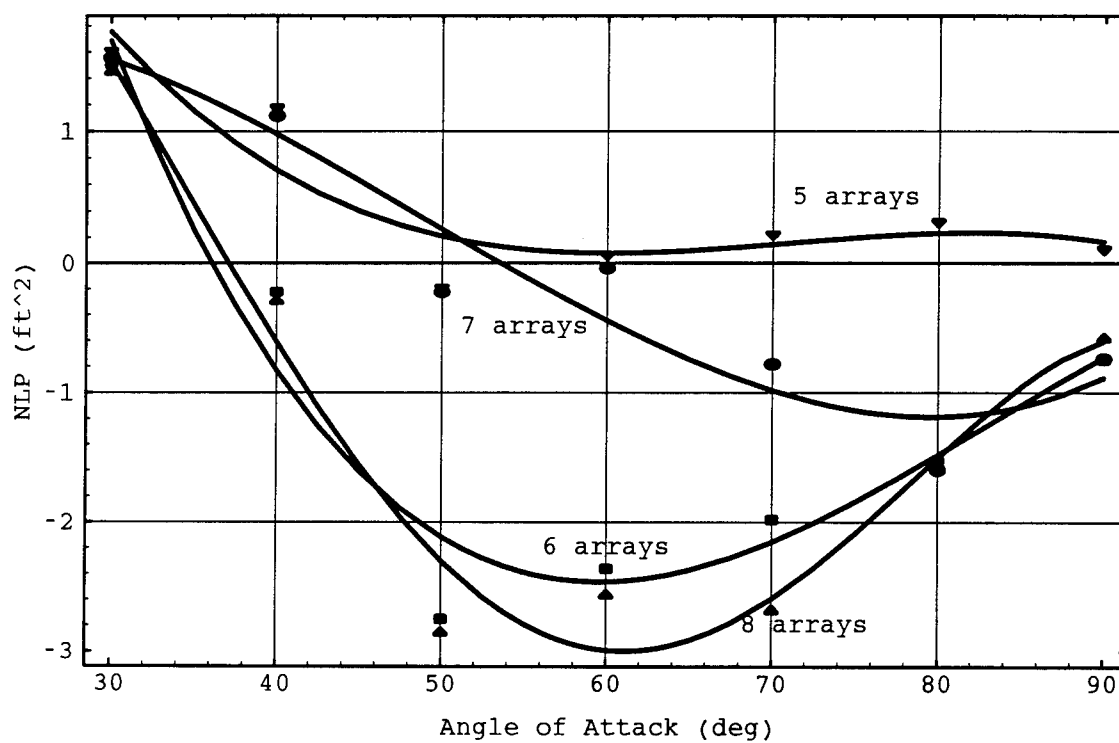


**Figure 27: Effect of Number of Arrays on NLP**  
(Test Run at Low Tow Velocity/11 Cylinders/Low Pre-tension)

positive region up to the  $60^\circ$  case. Similarly, the three and four array curves are comparable to each other, showing that lift drops off as angle-of-attack increases up to specific large angles-of-attack. Figure 28 is a continuation of the setup in Figure 27. Note that the five and seven array conditions seem to coincide at the early angles-of-attack and then begin to diverge at the  $50^\circ$  case. For this case, the seven array condition generates negative lift for a maximum separation of approximately  $1.0 \text{ ft}^2$  NLP at  $90^\circ$ . Note also that the six and eight array curves are also nearly coincident with the exception of a  $0.4 \text{ ft}^2$  separation at  $60^\circ$ . As seen in Figure 29, decreasing the number of cylinders per line from eleven to six alters the effect of the number of arrays on the net's NLP. The one and two array curves are similar until angle-of-attack equals  $72^\circ$ , at which point the two array case's NLP increases sharply to  $2.4 \text{ ft}^2$  as the one array case becomes slightly negative. The four array case is almost identical to the one array case. On the other hand, the three array case is predominantly negative as it falls well beneath the three other curves between  $35^\circ$  and  $80^\circ$ . Note that the upward jump experienced by the NLP for Granger's single line array on Figure 29 at high angles-of-attack is also seen in the NLP for net configurations with two and three lines.

When the number of cylinders per line is reduced to three (see Figure 30), it is the two array case which becomes predominantly negative as the three and four array cases are



## Legend

▼	5 Arrays
■	6 Arrays
●	7 Arrays
▲	8 Arrays

**Figure 28:** Effect of Number of Arrays on NLP  
(Test Run at Low Tow Velocity/11 Cylinders/Low Pre-tension)

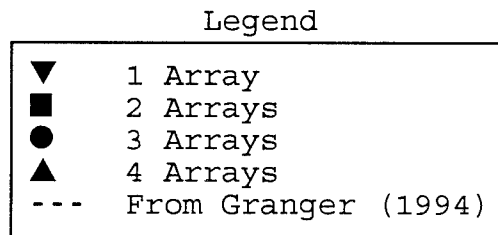
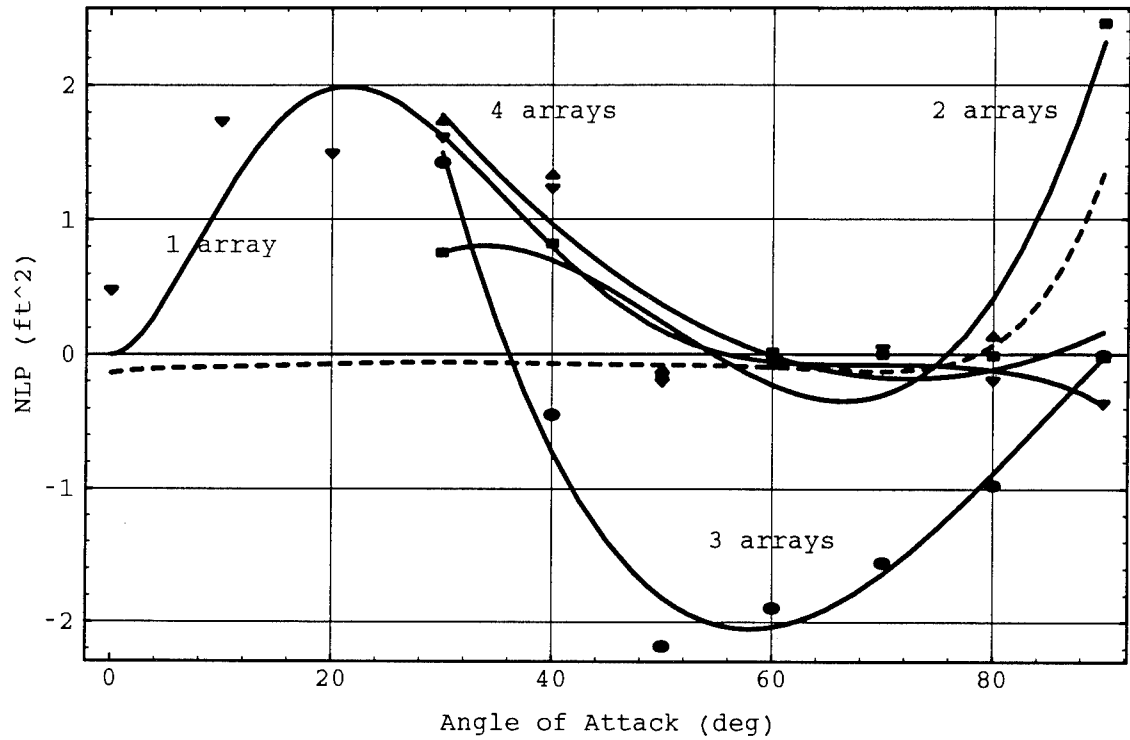


**Figure 29:** Effect of Number of Arrays on NLP  
(Test Run at Low Tow Velocity/6 Cylinders/Low Pre-tension)



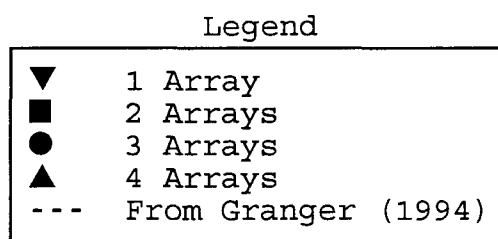
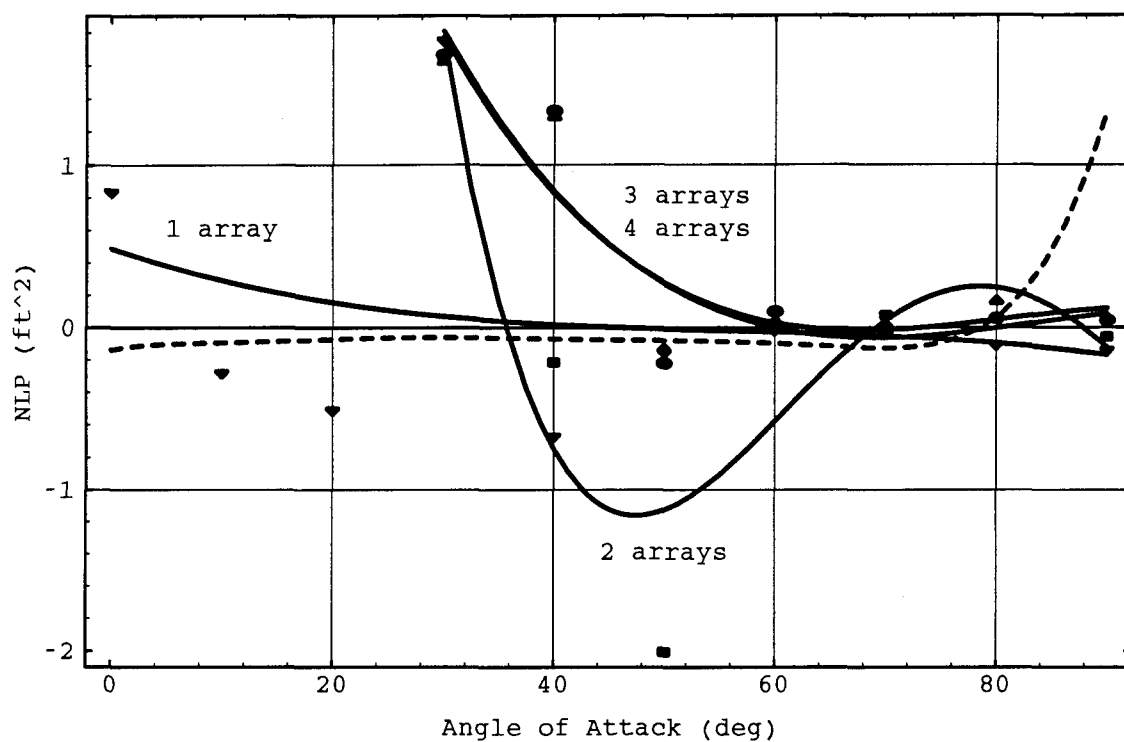


**Figure 30:** Effect of Number of Arrays on NLP  
(Test Run at Low Tow Velocity/3 Cylinders/Low Pre-tension)

nearly alike. Note that NLP for Granger's single array configuration behaves similarly to the present single line array NLP with three cylinders in Figure 30 between  $20^\circ$  and  $80^\circ$ . On the other hand, the one array case generates little to no lift. At high tension (see Figure 31), the effect of the number of arrays on lift is insignificant since all four curves are nearly identical in their behavior.

(c) Effect of Number of Cylinders per Line Array on NLP:

Figure 32 illustrates the effect of the number of cylinders per line on a single array net towed at low speed and at the low tension configuration. Note that the three cylinder per line case has very scattered data points, and the curve fit does not accurately reflect the behavior of the points. The six and eleven cylinder per line nets generate significant lift, reaching maximum lift at  $20^\circ$  and then diminishing after  $60^\circ$ . Figure 33 shows the curves for a two array configuration. The addition of a second array results in a decrease of lift (with the exception of the six cylinder per line case at high angles-of-attack). When a third array is attached to the net, the effect of the number of cylinders per line changes once again. This time, the three cylinder per line net has the greatest lift while the six and eleven cylinder per line net are almost identical, having predominantly negative lift values (see Figure 34). With four arrays per line (see Figure 35), the number of cylinders per line in the net has yet another effect. Lift for the net with

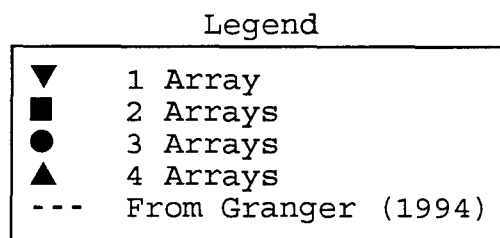
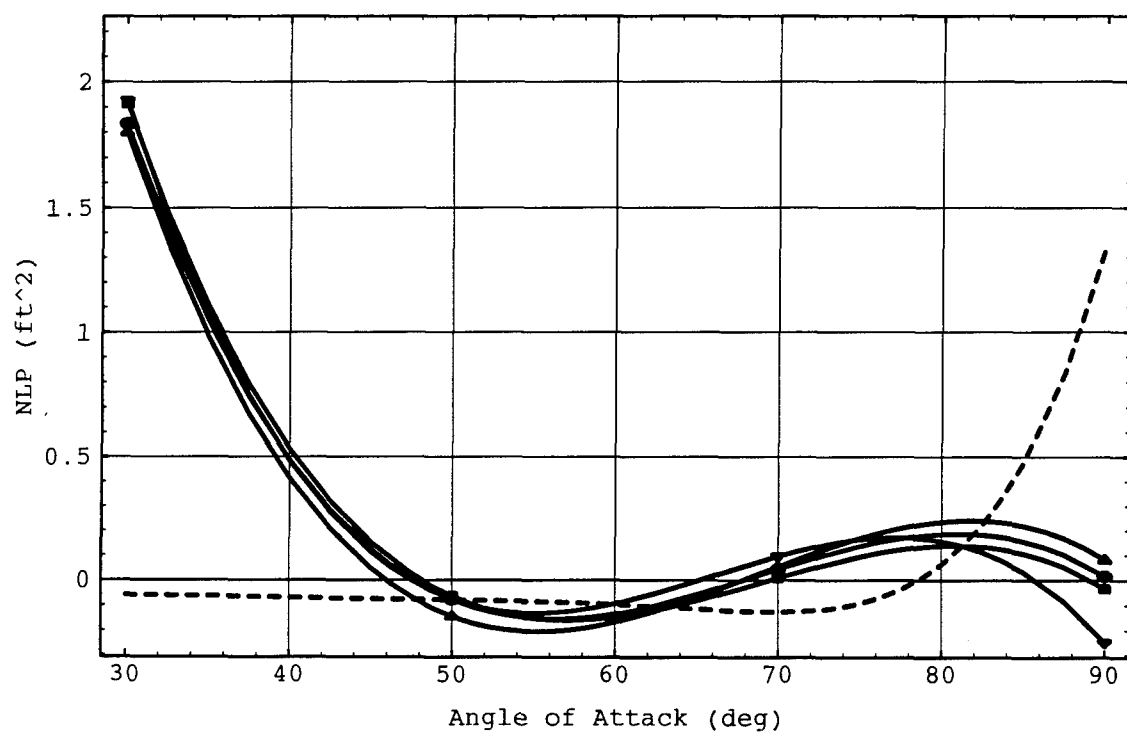


**Figure 31:** Effect of Number of Arrays on NLP  
(Test Run at Low Tow Velocity/6 Cylinders/High Pre-tension)

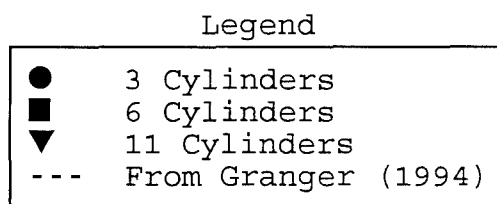
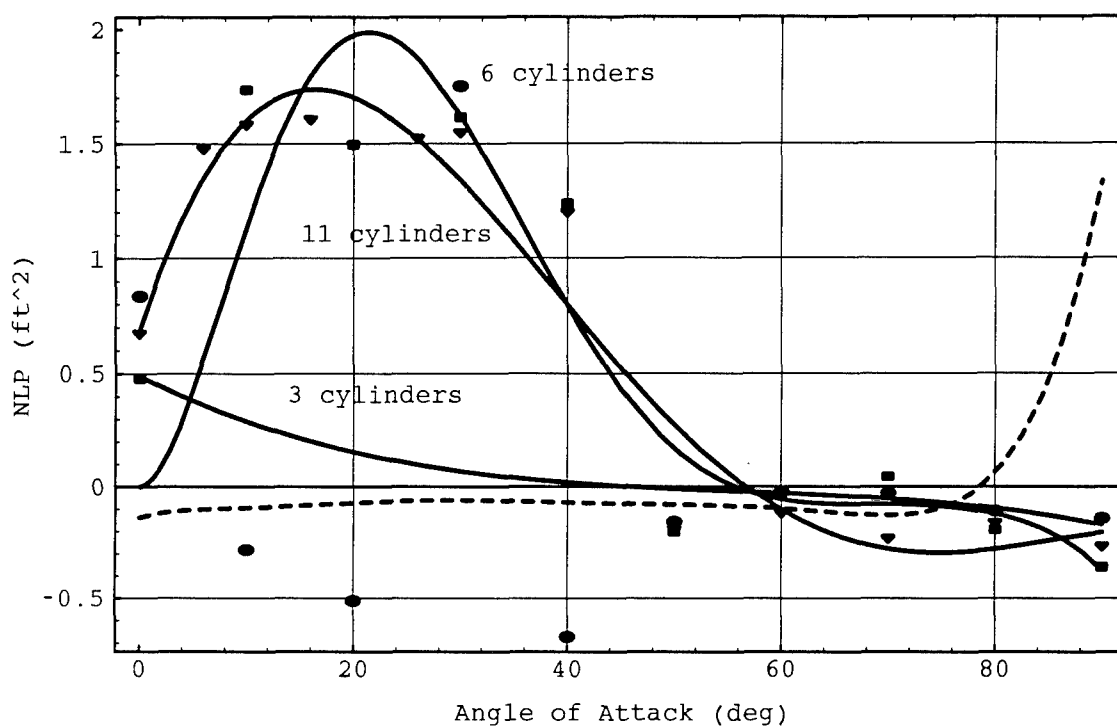
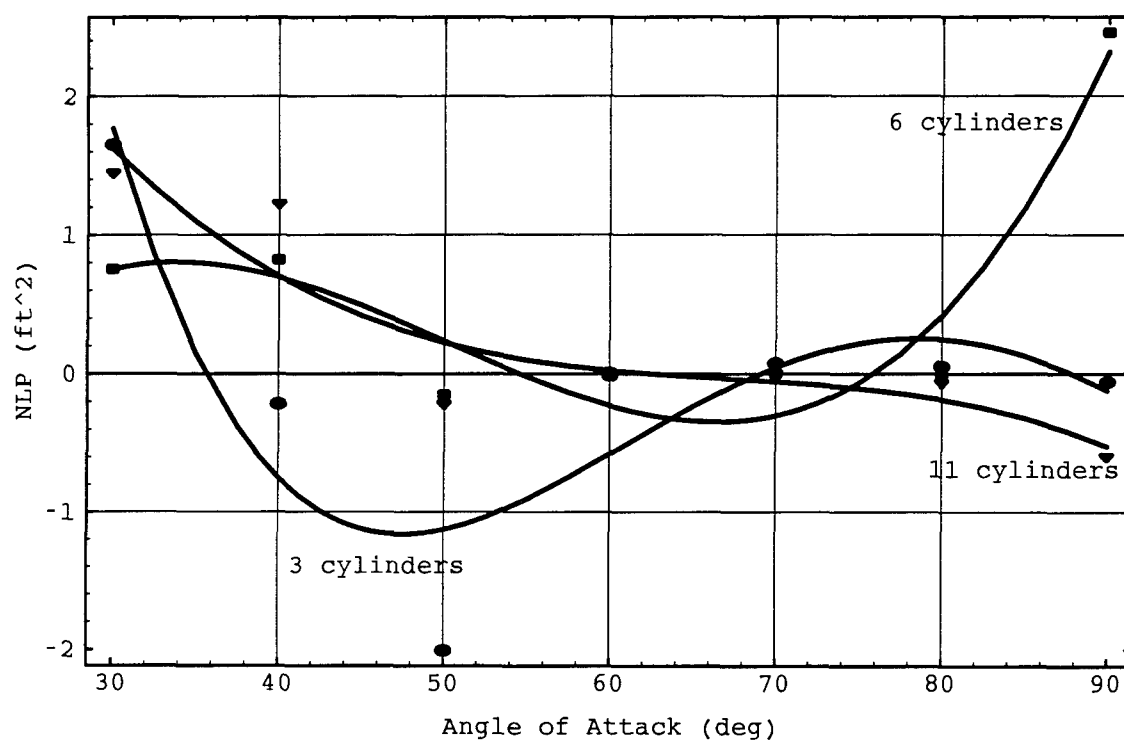


**Figure 32:** Effect of Number of Cylinders on NLP  
(Test Run at Low Tow Velocity/1 Array/Low Pre-tension)



## Legend

- |   |              |
|---|--------------|
| ● | 3 Cylinders  |
| ■ | 6 Cylinders  |
| ▼ | 11 Cylinders |

**Figure 33:** Effect of Number of Cylinders on NLP  
(Test Run at Low Tow Velocity/2 Arrays/Low Pre-tension)

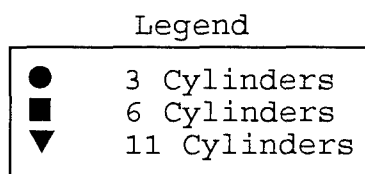
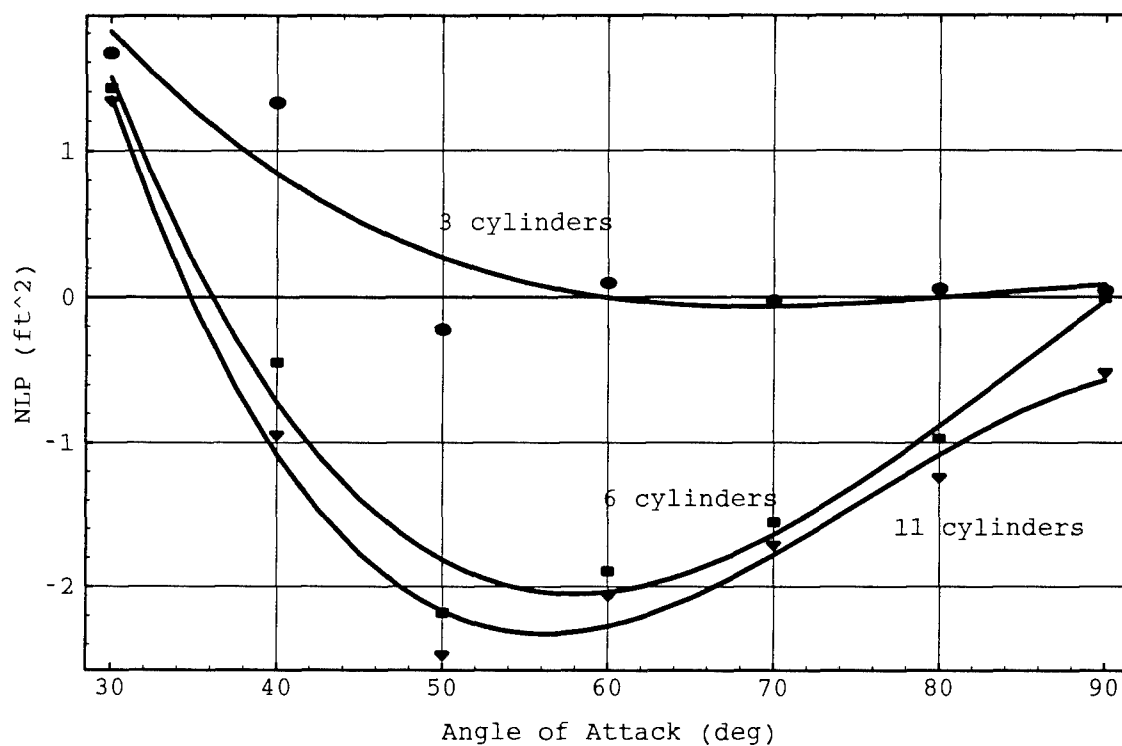
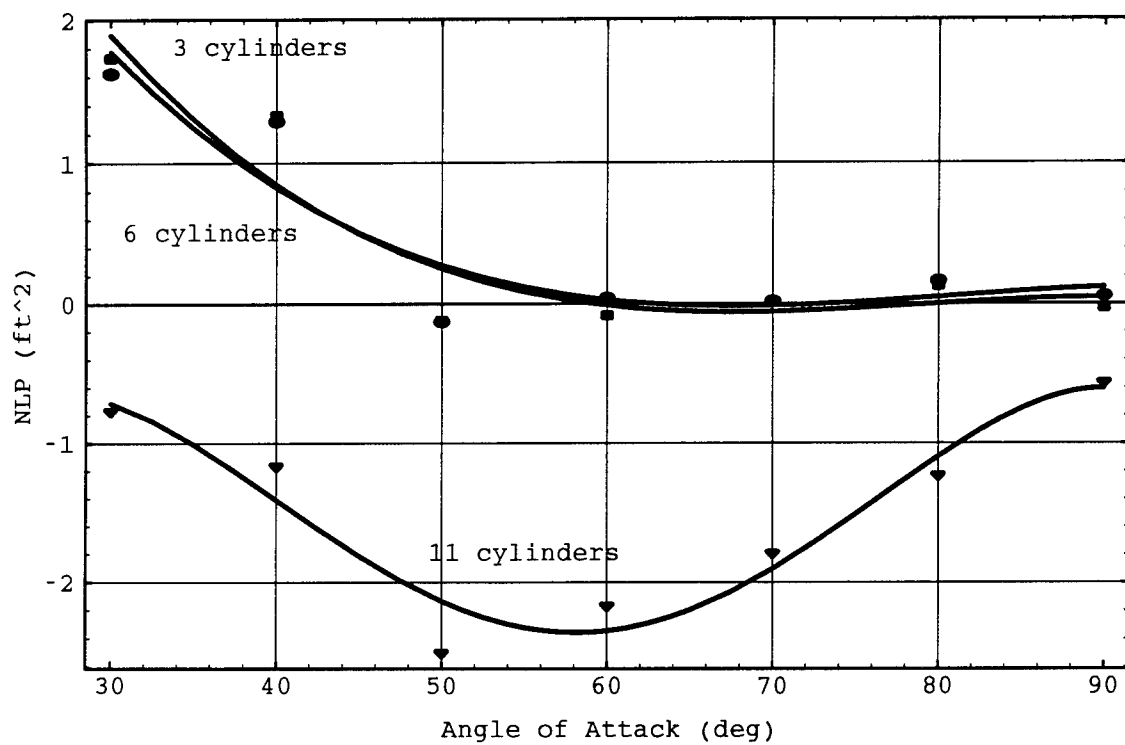


**Figure 34:** Effect of Number of Cylinders on NLP  
(Test Run at Low Tow Velocity/3 Arrays/Low Pre-tension)



## Legend

- |   |              |
|---|--------------|
| ● | 3 Cylinders  |
| ■ | 6 Cylinders  |
| ▼ | 11 Cylinders |

**Figure 35:** Effect of Number of Cylinders on NLP  
(Test Run at Low Tow Velocity/4 Arrays/Low Pre-tension)

eleven cylinders per line is negative for all values of angle-of-attack, while the three and six cylinder per line nets give identical results commencing at approximately  $1.8 \text{ ft}^2$  NLP before dropping to zero lift for angles-of-attack greater than or equal to  $60^\circ$ . High tension curtails the effect of the number of cylinders per line as seen in Figure 36. In summary, the effect of increasing or decreasing the number of cylinders plays no role in the behavior of lift.

(d) Effect of Tow Velocity on NLP: In general, the low velocity curves for NLP show a greater variation and range of lift than the high velocity cases. Figure 37 illustrates the characteristic behavior of both curves: the low velocity case has the greater lift at early angles-of-attack ( $0^\circ$  to  $59^\circ$ ). Peaking within these early angles ( $16^\circ$ ), it drops below the high velocity lift at a midrange angle-of-attack ( $59^\circ$ ) and hovers around or just beneath zero lift thereafter. Note that in Figure 37, NLP for Granger's five knot case starts at low angles-of-attack slightly above the three knot case before dropping under the three knot case at the  $50^\circ$  angle-of-attack.

A notable exception from the general trend occurs in Figure 38: instead of remaining at the low NLP condition at high angles-of-attack, both the low and high velocity NLP curves jump suddenly at approximately  $70^\circ$ . The low velocity NLP rises from  $-0.3 \text{ ft}^2$  to  $2.4 \text{ ft}^2$  in  $20^\circ$ , and the high velocity NLP grows from  $0.1 \text{ ft}^2$  to  $1.1 \text{ ft}^2$ .



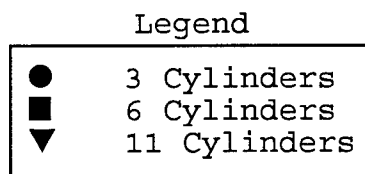
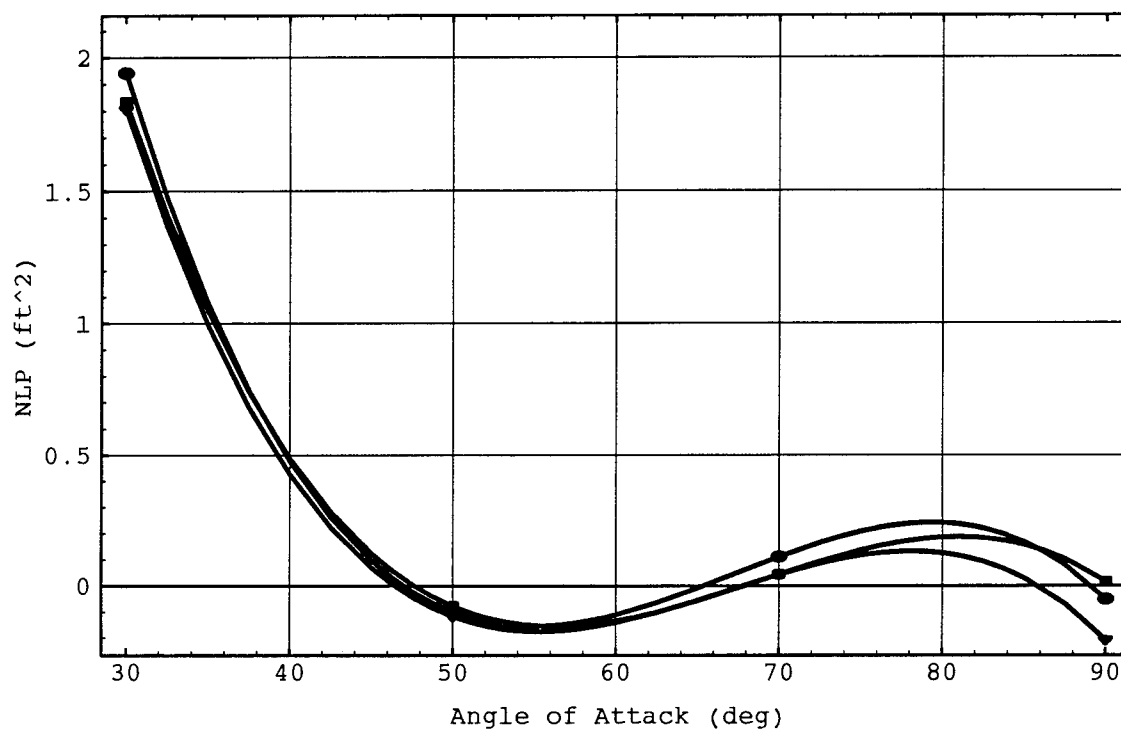
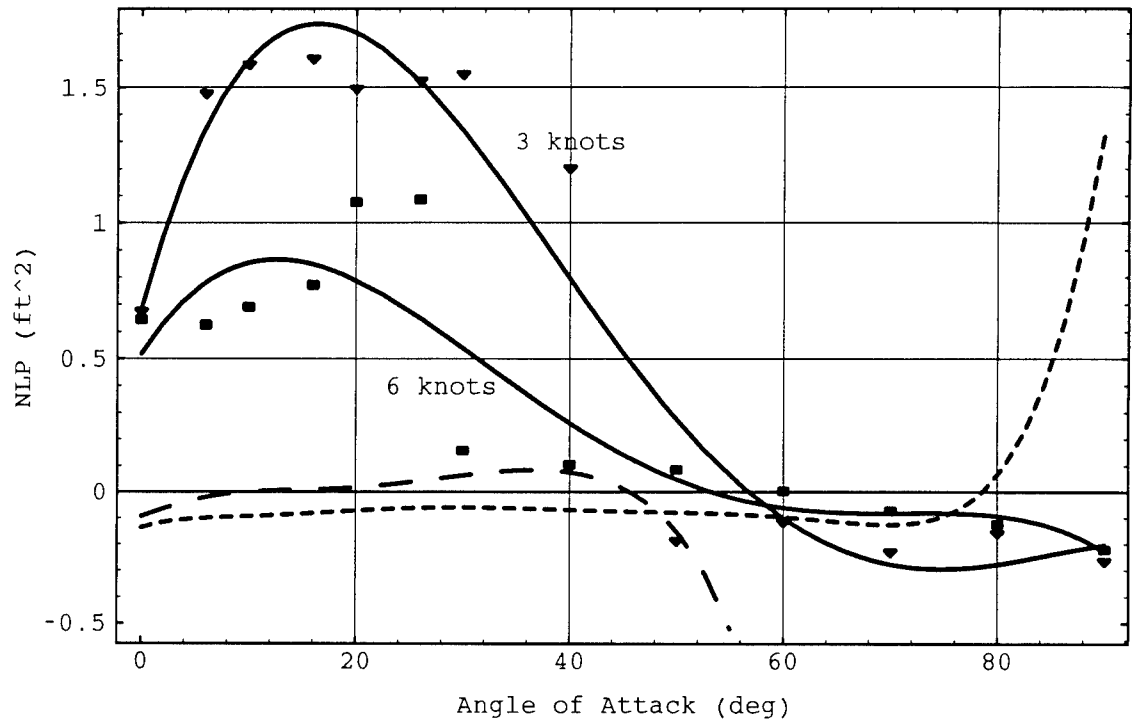


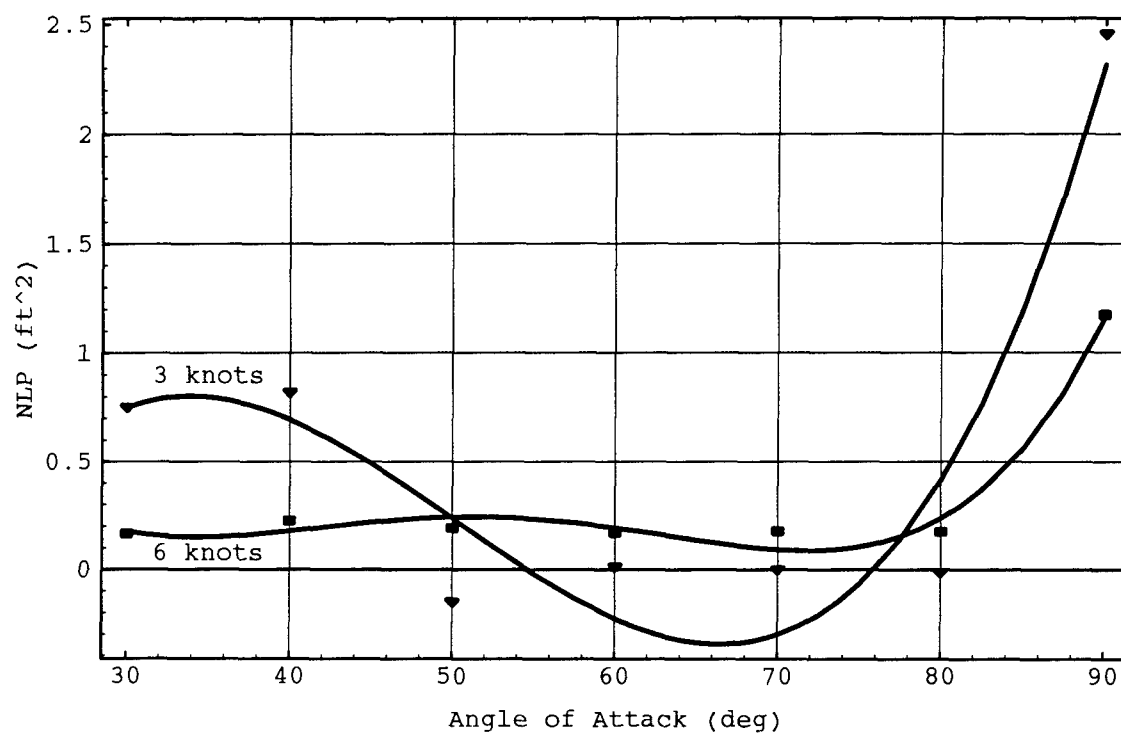
**Figure 36:** Effect of Number of Cylinders on NLP  
(Test Run at Low Tow Velocity/3 Arrays/High Pre-tension)



Legend

▼	3 Knots
■	6 Knots
---	From Granger (1994), 3 Knots
---	From Granger (1994), 5 Knots

**Figure 37:** Effect of Tow Velocity on NLP  
(Test Run at 11 Cylinders/1 Array/Low Pre-tension)



## Legend

▼	3 Knots
■	6 Knots

**Figure 38:** Effect of Tow Velocity on NLP  
(Test Run at 6 Cylinders/2 Arrays/Low Pre-tension)

(e) Effect of Pre-Tension on NLP: In general, the pre-tension does not significantly affect the NLP in the array. This conclusion was also reported earlier by Granger (1994). Figure 39 is representative of the effect that pre-tension has on NLP.

The only instance that pre-tension does make a difference is when there are a high number of cylinders per line combined with a high number of arrays. Figure 40 shows the results for an eleven cylinder per line, three array configuration. Note that the low tension net generates considerably less lift than the high tension net. This is especially evident between  $40^\circ$  and  $80^\circ$ . The addition of one more array increases the differences between the two NLP curves at small angles-of-attack as well as in the midrange angles (see Figure 41). Referring to the one array case with only six cylinders per line gives the result as shown in Figure 42. Note that this compares to the one array case with eleven cylinders per line. Similar trends occur for the rest of the six cylinder per line family of curves except for the four array case (see Figure 43). Likewise, the low and high tension curves for the one array, three cylinder per line case seen in Figure 44 are separated by a difference of almost  $1.9 \text{ ft}^2$  at the  $30^\circ$  angle-of-attack, which is a rather excessive difference. Note that the data looks questionable at the  $30^\circ$  angle-of-attack. The last plot of significance in this section is Figure 45. Although the low and high tension curves are very similar for

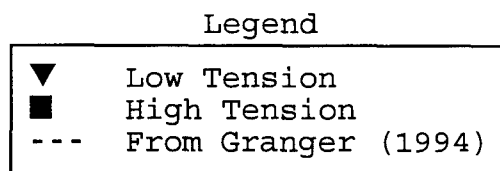
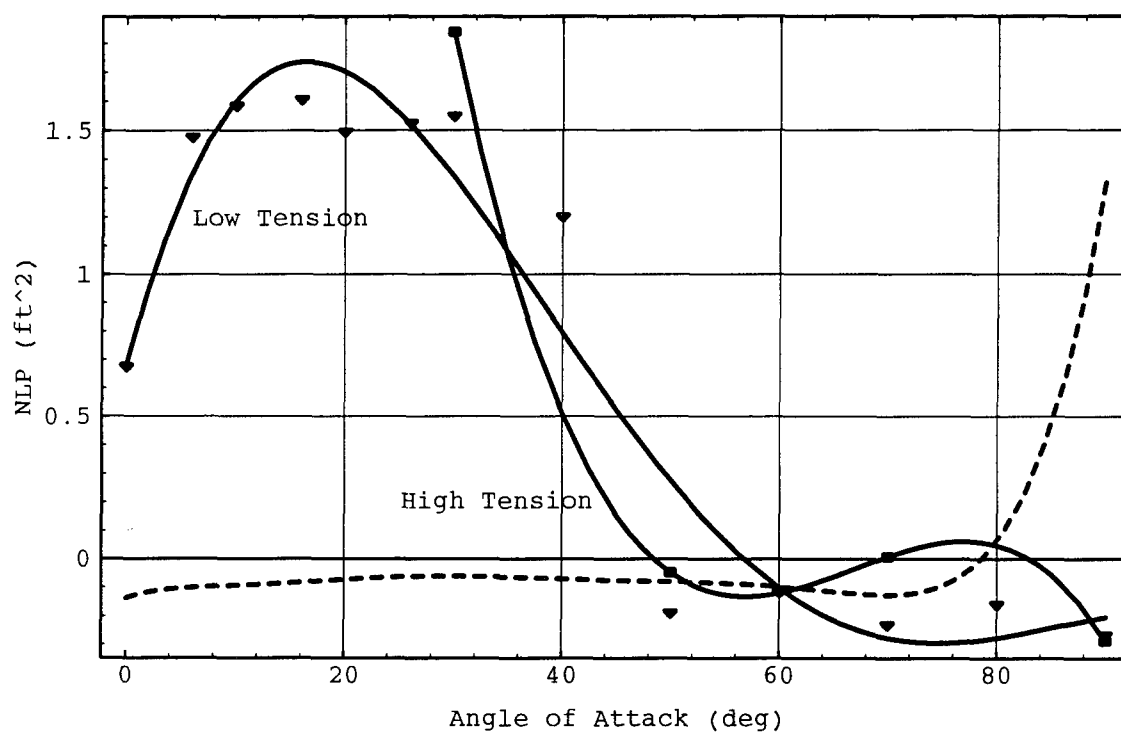


**Figure 39:** Effect of Pre-tension on NLP  
(Test Run at 11 Cylinders/1 Array/Low Tow Velocity)

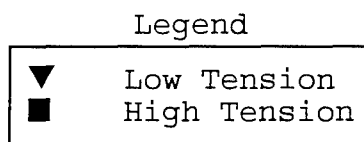
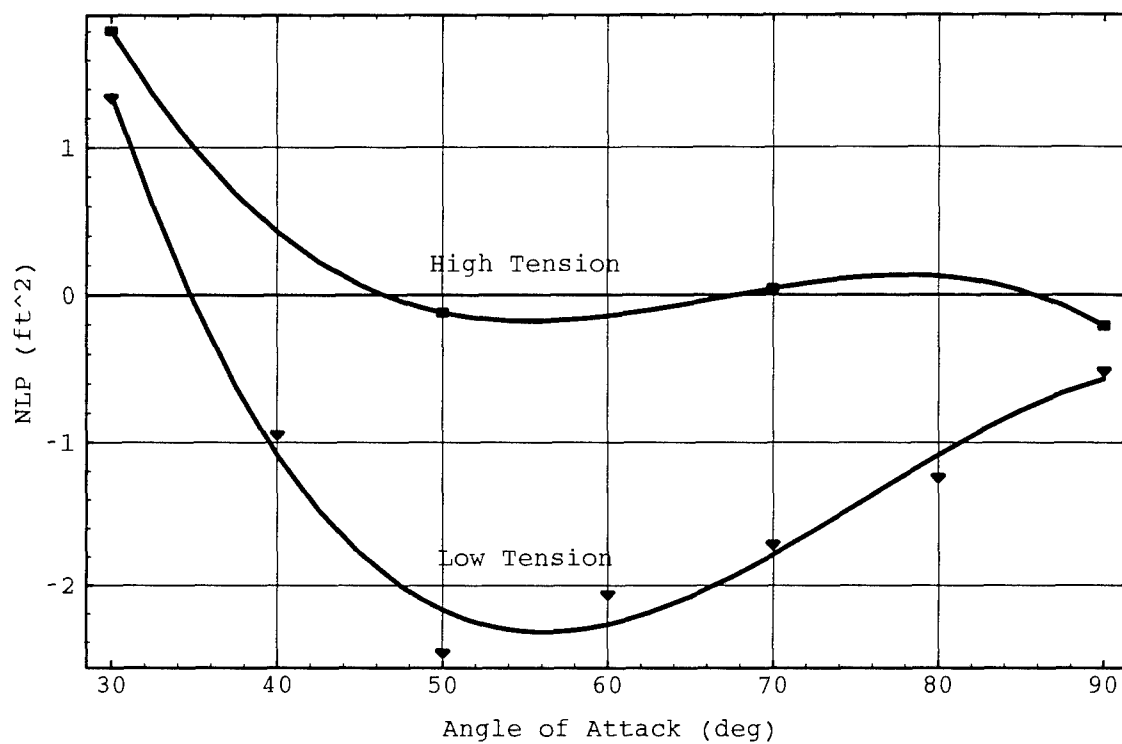
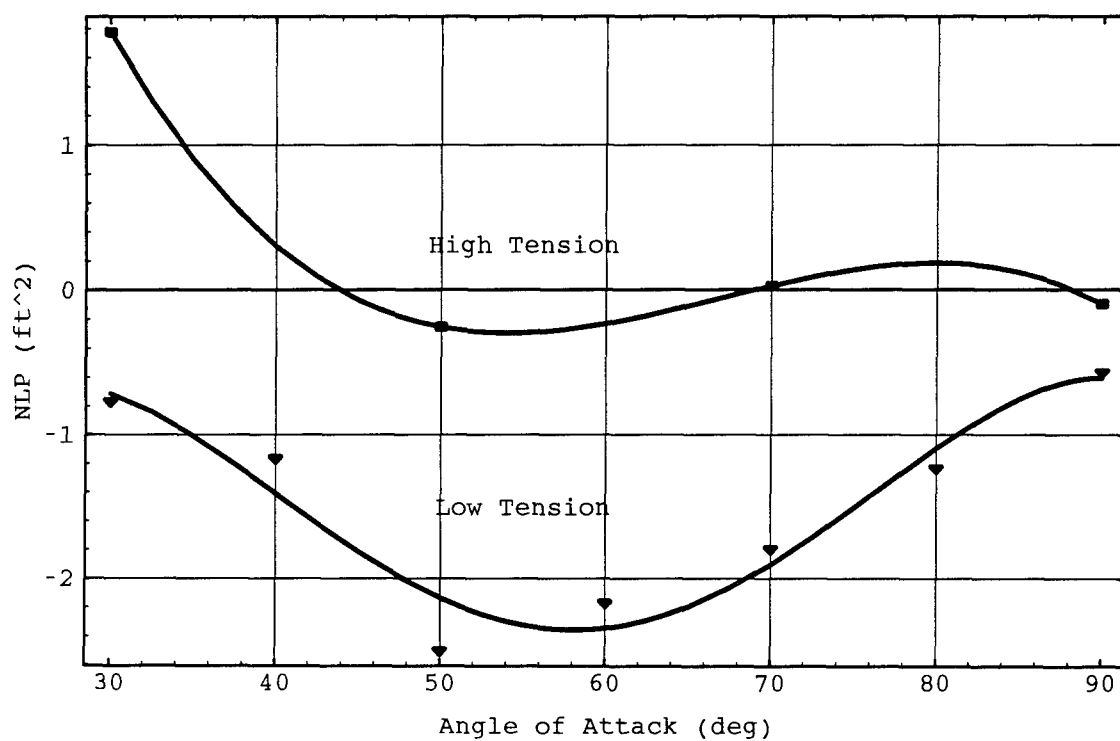


**Figure 40:** Effect of Pre-tension on NLP  
(Test Run at 11 Cylinders/3 Arrays/Low Tow Velocity)



Legend

- |   |              |
|---|--------------|
| ▼ | Low Tension  |
| ■ | High Tension |

**Figure 41:** Effect of Pre-tension on NLP  
(Test Run at 11 Cylinders/4 Arrays/Low Tow Velocity)

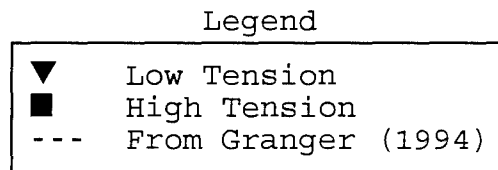
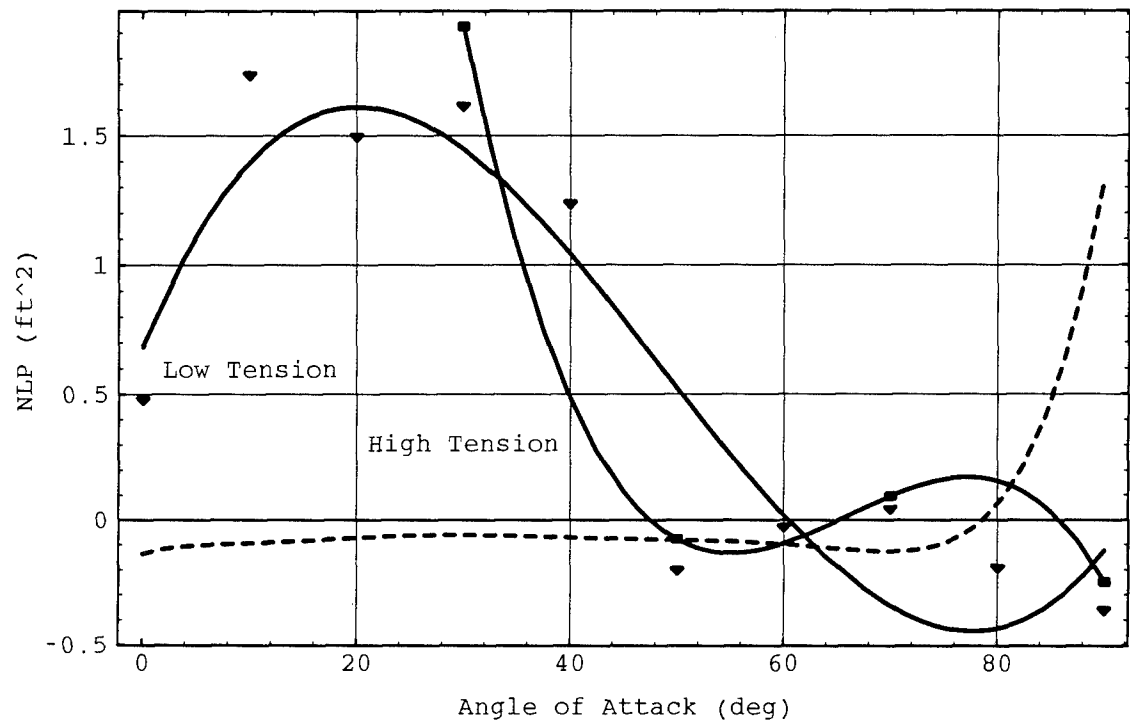
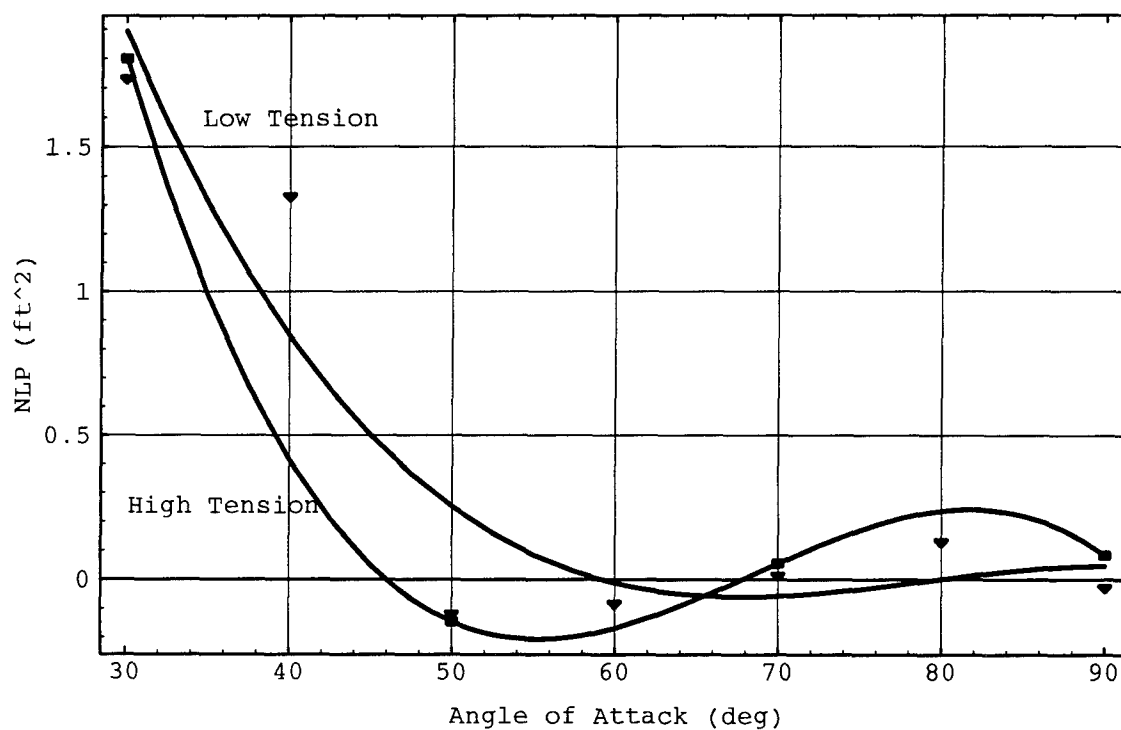


**Figure 42:** Effect of Pre-tension on NLP  
(Test Run at 6 Cylinders/1 Array/Low Tow Velocity)





## Legend

▼	Low Tension
■	High Tension

**Figure 43:** Effect of Pre-tension on NLP  
(Test Run at 6 Cylinders/4 Arrays/Low Tow Velocity)

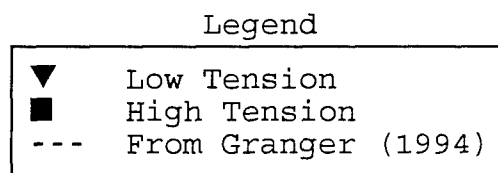
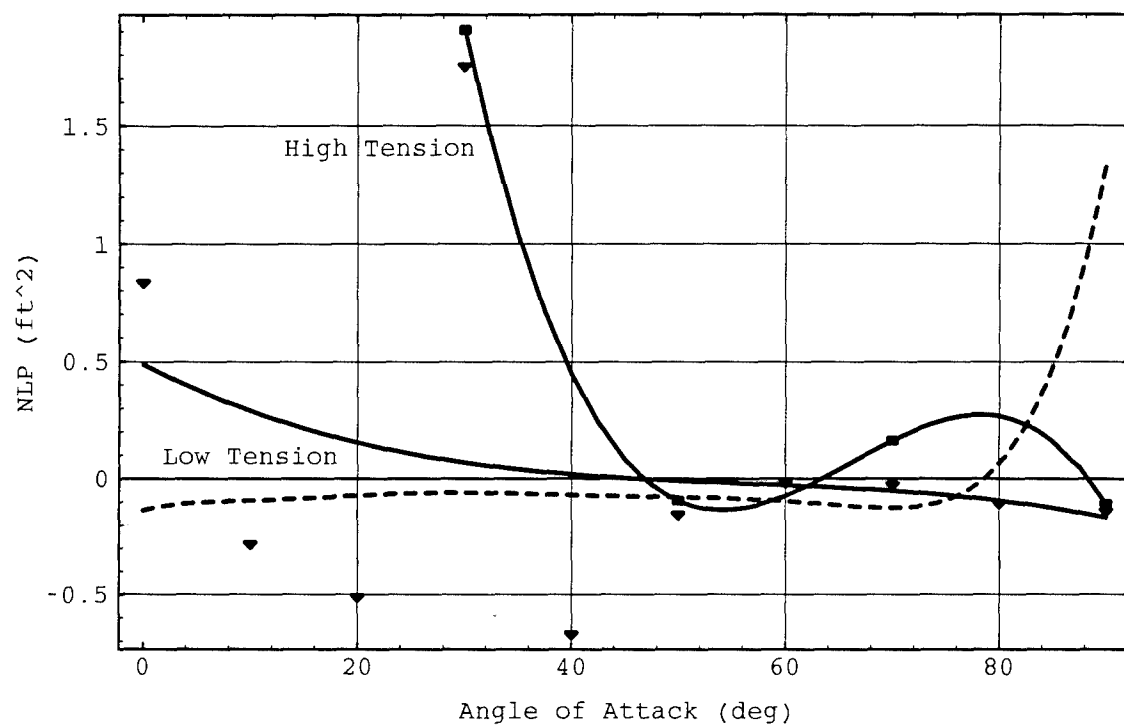


**Figure 44:** Effect of Pre-tension on NLP  
(Test Run at 3 Cylinders/1 Array/Low Tow Velocity)

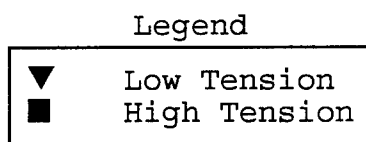
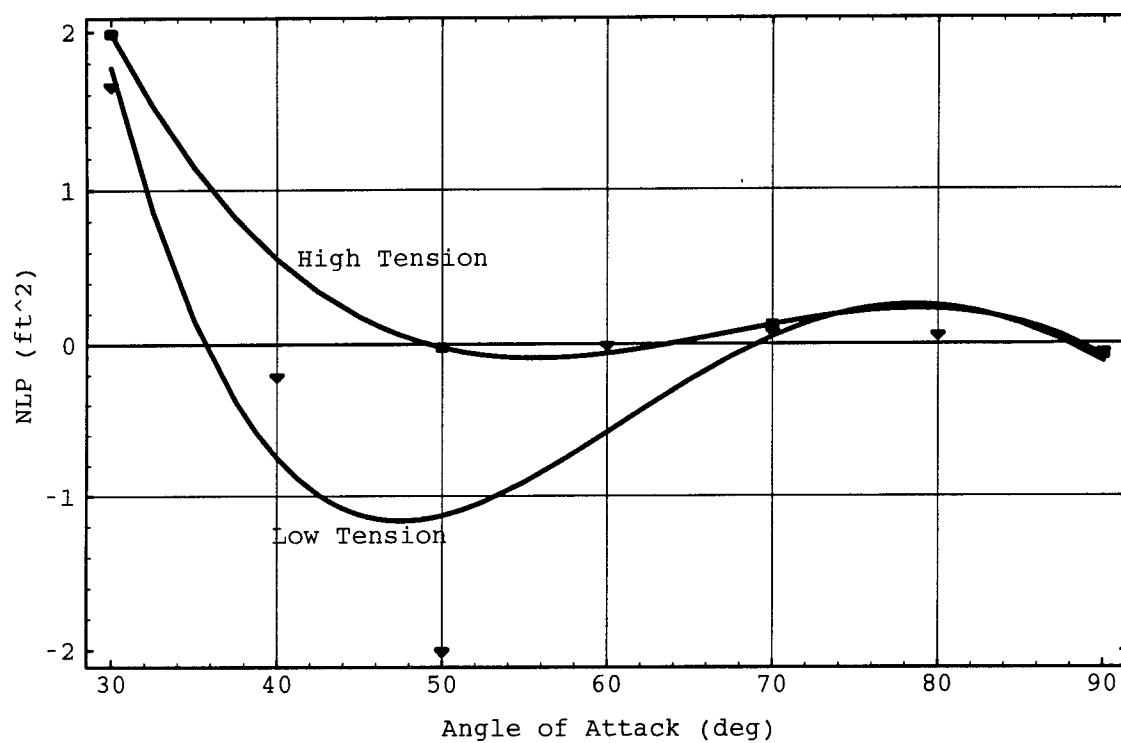


**Figure 45:** Effect of Pre-tension on NLP  
(Test Run at 3 Cylinders/2 Arrays/Low Tow Velocity)

angles-of-attack greater than  $70^\circ$ , there is a substantial difference between  $30^\circ$  and  $70^\circ$ , with as much as a  $1.1 \text{ ft}^2$  difference at approximately  $45^\circ$ . Again, this is considered rather excessive.

## 5. A Resume of the Findings

(i) Generally, drag acting on the towed net array increased nonlinearly with increasing angle-of-attack. The drag curve had a fairly constant positive slope up to an angle-of-attack of approximately  $60^\circ$ . At greater angles-of-attack, however, slope began to decrease, either leveling out at zero slope or becoming slightly negative.

(ii) The addition of line arrays to the towed net increased the drag significantly. In general, the magnitude of the increase depended on the number of cylinders present on the added line array. With the addition of a line with eleven cylinders, NDP increased by approximately  $0.6 \text{ ft}^2$ . With the addition of a line with six cylinders, NDP increased by approximately  $0.5 \text{ ft}^2$ . With the addition of a line with three cylinders, NDP increased by approximately  $0.4 \text{ ft}^2$ .

(iii) Increasing the number of cylinders per line array in the towed net raised the amount of drag that it produced. In general, the magnitude of increase in drag depended largely on the number of arrays present. With nets containing one or two arrays, changing from three to six cylinders per line increased NDP by  $0.2 \text{ ft}^2$ , and changing from six to eleven cylinders per line increased NDP by  $0.4 \text{ ft}^2$ . With nets containing three or four arrays, changing from three to six cylinders per line increased NDP by  $0.4 \text{ ft}^2$ , and changing from six to eleven cylinders per line increased NDP by  $0.6 \text{ ft}^2$ .

(iv) For net configurations containing a low number of line arrays, tow velocity did not have a significant impact on drag. However, as more line arrays were attached to the net, the low velocity runs developed greater drag between  $50^\circ$  and  $80^\circ$  relative to the high velocity runs for the same net configuration.

(v) Applying higher pre-tension loads to the leading line array for the towed net increased the drag.

(vi) Generally, lift acting on the towed net was low at small angles-of-attack and increased with a positive slope to peak around the  $20^\circ$  angle-of-attack. At the  $20^\circ$  angle-of-attack, the NLP curve's slope became negative, and NLP decreased in a linear manner to the  $60^\circ$  angle-of-attack. The NLP curve's slope then approached zero with increasing angle-of-attack, causing NLP to settle out near zero lift at high angles-of-attack. Significant deviation from this trend occurred at high angles-of-attack for nets with a lower number of cylinders per line and a lower number of arrays.

(vii) In general, the one and two array nets had comparable lift curves, as did the three and four array nets. This suggests a "group" effect of line arrays with regard to the lift acting on the net.

(viii) The effect of the number of cylinders per line array on lift is highly dependent on the number of arrays in the towed configuration.

(ix) The NLP values for the low velocity runs seem more erratic and unpredictable than the high velocity runs, especially when there are fewer line arrays and fewer cylinders per line array.

(x) Pre-tension of the leading array only affects the lift characteristics when there are a high number of cylinders per line array and a high number of arrays. In these cases, the low tension array generates less lift than the high tension array. In addition, high pre-tension reduces the effect that the number of cylinders per line array and the number of line arrays have on lift.

Taken as a whole, these conclusions make a general statement about the net array's stability. Variations from the general trends observed in the net's behavior occurred when the net's geometric dimensions were reduced (lower number of arrays, fewer cylinders per line, lower velocity, and lower pre-tension). This conclusion is supported by the video images of the test runs recorded by Ahn (1995). The video reveals that vertical oscillation of the individual lines and cylinders in the net array was present to some degree in all test runs. Furthermore, the video reveals that the magnitude and frequency of these oscillations were reduced in nets containing a low number of cylinders per line array or a high number of line arrays. However, in some cases, having a high number of line arrays also contributed to the net's instability during the test runs. This is evidenced by the

chaotic out-of-phase oscillation between consecutive line arrays in some of the multi-line net configurations.

It is the opinion of the author that the unstable and unpredictable behavior of a towed net array makes it unsuitable for military application, posing potential safety risks and producing unreliable deployment configurations. An exploratory investigation was done to examine a more stable method for deploying the cylindrical charges to destroy mines in the surf zone, and is outlined in Appendix C.



## 6. References

Granger, Robert A. "An Experimental Investigation of a Line Array of Charges Descending and Being Towed." USNA Contract No. N6133193WR32030, 1993.

Granger, Robert A. "Towing Basin Tests of a Line Charge Final Report." USNA Contract No. N0002494WR70145, 1994.

Munson, Bruce R., Donald F. Young, Theodore H. Okiishi. Fundamentals of Fluid Mechanics. New York: John Wiley and Sons, Inc., 1994.

Ahn, So Won Silas, "Towed Net Array" (Videotape). USNA ERC Library Catalog No. 953267, 1995.

Truver, Scott C. "Exploding the Mine Warfare Myth." Proceedings of the U.S. Naval Institute, Volume 120/10/1,100, October, 1994.

## Appendix A: Experimental Results and Method

Table A.1 is a representative portion of the pre-test matrix which served as a guideline for the order in which the test runs were conducted. As stated in the body of the report, not all of the pre-test matrix runs were performed. This was due to one of two reasons. First, the maximum moment that each streamlined strut could withstand was 2000 ft-lbf. Since each strut was four feet in length, the maximum force limitation was 500 lbs. Second, tow tank use for this experiment was limited to just under three weeks. Thus, the pre-test matrix was abbreviated in order to run as many different net configurations as possible. The first six columns in Table A.1 identify the towed net configuration for each individual run. The last four columns were filled in after obtaining and correcting the force data from the two struts with the tare readings and pre-tension values.

Table A.2 contains the test data obtained from the experiment. Note that there are 31 groups of data, each of which are labeled by a two digit number in the upper left corner of each block. This two digit number is called the Test Set Number, and designates all the test runs performed for a particular towed net configuration. The first three columns identify the tow configuration for each individual run, and the next four columns list the force data obtained from the experiment. The two "Pre-Tension" columns show the

tension force reading from each of the two struts. Finally, the last two columns represent the calculated NDP and NLP for each individual run.

Table A.1: Portion of the Pre-test Matrix

Test Number	Number of Arrays	Cylinder Spacing (inches)	Line Tension (lbs)	Tow Speed (knots)	Angle of Attack (deg)	X1 (lbf)	X2 (lbf)	Y1 (lbf)	Y2 (lbf)
1	1	12	75	3	0				
2	1	12	75	6	0				
3	1	12	75	3	5				
4	1	12	75	6	5				
5	1	12	75	3	10				
6	1	12	75	6	10				
7	1	12	75	3	15				
8	1	12	75	6	15				
9	1	12	75	3	20				
10	1	12	75	6	20				
11	1	12	75	3	25				
12	1	12	75	6	25				
13	1	12	75	3	30				
14	1	12	75	6	30				
15	1	12	75	3	40				
16	1	12	75	6	40				
17	1	12	75	3	50				
18	1	12	75	6	50				
19	1	12	75	3	60				
20	1	12	75	6	60				
21	1	12	75	3	70				

Table A.1: Portion of the Pre-test Matrix (continued)

Test Number	Number of Arrays	Cylinder Spacing (inches)	Line Tension (lbs)	Tow Speed (knots)	Angle of Attack (deg)	X1 (lbf)	X2 (lbf)	Y1 (lbf)	Y2 (lbf)
22	1	12	75	6	70				
23	1	12	75	3	80				
24	1	12	75	6	80				
25	1	12	75	3	90				
26	1	12	75	6	90				
27	2	12	75	3	0				
28	2	12	75	6	0				
29	2	12	75	3	5				
30	2	12	75	6	5				
31	2	12	75	3	10				
32	2	12	75	6	10				
33	2	12	75	3	15				
34	2	12	75	6	15				
35	2	12	75	3	20				
36	2	12	75	6	20				
37	2	12	75	3	25				
38	2	12	75	6	25				
39	2	12	75	3	30				

Table A.2: Experimental Data

00: Tare Tests									
Test Number	Tow Speed (ft/sec)	Angle of Attack (deg)	X1 (lbs)	X2 (lbs)	Y1 (lbs)	Y2 (lbs)			
T1	5.04	0	6.56	9.58	15.21	-3.78			
T2	10.07	0	29.71	36.10	-100.40	-20.94			
T3	5.04	6	9.12	9.91	-30.20	-7.01			
T4	10.07	6	17.39	31.76	-87.06	-33.01			
T5	5.04	10	8.18	9.79	-36.06	-6.71			
T6	10.07	10	12.71	29.61	-98.45	-29.54			
T7	5.04	12	7.17	9.19	-36.06	-6.98			
T8	10.08	12	12.43	29.61	-80.26	-30.16			
T8R	5.04	16	2.42	9.26	-26.62	-5.83			
T9R	10.08	16	4.25	23.12	-89.61	-46.87			
T9	5.04	20	-3.24	9.36	-40.53	-5.57			
T10	10.08	20	-13.42	15.54	-136.89	-50.15			
T11	5.04	26	-2.98	4.96	-28.27	-12.86			
T12	10.08	26	-27.91	17.64	-137.73	-40.78			
T13	5.04	30	-4.83	7.40	-40.38	-8.21			
T14	10.07	30	45.52	15.94	36.62	-39.59			
T15	5.04	40	12.20	6.43	-38.24	-9.78			
T16	10.08	40	55.35	6.88	30.30	-46.13			
T17	5.04	50	42.67	4.93	22.82	-10.19			

Table A.2: Experimental Data (continued)

00: Tare Tests (continued)									
Test Number	Tow Speed (ft/sec)	Angle of Attack (deg)	X1 (lbs)	X2 (lbs)	Y1 (lbs)	Y2 (lbs)			
T18	10.08	50	59.07	-3.21	18.90	-48.86			
T19	5.04	60	37.47	1.18	11.66	-11.55			
T20	10.08	60	52.26	-12.09	2.88	-45.79			
T21	5.04	70	35.37	0.02	4.04	-10.73			
T22	10.08	70	44.70	-22.73	-8.51	-42.01			
T23	5.04	80	26.45	-2.20	-2.09	-10.31			
T24	10.08	80	27.88	-29.83	-17.97	-36.85			
T25	5.04	90	13.64	-4.66	-7.38	-9.78			
T26	10.08	90	5.90	-37.14	-22.95	-30.58			

01: One Array, Low Tension, 11 Cylinders per Line									
Test Number	Tow Speed (ft/sec)	Angle of Attack (deg)	X1 Gauge (lbs)	X2 Gauge (lbs)	Y1 Gauge (lbs)	Y2 Gauge (lbs)	X1 Pre Tension (lbs)	X2 Pre Tension (lbs)	NLP (ft^2)
1	5.04	0	89.40	-57.45	49.33	-4.68	75.32	-69.54	0.2037
2	10.08	0	108.44	-33.76	23.05	-17.34	75.62	-70.00	0.0165
3	5.04	6	92.33	-57.06	42.40	-7.63	75.92	-70.47	0.0651
									1.4771

Table A.2: Experimental Data (continued)

01: One Array, Low Tension, 11 Cylinders per Line (continued)																
Test Number	Tow Speed (ft/sec)	Angle of Attack (deg)	X1 Gauge (lbs)		X2 Gauge (lbs)		Y1 Gauge (lbs)		Y2 Gauge (lbs)		X1 Pre Tension (lbs)		X2 Pre Tension (lbs)		NDP (ft^2)	NLP (ft^2)
4	10.08	6	118.77	-38.69	33.58	-32.46	75.70	-70.13	0.0638	0.6255						
5	5.04	10	94.76	-56.10	41.29	-7.54	75.97	-70.52	0.0350	1.5845						
6	10.07	10	134.39	-41.34	43.01	-40.94	75.46	-69.91	0.1115	0.6917						
7	5.04	16	106.14	-56.22	50.88	-10.44	74.53	-68.89	0.2284	1.6058						
8	10.07	16	165.21	-51.76	55.84	-57.55	75.87	-70.39	0.2052	0.7723						
9	5.04	20	107.52	-59.50	32.01	-13.02	74.38	-68.80	0.2411	1.4948						
10	10.07	20	192.36	-69.02	68.55	-72.71	75.02	-69.37	0.2343	1.0756						
11	5.04	26	122.89	-62.84	33.55	-16.90	74.64	-69.25	0.4473	1.5240						
12	10.07	26	226.56	-82.50	69.68	-83.58	75.02	-69.55	0.3136	1.0849						
13	5.04	30	127.20	-66.03	27.13	-18.41	74.65	-69.24	0.3536	1.5484						
14	10.07	30	245.83	-89.63	62.07	-81.00	75.48	-69.97	0.4338	0.1567						
15	5.04	40	145.35	-78.37	16.72	-23.72	76.55	-71.20	0.1335	1.1998						
16	10.07	40	281.67	-114.52	31.18	-104.39	76.13	-71.10	0.5770	0.1031						
17	5.04	50	158.18	-88.49	5.35	-27.64	76.75	-71.89	0.7684	-0.1878						
18	10.07	50	306.65	-145.49	-2.93	-120.98	76.93	-71.99	0.6945	0.0839						
19	5.04	60	159.32	-99.58	-7.26	-31.99	78.30	-73.32	0.8560	-0.1164						
20	10.07	60	295.01	-168.76	-52.27	-130.28	77.98	-73.20	0.8222	0.0030						
21	5.04	70	154.54	-109.64	-21.04	-32.20	80.21	-75.60	0.9226	-0.2299						
22	10.07	70	267.28	-192.76	-90.92	-133.02	79.78	-75.06	0.9125	-0.0731						



Table A.2: Experimental Data (continued)

01: One Array, Low Tension, 11 Cylinders per Line (continued)														
Test Number	Tow Speed (ft/sec)	Angle of Attack (deg)	X1		X2		Y1		Y2		X1 Pre Tension (lbs)	X2 Pre Tension (lbs)	NDP (ft^2)	NLP (ft^2)
			Gauge (lbs)	(lbs)	Gauge (lbs)	(lbs)	Gauge (lbs)	(lbs)	Gauge (lbs)	(lbs)				
23	5.04	80	155.23		-125.57		-30.40		-36.35		102.30	-98.53	1.0931	-0.1589
24	10.07	80	232.46		-219.77		-113.87		-141.34		89.20	-85.23	1.0136	-0.1236
25	5.04	90	130.39		-128.70		-36.66		-37.67		97.79	-92.02	1.1613	-0.2653
26	10.07	90	172.71		-242.01		-122.54		-138.65		86.31	-80.73	1.0567	-0.2221

02: Two Arrays, Low Tension, 11 Cylinders Per Line

Test Number	Tow Speed (ft/sec)	Angle of Attack (deg)	X1 Gauge (lbs)	X2 Gauge (lbs)	Y1 Gauge (lbs)	Y2 Gauge (lbs)	X1 Pre Tension (lbs)	X2 Pre Tension (lbs)	NDP (ft^2)	NLP (ft^2)
39	5.04	30	140.86	-63.03	17.56	-23.71	74.77	-68.55	0.7835	1.4478
40	10.07	30	303.10	-89.73	40.78	-99.66	75.34	-69.19	0.7846	0.1245
41	5.04	40	170.77	-81.34	8.08	-31.50	74.21	-67.98	0.6836	1.2259
42	10.07	40	362.41	-132.80	5.89	-127.68	74.21	-67.98	0.9747	0.1141
43	5.04	50	178.62	-94.07	-5.22	-35.94	74.28	-68.53	1.2444	-0.2168
44	10.07	50	379.36	-165.37	-39.64	-144.50	75.35	-69.59	1.0994	0.0896
45	5.04	60	187.76	-107.04	-19.05	-42.20	74.98	-68.57	1.4416	0.0041
46	10.07	60	392.02	-197.38	-94.28	-163.32	74.72	-68.79	1.3240	0.1084

Table A.2: Experimental Data (continued)

02: Two Arrays, Low Tension, 11 Cylinders Per Line (continued)																
Test Number	Tow Speed (ft/sec)	Angle of Attack (deg)	X1		X2		Y1		Y2		X1		X2		NDP	NLP
			Gauge (lbs)		Gauge (lbs)		Gauge (lbs)		Gauge (lbs)		Pre Tension (lbs)		Pre Tension (lbs)			
47	5.04	70	181.37		-116.04		-30.92		-41.01		75.60		-69.70		1.4124	0.0056
48	10.08	70	361.22		-228.82		-139.82		-175.14		75.44		-69.60		1.4436	0.0398
49	5.05	80	170.73		-131.28		-40.70		-47.12		76.82		-71.71		1.5383	-0.0639
50	10.08	80	331.64		-257.73		-164.42		-182.68		76.40		-71.16		1.5240	0.0954
51	5.04	90	136.78		-151.95		-49.35		-48.12		97.61		-92.53		1.6314	-0.5938
52	10.08	90	208.80		-295.73		-178.13		-186.08		85.50		-80.35		1.5778	-0.3090

03: Three Arrays, Low Tension, 11 Cylinders per Line																
Test Number	Tow Speed (ft/sec)	Angle of Attack (deg)	X1		X2		Y1		Y2		X1		X2		NDP	NLP
			Gauge (lbs)		Gauge (lbs)		Gauge (lbs)		Gauge (lbs)		Pre Tension (lbs)		Pre Tension (lbs)			
65	5.04	30	171.65		-80.62		9.52		-29.65		103.20		-97.57		1.1681	1.3420
66	10.08	30	345.13		-101.41		10.36		-115.19		100.80		-95.33		1.0362	0.0009
67	5.04	40	143.83		-103.09		-78.33		-44.32		96.68		-91.06		1.2311	-0.9460
68	10.08	40	271.79		-152.59		-237.74		-149.03		95.57		-90.03		1.4109	-1.2752
69	5.04	50	137.89		-115.37		-94.17		-45.58		93.39		-87.56		1.9676	-2.4707
70	10.08	50	259.48		-185.80		-269.24		-169.57		92.37		-87.00		1.6312	-1.2862

Table A.2: Experimental Data (continued)

03: Three Arrays, Low Tension, 11 Cylinders per Line (continued)																
Test Number	Tow Speed (ft/sec)	Angle of Attack (deg)	X1		X2		Y1		Y2		X1		X2		NDP (ft^2)	NLP (ft^2)
			Gauge (lbs)	(lbs)	Gauge (lbs)	(lbs)	Gauge (lbs)	(lbs)	Gauge (lbs)	(lbs)	Tension (lbs)	Pre (lbs)	Tension (lbs)	Pre (lbs)		
71	5.04	60	135.65	-127.82	-90.41	-48.87	91.83	-85.98	2.0797	-2.0609						
72	10.08	60	261.05	-223.45	-272.72	-195.23	91.07	-85.30	1.8482	-1.1159						
73	5.04	70	136.89	-137.65	-81.52	-55.07	90.52	-84.31	2.1853	-1.7111						
74	10.08	70	229.79	-263.90	-276.36	-207.09	89.41	-83.17	1.9577	-1.0494						
75	5.04	80	138.10	-147.86	-74.26	-60.50	88.73	-82.18	2.3047	-1.2430						
76	10.08	80	242.32	-296.81	-250.05	-230.96	87.49	-81.09	2.0795	-0.6706						
77	5.04	90	150.77	-160.55	-62.69	-60.71	87.97	-81.41	2.1581	-0.5143						
78	10.07	90	246.33	-338.65	-224.65	-230.63	86.92	-80.54	2.0443	-0.3433						

04: Four Arrays, Low Tension, 11 Cylinders per Line										
Test Number	Tow Speed (ft/sec)	Angle of Attack (deg)	X1 Gauge (lbs)	X2 Gauge (lbs)	Y1 Gauge (lbs)	Y2 Gauge (lbs)	X1 Pre Tension (lbs)	X2 Pre Tension (lbs)	NDP (ft^2)	NLP (ft^2)
91	5.04	30	158.94	-88.46	-91.51	-36.24	111.2	-104.7	1.8843	-0.7689
92	10.07	30	297.80	-112.49	-245.68	-122.46	110.3	-103.4	1.4444	-1.3117
93	5.04	40	158.36	-104.08	-101.96	-45.98	104.6	-98.67	1.7672	-1.1668
94	10.07	40	304.03	-152.29	-294.78	-153.25	104.4	-98.09	1.7380	-1.4126

Table A.2: Experimental Data (continued)

04: Four Arrays, Low Tension, 11 Cylinders per Line (continued)											
Test Number	Tow Speed (ft/sec)	Angle of Attack (deg)	X1 Gauge (lbs)	X2 Gauge (lbs)	Y1 Gauge (lbs)	Y2 Gauge (lbs)	X1 Pre Tension (lbs)	X2 Pre Tension (lbs)	NDP (ft <sup>2</sup> )	NLP (ft <sup>2</sup> )	
95	5.04	50	160.47	-123.37	-104.91	-53.97	102.7	-96.28	2.4479	-2.5027	
96	10.07	50	306.12	-196.75	-310.56	-186.61	101.6	-95.06	1.9748	-1.3451	
97	5.04	60	155.24	-137.89	-105.20	-58.39	101.3	-93.75	2.5868	-2.1702	
98	10.07	60	300.51	-236.86	-310.54	-211.14	100.2	-93.22	2.1518	-1.1454	
99	5.04	70	152.78	-148.14	-95.01	-63.01	101.1	-92.84	2.6176	-1.7960	
100	10.07	70	266.19	-285.15	-320.54	-240.36	99.25	-91.46	2.3556	-1.1212	
101	5.04	80	155.55	-159.48	-86.89	-68.75	99.63	-91.36	2.7369	-1.2344	
102	10.07	80	282.06	-319.53	-287.26	-255.00	97.75	-89.4	2.4039	-0.6505	
103	5.04	90	164.17	-175.63	-73.57	-69.72	98.26	-90.69	2.5621	-0.5690	
104	10.07	90	273.70	-366.70	-260.18	-269.01	97.56	-89.27	2.4204	-0.3564	

05: Five Arrays, Low Tension, 11 Cylinders per Line											
Test Number	Tow Speed (ft/sec)	Angle of Attack (deg)	X1 Gauge (lbs)	X2 Gauge (lbs)	Y1 Gauge (lbs)	Y2 Gauge (lbs)	X1 Pre Tension (lbs)	X2 Pre Tension (lbs)	NDP (ft <sup>2</sup> )	NLP (ft <sup>2</sup> )	
117	5.04	30	208.96	-77.44	8.33	-38.67	108.8	-106.30	2.0392	1.6054	
119	5.04	40	237.85	-104.68	-14.11	-52.52	107.9	-105.50	1.9880	1.1747	

Table A.2: Experimental Data (continued)

05: Five Arrays, Low Tension, 11 Cylinders per Line (continued)													
Test Number	Tow Speed (ft/sec)	Angle of Attack (deg)	X1		X2		Y1		Y2		X1		NLP
			Gauge (lbs)	(lbs)	Gauge (lbs)	(lbs)	Gauge (lbs)	(lbs)	Pre Tension (lbs)	Post Tension (lbs)			
121	5.04	50	259.96	-129.56	-36.34	-61.74	107.6	-105.20	2.7726	-0.1945			
123	5.04	60	260.35	-145.47	-54.02	-67.72	107.5	-105.00	2.8924	0.0595			
125	5.04	70	258.62	-159.43	-69.78	-73.60	108.4	-105.80	3.0344	0.2185			
127	5.04	80	240.35	-173.95	-77.60	-77.71	106.4	-105.10	3.0030	0.3131			
128	10.07	80	493.93	-337.83	-294.57	-281.05	107.7	-106.10	2.7481	0.3238			
129	5.04	90	211.66	-197.57	-81.36	-76.87	108.3	-108.40	2.8656	0.1058			
130	10.07	90	409.87	-377.62	-300.76	-295.52	111.8	-111.90	2.7618	0.3236			

06: Six Arrays, Low Tension, 11 Cylinders per Line													
Test Number	Tow Speed (ft/sec)	Angle of Attack (deg)	X1		X2		Y1		Y2		X1		NLP
			Gauge (lbs)	(lbs)	Gauge (lbs)	(lbs)	Gauge (lbs)	(lbs)	Gauge (lbs)	(lbs)	Pre Tension (lbs)	Post Tension (lbs)	
169	5.04	30	226.76	-82.76	-0.45	-42.78	123.40	-121.10	2.3931	1.5074			
171	5.04	40	214.53	-116.45	-68.01	-59.17	122.80	-120.50	2.2341	-0.2244			
173	5.04	50	200.21	-145.57	-131.14	-72.89	121.90	-119.90	3.4373	-2.7506			
175	5.04	60	194.21	-164.61	-133.08	-79.61	120.80	-118.60	3.6293	-2.3593			
177	5.04	70	185.20	-177.82	-124.02	-84.97	120.00	-117.90	3.6524	-1.9803			

Table A.2: Experimental Data (continued)

06: Six Arrays, Low Tension, 11 Cylinders per Line (continued)

Test Number	Tow Speed (ft/sec)	Angle of Attack (deg)	X1 Gauge (lbs)	X2 Gauge (lbs)	Y1 Gauge (lbs)	Y2 Gauge (lbs)	X1 Pre Tension (lbs)	X2 Pre Tension (lbs)	NDP (ft <sup>2</sup> )	NLP (ft <sup>2</sup> )
179	5.04	80	176.08	-192.61	-113.73	-88.90	119.10	-117.10	3.6546	-1.5268
181	5.04	90	182.19	-208.12	-97.49	-89.30	118.40	-116.40	3.4458	-0.7498

07: Seven Arrays, Low Tension, 11 Cylinders per Line

Test Number	Tow Speed (ft/sec)	Angle of Attack (deg)	X1 Gauge (lbs)	X2 Gauge (lbs)	Y1 Gauge (lbs)	Y2 Gauge (lbs)	X1 Pre Tension (lbs)	X2 Pre Tension (lbs)	NDP (ft <sup>2</sup> )	NLP (ft <sup>2</sup> )
195	5.04	30	243.98	-82.43	-4.69	-46.55	129.50	-128.30	2.8026	1.5559
197	5.04	40	279.52	-116.06	-31.31	-65.54	128.70	-127.60	2.8742	1.1169
199	5.04	50	303.73	-145.91	-56.86	-78.03	128.30	-127.30	3.7217	-0.2266
201	5.04	60	304.80	-169.72	-82.28	-86.76	128.60	-127.50	3.9439	-0.0410
203	5.04	70	253.95	-188.23	-105.49	-93.58	128.90	-127.60	3.8739	-0.7824
205	5.04	80	190.98	-206.81	-131.16	-99.07	130.90	-129.50	4.2144	-1.5982
207	5.04	90	209.60	-235.60	-110.15	-103.44	138.90	-137.30	3.9902	-0.7431

Table A.2: Experimental Data (continued)

08: Eight Arrays, Low Tension, 11 Cylinders per Line												
Test Number	Tow Speed (ft/sec)	Angle of Attack (deg)	X1 Gauge (lbs)	X2 Gauge (lbs)	Y1 Gauge (lbs)	Y2 Gauge (lbs)	X1 Pre Tension (lbs)	X2 Pre Tension (lbs)	NDP (ft <sup>2</sup> )	NLP (ft <sup>2</sup> )		
221	5.04	30	255.09	-84.39	-13.68	-49.07	142.10	-141.50	3.0910	1.4525		
223	5.04	40	251.95	-126.54	-84.72	-71.81	140.50	-140.40	3.0769	-0.2956		
225	5.04	50	239.72	-161.21	-154.47	-87.69	140.70	-140.20	4.3619	-2.8537		
227	5.04	60	228.14	-182.14	-163.45	-100.34	139.20	-138.50	4.7101	-2.5634		
229	5.04	70	214.05	-200.77	-162.76	-105.47	137.70	-137.10	4.6775	-2.6822		
231	5.04	80	209.07	-219.01	-144.65	-113.81	136.90	-136.40	4.8000	-1.5619		
233	5.04	90	216.40	-235.79	-126.39	-117.25	136.30	-135.90	4.6006	-0.5844		

09: One Array, Low Tension, 6 Cylinders per Line												
Test Number	Tow Speed (ft/sec)	Angle of Attack (deg)	X1 Gauge (lbs)	X2 Gauge (lbs)	Y1 Gauge (lbs)	Y2 Gauge (lbs)	X1 Pre Tension (lbs)	X2 Pre Tension (lbs)	NDP (ft <sup>2</sup> )	NLP (ft <sup>2</sup> )		
267	5.04	0	104.36	-86.01	40.26	-5.26	95.00	-97.35	0.0926	0.4788		
268	10.06	0	123.53	-66.95	30.05	-30.36	95.27	-97.41	-0.0361	0.6171		
269	5.04	10	116.19	-83.53	48.39	-7.42	94.63	-96.98	0.0455	1.7353		
270	10.06	10	138.60	-65.61	53.04	-36.23	95.15	-97.56	0.0379	0.7563		

Table A.2: Experimental Data (continued)

09: One Array, Low Tension, 6 Cylinders per Line (continued)																
Test Number	Tow Speed (ft/sec)	Angle of Attack (deg)	X1		X2		Y1		Y2		X1		X2		NDP (ft^2)	NLP (ft^2)
			Gauge	(lbs)	Gauge	(lbs)	Gauge	(lbs)	Gauge	(lbs)	Pre Tension (lbs)	Pre Tension (lbs)				
271	5.04	20		119.54	-84.31	32.07	-11.23				93.68	-95.92	0.1333		1.4956	
272	10.06	20		180.49	-79.71	77.87	-56.96				96.25	-98.50	0.1208		1.1723	
273	5.04	30		135.56	-86.55	29.82	-14.78				92.69	-94.98	0.2110		1.6143	
274	10.07	30		232.92	-100.08	74.86	-68.39				93.26	-95.50	0.3004		0.2289	
275	5.04	40		142.92	-91.45	20.78	-19.05				92.12	-94.69	-0.0986		1.2365	
276	10.06	40		257.37	-124.99	38.72	-79.60				92.97	-95.26	0.3650		0.1396	
277	5.04	50		149.67	-97.79	10.77	-21.21				91.83	-94.01	0.4433		-0.2007	
278	10.07	50		272.16	-143.16	9.46	-87.45				92.17	-94.58	0.4343		0.1374	
279	5.04	60		154.53	-106.16	-0.25	-23.42				94.42	-96.89	0.5421		-0.0271	
280	10.07	60		263.38	-163.27	-26.63	-89.65				94.64	-96.89	0.4815		0.0874	
281	5.04	70		157.62	-113.00	-8.75	-24.07				98.98	-101.60	0.5811		0.0447	
282	10.07	70		249.48	-184.60	-56.11	-94.22				98.99	-101.60	0.5565		0.0440	
283	5.04	80		140.66	-122.83	-20.15	-24.90				99.77	-102.40	0.6398		-0.1910	
284	10.07	80		209.20	-207.45	-82.02	-97.72				99.43	-102.20	0.6317		-0.0780	
285	5.04	90		123.49	-134.82	-25.17	-25.17				102.80	-105.40	0.6740		-0.3598	
286	10.06	90		157.58	-232.16	-87.08	-99.06				101.50	-104.20	0.6761		-0.2072	



Table A.2: Experimental Data (continued)

10: Two Arrays, Low Tension, 6 Cylinders per Line, 12 Inch Consecutive Spacing																				
Test Number	Tow Speed (ft/sec)	Angle of Attack (deg)	X1			X2			Y1			Y2			X1		X2		NDP (ft^2)	NLP (ft^2)
			Gauge	(lbs)		Gauge	(lbs)		Gauge	(lbs)		Gauge	(lbs)		Pre Tension (lbs)		Pre Tension (lbs)			
287	5.04	30		116.05		-95.83		-64.6		-19.95		100.70		-102.80		0.3859		0.1339		
288	10.06	30		179.68		-117.26		-158.36		-80.2		99.59		-101.70		0.8084		-1.3689		
289	5.04	40		114.2		-106.28		-62.38		-29.01		97.51		-99.89		0.0651		-0.3408		
290	10.06	40		178.09		-151.40		-182.75		-100.44		96.63		-99.09		0.9975		-1.4512		
291	5.04	50		114.86		-114.52		-60.12		-28.07		95.31		-97.56		1.4948		-2.4479		
292	10.07	50		169.43		-175.06		-188.88		-112.25		95.06		-97.54		1.1281		-1.3386		
293	5.04	60		108.41		-122.27		-59.43		-31.39		93.88		-96.50		1.5012		-2.0370		
294	10.07	60		151.46		-199.10		-182.39		-119.78		93.28		-95.80		1.1400		-1.1593		
295	5.04	70		107.71		-125.42		-47.96		-31.61		93.38		-95.64		1.3199		-1.5794		
296	10.06	70		146.55		-221.55		-163.94		-125.32		92.70		-94.74		1.1388		-0.9296		
297	5.04	80		108.34		-134.92		-43.07		-33.02		94.63		-96.68		1.2665		-1.2295		
298	10.06	80		146.34		-252.13		-149.13		-133.82		92.09		-94.53		1.1505		-0.7278		
299	5.04	90		118.07		-140.16		-35.65		-33.04		91.65		-94.11		1.0955		-0.5811		
300	10.06	90		185.04		-264.46		-126.24		-132.25		92.87		-95.27		1.0839		-0.2334		

Table A.2: Experimental Data (continued)

11: Two Arrays, Low Tension, 6 Cylinders per Line, 24 Inch Consecutive Spacing																	
Test Number	Tow Speed (ft/sec)	Angle of Attack (deg)	X1 Gauge		X2 Gauge		Y1 Gauge		Y2 Gauge		X1 Pre Tension		X2 Pre Tension		NDP (ft^2)	NLP (ft^2)	
			(lbs)	(lbs)	(lbs)	(lbs)	(lbs)	(lbs)	(lbs)	(lbs)	(lbs)	(lbs)					
301	5.04	30	141.65	-82.42	-21.09	-19.21	90.63	-93.68	0.9662	0.7523							
302	10.06	30	274.91	-101.25	49.24	-80.78	91.54	-93.88	0.5786	0.1658							
303	5.04	40	164.06	-93.36	-15.78	-25.31	90.38	-92.85	0.7582	0.8200							
304	10.06	40	323.59	-129.45	29.43	-100.12	91.15	-93.33	0.7035	0.2252							
305	5.04	50	175.90	-106.70	2.54	-29.73	89.19	-91.42	0.9308	-0.1491							
306	10.06	50	352.55	-167.01	-9.14	-119.99	90.35	-92.75	0.8202	0.1909							
307	5.04	60	178.55	-116.88	-9.19	-32.91	89.38	-91.53	0.9982	0.0141							
308	10.07	60	352.37	-195.37	-54.40	-128.47	89.70	-92.18	0.9203	0.1697							
309	5.04	70	174.84	-124.17	-20.62	-33.71	89.94	-92.05	1.0302	0.0010							
310	10.07	70	333.93	-217.59	-89.69	-124.80	89.86	-92.29	0.9525	0.1775							
311	5.04	80	162.00	-131.51	-29.63	-34.04	90.23	-92.45	1.0555	-0.0116							
312	10.06	80	303.10	-239.64	-115.28	-127.48	89.56	-92.00	1.0037	0.1743							
313	5.04	90	141.47	-13.76	-33.82	-33.61	93.26	-95.46	1.0212	2.4565							
314	10.06	90	220.56	-24.21	-125.00	-133.12	91.53	-93.80	1.0431	1.1720							

Table A.2: Experimental Data (continued)

12: Three Arrays, Low Tension, 6 Cylinders per Line, 24 Inch Consecutive Spacing																
Test Number	Tow Speed (ft/sec)	Angle of Attack (deg)	X1 Gauge		X2 Gauge		Y1 Gauge		Y2 Gauge		X1 Pre Tension		X2 Pre Tension		NDP (ft^2)	NLP (ft^2)
			(lbs)	(lbs)	(lbs)	(lbs)	(lbs)	(lbs)	(lbs)	(lbs)	(lbs)	(lbs)				
315	5.04	30	157.35	-86.29	14.14	-22.48	99.44	-101.60	0.8341						1.4257	
316	10.06	30	311.91	-109.13	23.85	-90.59	98.56	-100.90	0.7969						0.0847	
317	5.04	40	138.00	-107.38	-54.07	-34.56	98.50	-100.60	0.7495						-0.4480	
318	10.06	40	250.10	-149.76	-174.18	-113.35	97.66	-99.94	1.0482						-0.9288	
319	5.04	50	135.98	-124.72	-76.02	-38.32	96.25	-99.02	1.5375						-2.1803	
320	10.06	50	224.48	-191.83	-232.48	-144.77	95.92	-98.47	1.2887						-1.2189	
321	5.04	60	132.16	-136.08	-71.72	-44.37	95.63	-97.61	1.6319						-1.8943	
322	10.06	60	223.75	-222.36	-217.20	-152.33	94.29	-96.85	1.3499						-0.9926	
323	5.04	70	132.22	-143.86	-63.53	-44.38	94.56	-96.93	1.6219						-1.5557	
324	10.06	70	193.88	-249.90	-214.87	-162.66	93.32	-95.70	1.4349						-0.9325	
325	5.04	80	137.41	-149.12	-51.31	-45.79	93.72	-95.99	1.5756						-0.9727	
326	10.06	80	358.61	-269.72	-154.66	-165.32	92.07	-94.34	1.4138						0.2328	
327	5.04	90	159.36	-152.96	-46.71	-45.66	92.45	-94.55	1.5278						-0.0098	
328	10.06	90	304.35	-288.32	-169.43	-170.03	91.00	-93.37	1.4578						0.2531	

Table A.2: Experimental Data (continued)

13: Four Arrays, Low Tension, 6 Cylinders per Line, 24 Inch Consecutive Spacing																
Test Number	Tow Speed (ft/sec)	Angle of Attack (deg)	X1 Gauge (lbs)		X2 Gauge (lbs)		Y1 Gauge (lbs)		Y2 Gauge (lbs)		X1 Pre Tension (lbs)		X2 Pre Tension (lbs)		NDP (ft^2)	NLP (ft^2)
			X1 Gauge	X2 Gauge	X1 Gauge	X2 Gauge	Y1 Gauge	Y2 Gauge	X1 Pre	X2 Pre	X1 Tension	X2 Tension				
329	5.04	30	179.35	-81.97	20.88	-27.18	97.83	-100.20	1.2801	1.7310						
330	10.07	30	363.67	-101.85	54.86	-97.31	98.03	-100.60	0.9947	0.3423						
331	5.04	40	204.45	-104.34	3.75	-36.92	96.22	-98.88	1.1154	1.3297						
332	10.07	40	417.85	-145.84	0.14	-125.59	97.10	-99.72	1.1865	0.2674						
333	5.04	50	225.43	-127.06	-14.61	-45.74	95.61	-98.38	1.8347	0.1198						
334	10.07	50	460.04	-196.67	-55.90	-161.22	96.09	-98.72	1.4169	0.2070						
335	5.04	60	225.62	-144.89	-33.02	-52.39	95.91	-98.43	1.9575	-0.0840						
336	10.07	60	453.05	-232.97	-120.16	-178.91	95.14	-97.85	1.5935	0.1530						
337	5.04	70	222.42	-154.41	-45.48	-55.33	96.53	-98.85	2.0394	0.0130						
338	10.06	70	447.14	-270.45	-165.75	-197.46	94.90	-97.44	1.7724	0.2082						
339	5.04	80	206.53	-161.64	-52.21	-56.51	97.21	-100.00	2.0095	0.1290						
340	10.06	80	399.31	-282.07	-196.44	-201.55	95.47	-98.41	1.8312	0.3094						
341	5.04	90	183.82	-178.94	-57.34	-54.82	101.70	-104.40	1.9298	-0.0284						
342	10.07	90	340.97	-303.47	-207.40	-204.08	97.93	-100.90	1.8214	0.3649						

Table A.2: Experimental Data (continued)

14: One Array, Low Tension, 3 Cylinders per Line																		
Test Number	Tow Speed (ft/sec)	Angle of Attack (deg)	X1 Gauge (lbs)		X2 Gauge (lbs)		Y1 Gauge (lbs)		Y2 Gauge (lbs)		X1 Pre Tension (lbs)		X2 Pre Tension (lbs)		NDP (ft^2)	NLP (ft^2)		
			Gauge	(lbs)	Gauge	(lbs)	Gauge	(lbs)	Gauge	(lbs)	Pre Tension	(lbs)	Pre Tension	(lbs)				
343	5.04	0	113.93	-94.29	46.84	5.69	102.30	-104.10	0.1077	0.8349								
344	10.06	0	128.48	-76.84	33.59	-30.91	102.20	-104.70	-0.0595	0.6323								
345	5.04	10	113.75	-93.69	-48.00	-9.68	101.90	-104.40	0.1444	-0.2821								
346	10.07	10	125.67	-77.53	-105.31	-32.48	101.00	-103.70	0.0514	-0.0416								
347	5.04	20	104.40	-96.13	-65.46	-9.07	99.07	-101.50	0.2849	-0.5109								
348	10.07	20	118.07	-93.26	-125.85	-54.99	101.30	-104.00	0.1106	0.0738								
349	5.04	30	141.38	-91.73	36.38	-14.21	98.38	-101.10	0.1574	1.7506								
350	10.07	30	209.39	-99.85	74.02	-62.33	99.81	-102.50	0.1864	0.1938								
351	5.04	40	94.34	-100.26	-54.67	-17.90	96.68	-99.07	-0.0243	-0.6714								
352	10.06	40	103.98	-124.16	-142.76	-73.54	98.81	-101.30	0.3449	-1.0449								
353	5.04	50	145.34	-96.45	15.62	-19.89	92.18	-95.03	0.3170	-0.1562								
354	10.06	50	255.16	-137.67	19.62	-87.29	93.81	-96.29	0.3574	0.1268								
355	5.04	60	145.44	-100.34	4.21	-21.19	91.75	-94.03	0.3893	-0.0200								
356	10.07	60	251.09	-157.41	-15.38	-87.38	92.43	-94.71	0.4057	0.0936								
357	5.04	70	140.14	-101.21	-5.12	-21.28	90.00	-92.19	0.4160	-0.0276								
358	10.07	70	244.03	-172.53	-41.17	-89.68	90.76	-92.94	0.4741	0.1075								
359	5.04	80	128.10	-107.08	-15.48	-21.77	89.85	-92.05	0.4935	-0.1083								

Table A.2: Experimental Data (continued)

14: One Array, Low Tension, 3 Cylinders per Line (continued)										
Test Number	Tow Speed (ft/sec)	Angle of Attack (deg)	X1 Gauge (lbs)	X2 Gauge (lbs)	Y1 Gauge (lbs)	Y2 Gauge (lbs)	X1 Pre Tension (lbs)	X2 Pre Tension (lbs)	NDP (ft^2)	NLP (ft^2)
360	10.07	80	207.14	-189.06	-65.79	-85.16	89.97	-92.25	0.5014	0.0269
361	5.04	90	109.02	-109.27	-18.95	-20.75	89.25	-91.53	0.4579	-0.1412
362	10.07	90	161.81	-205.83	-73.89	-81.24	89.39	-91.66	0.5170	-0.0535

15: Two Arrays, Low Tension, 3 Cylinders per Line, 12 Inches Consecutive Spacing										
Test Number	Tow Speed (ft/sec)	Angle of Attack (deg)	X1 Gauge (lbs)	X2 Gauge (lbs)	Y1 Gauge (lbs)	Y2 Gauge (lbs)	X1 Pre Tension (lbs)	X2 Pre Tension (lbs)	NDP (ft^2)	NLP (ft^2)
363	5.04	30	140.25	-82.97	30.86	-16.06	87.77	-89.80	0.5695	1.8157
364	10.06	30	239.89	-102.48	63.34	-79.29	90.20	-92.42	0.2476	0.0666
365	5.04	40	153.42	-90.99	21.18	-21.24	87.50	-89.55	-0.0025	1.2696
366	10.06	40	279.35	-129.27	34.71	-86.88	89.49	-91.88	0.2822	-0.0050
367	5.04	50	160.36	-101.36	8.24	-25.11	87.29	-89.54	0.1445	-0.7601
368	10.07	50	311.95	-158.76	13.02	-102.06	88.77	-91.16	0.3528	-0.0473
369	5.04	60	160.19	-108.69	-1.53	-26.62	87.67	-89.78	0.2805	-0.6623
370	10.07	60	307.38	-179.73	-28.34	-107.35	88.25	-90.68	0.4739	-0.1234
371	5.04	70	160.74	-111.95	-11.17	-27.12	88.01	-90.14	0.4655	-0.5979

Table A.2: Experimental Data (continued)

15: Two Arrays, Low Tension, 3 Cylinders per Line, 12 Inches Consecutive Spacing (continued)																
Test Number	Tow Speed (ft/sec)	Angle of Attack (deg)	X1		X2		Y1		Y2		X1		X2		NDP	NLP
			Gauge (lbs)		Gauge (lbs)		Gauge (lbs)		Gauge (lbs)		Pre Tension (lbs)		Pre Tension (lbs)			
372	10.07	70	301.27		-199.99		-59.82		-110.62		88.43		-90.56		0.5978	-0.1417
373	5.04	80	147.25		-119.04		-21.12		-27.84		88.56		-90.90		0.6525	-0.5761
374	10.07	80	264.96		-222.54		-88.31		-110.77		88.73		-91.02		0.7131	-0.1828
375	5.04	90	131.93		-128.57		-26.52		-27.91		93.55		-95.93		0.7571	-0.4376
376	10.07	90	203.77		-235.30		-90.45		-103.50		92.04		-94.51		0.7145	-0.2079

16: Two Arrays, Low Tension, 3 Cylinders per Line, 36 Inches Consecutive Spacing																
Test Number	Tow Speed (ft/sec)	Angle of Attack (deg)	X1		X2		Y1		Y2		X1		X2		NDP (ft^2)	NLP (ft^2)
			Gauge (lbs)		Gauge (lbs)		Gauge (lbs)		Gauge (lbs)		Tension (lbs)	Pre	Tension (lbs)	Pre		
377	5.04	30	139.19		-82.17		28.73		-16.17		90.41		-92.59		0.3752	1.6509
378	10.06	30	246.48		-96.23		68.78		-71.76		92.07		-94.51		0.4029	0.2325
379	5.04	40	105.36		-93.81		-35.44		-22.19		90.83		-92.96		0.0485	-0.2142
380	10.07	40	171.45		-125.54		-115.52		-84.36		90.40		-92.62		0.5470	-0.7635
381	5.04	50	98.12		-103.34		-55.76		-25.96		88.41		-91.42		0.8178	-2.0071
382	10.06	50	140.05		-158.70		-162.92		-102.45		88.14		-90.82		0.6840	-1.0521
383	5.04	60	159.72		-106.97		-2.30		-26.99		86.29		-88.50		0.6829	-0.0117

Table A.2: Experimental Data (continued)

16: Two Arrays, Low Tension, 3 Cylinders per Line, 36 Inches Consecutive Spacing (continued)												
Test Number	Tow Speed (ft/sec)	Angle of Attack (deg)	X1 Gauge (lbs)	X2 Gauge (lbs)	Y1 Gauge (lbs)	Y2 Gauge (lbs)	X1 Pre Tension (lbs)	X2 Pre Tension (lbs)	NDP (ft <sup>2</sup> )	NLP (ft <sup>2</sup> )		
384	10.07	60	315.76	-178.73	-28.99	-110.63	85.70	-88.04	0.6786	0.1911		
385	5.04	70	162.79	-113.08	-12.95	-28.63	85.84	-88.22	0.7820	0.0764		
386	10.07	70	320.05	-200.15	-60.14	-108.79	85.28	-87.62	0.7407	0.2734		
387	5.04	80	147.23	-116.43	-22.16	-28.27	84.91	-87.70	0.7937	0.0527		
388	10.07	80	280.43	-219.19	-88.45	-107.96	84.91	-87.29	0.7675	0.2035		
389	5.04	90	125.96	-122.04	-26.65	-27.09	85.05	-87.29	0.7431	-0.0573		
390	10.06	90	224.96	-227.27	-98.32	-103.57	84.39	-86.75	0.7564	0.1595		

17: Three Arrays, Low Tension, 3 Cylinders per Line, 36 Inches Consecutive Spacing												
Test Number	Tow Speed (ft/sec)	Angle of Attack (deg)	X1 Gauge (lbs)	X2 Gauge (lbs)	Y1 Gauge (lbs)	Y2 Gauge (lbs)	X1 Pre Tension (lbs)	X2 Pre Tension (lbs)	NDP (ft <sup>2</sup> )	NLP (ft <sup>2</sup> )		
391	5.04	30	143.67	-77.70	25.34	-17.51	86.70	-89.36	0.5891	1.6635		
392	10.06	30	272.26	-97.75	60.55	-76.25	88.00	-90.24	0.5415	0.2377		
393	5.04	40	162.20	-91.47	16.10	-24.55	86.52	-88.69	0.3278	1.3244		
394	10.07	40	312.46	-133.85	16.60	-96.33	86.72	-89.40	0.6731	0.1403		
395	5.04	50	171.37	-106.55	2.20	-29.81	86.26	-88.61	0.8817	-0.2209		



Table A.2: Experimental Data (continued)

17: Three Arrays, Low Tension, 3 Cylinders per Line, 36 Inches Consecutive Spacing (continued)																		
Test Number	Tow Speed (ft/sec)	Angle of Attack (deg)	X1			X2			Y1			Y2			X1 Pre Tension (lbs)	X2 Pre Tension (lbs)	NDP (ft^2)	NLP (ft^2)
			Gauge	(lbs)		Gauge	(lbs)		Gauge	(lbs)		Gauge	(lbs)					
396	10.06	50	355.81	-168.77	-5.25	-117.90	86.19	-88.59	86.19	-117.90	86.19	-88.59	86.19	-88.59	0.8018	0.2163		
397	5.04	60	184.81	-117.79	-9.76	-33.40	86.49	-88.68	86.49	-33.40	86.49	-88.68	86.49	-88.68	1.0716	0.0981		
398	10.06	60	358.89	-197.43	-51.61	-126.26	85.66	-88.24	85.66	-126.26	85.66	-88.24	85.66	-88.24	0.9117	0.2029		
399	5.04	70	176.72	-126.37	-21.12	-36.50	86.99	-89.33	86.99	-36.50	86.99	-89.33	86.99	-89.33	1.0924	-0.0236		
400	10.07	70	349.85	-221.12	-85.21	-132.76	85.85	-88.36	85.85	-132.76	87.05	-89.34	86.44	-88.82	0.9908	0.2311		
401	5.04	80	166.28	-132.17	-30.47	-34.92	87.05	-89.34	87.05	-34.92	86.44	-88.82	86.44	-88.82	1.1029	0.0561		
402	10.07	80	309.86	-239.85	-113.42	-134.89	86.44	-88.82	86.44	-134.89	89.34	-91.68	89.34	-91.68	1.0353	0.2016		
403	5.04	90	148.14	-139.37	-34.17	-33.81	89.34	-91.68	89.34	-33.81	88.06	-90.53	88.06	-90.53	1.0323	0.0433		
404	10.07	90	268.55	-241.28	-123.88	-132.77	88.06	-90.53	88.06	-132.77					1.0336	0.3103		

18: Four Arrays, Low Tension, 3 Cylinders per Line, 36 Inches Consecutive Spacing															
Test Number	Tow Speed (ft/sec)	Angle of Attack (deg)	X1		X2		Y1		Y2		X1		X2		NLP
			Gauge	(lbs)	Gauge	(lbs)	Gauge	(lbs)	Gauge	(lbs)	Pre Tension (lbs)	Pre Tension (lbs)			
405	5.04	30	154.05		-80.71		22.98		-21.32		94.80		-96.88		1.6239
406	10.07	30	305.79		-101.65		67.95		-86.92		93.69		-96.05		0.2985
407	5.04	40	175.62		-97.18		11.84		-29.11		93.09		-95.45		1.2903

Table A.2: Experimental Data (continued)

18: Four Arrays, Low Tension, 3 Cylinders per Line, 36 Inches Consecutive Spacing (continued)												
Test Number	Tow Speed (ft/sec)	Angle of Attack (deg)	X1 Gauge (lbs)	X2 Gauge (lbs)	Y1 Gauge (lbs)	Y2 Gauge (lbs)	X1 Pre Tension (lbs)	X2 Pre Tension (lbs)	NDP (ft <sup>2</sup> )	NLP (ft <sup>2</sup> )		
408	10.07	40	355.36	-140.13	20.98	-110.76	92.10	-94.48	0.8475	0.2200		
409	5.04	50	192.02	-113.81	-2.62	-33.61	92.29	-94.38	1.1873	-0.1291		
410	10.06	50	406.57	-185.89	-12.70	-135.74	90.80	-93.20	1.0108	0.2648		
411	5.04	60	199.51	-127.82	-16.59	-40.26	91.22	-93.40	1.3598	0.0411		
412	10.07	60	409.05	-213.68	-65.63	-142.52	89.83	-92.14	1.1289	0.2737		
413	5.04	70	194.18	-136.91	-28.30	-41.92	90.28	-92.45	1.3798	0.0177		
414	10.07	70	388.77	-241.30	-108.27	-145.00	89.33	-91.56	1.1918	0.2579		
415	5.04	80	184.07	-142.20	-36.97	-41.13	89.53	-91.61	1.3838	0.1623		
416	10.07	80	345.68	-255.17	-136.04	-145.07	88.43	-90.81	1.2178	0.2753		
417	5.04	90	158.58	-149.11	-41.39	-41.10	89.06	-91.27	1.3271	0.0548		
418	10.06	90	302.30	-269.14	-148.98	-154.90	87.77	-90.11	1.2764	0.3403		

19: Four Arrays, High Tension, 3 Cylinders per Line, 36 Inches Consecutive Spacing												
Test Number	Tow Speed (ft/sec)	Angle of Attack (deg)	X1 Gauge (lbs)	X2 Gauge (lbs)	Y1 Gauge (lbs)	Y2 Gauge (lbs)	X1 Pre Tension (lbs)	X2 Pre Tension (lbs)	NDP (ft <sup>2</sup> )	NLP (ft <sup>2</sup> )		
419	5.04	30	280.52	-193.80	33.47	-21.27	208.60	-213.00	0.9403	1.9688		

Table A.2: Experimental Data (continued)

19: Four Arrays, High Tension, 3 Cylinders per Line, 36 Inches Consecutive Spacing (continued)												
Test Number	Tow Speed (ft/sec)	Angle of Attack (deg)	X1 Gauge (lbs)	X2 Gauge (lbs)	Y1 Gauge (lbs)	Y2 Gauge (lbs)	X1 Pre Tension (lbs)	X2 Pre Tension (lbs)	NDP (ft <sup>2</sup> )	NLP (ft <sup>2</sup> )		
420	5.04	50	298.90	-211.67	-3.35	-38.43	207.80	-212.30	1.4229	-0.0237		
421	5.04	70	309.50	-242.67	-35.15	-46.48	227.10	-231.40	1.6788	0.1616		
422	10.07	70	484.49	-317.43	-110.99	-168.22	222.90	-227.40	1.3538	0.3173		
423	5.04	90	238.74	-232.48	-45.24	-45.43	194.10	-198.30	1.4932	0.0301		
424	10.07	90	354.07	-324.53	-153.69	-167.82	184.70	-189.00	1.3636	0.3312		

20: Three Arrays, High Tension, 3 Cylinders per Line, 36 Inches Consecutive Spacing												
Test Number	Tow Speed (ft/sec)	Angle of Attack (deg)	X1 Gauge (lbs)	X2 Gauge (lbs)	Y1 Gauge (lbs)	Y2 Gauge (lbs)	X1 Pre Tension (lbs)	X2 Pre Tension (lbs)	NDP (ft <sup>2</sup> )	NLP (ft <sup>2</sup> )		
425	5.04	30	271.50	-194.36	35.31	-19.26	207.70	-212.40	0.7380	1.9423		
426	5.04	50	283.21	-207.10	1.36	-35.64	207.60	-212.10	1.1610	-0.0988		
427	5.04	70	277.69	-220.06	-24.65	-39.55	205.70	-210.20	1.2836	0.1109		
428	5.04	90	238.38	-236.35	-37.94	-39.93	204.70	-209.10	1.2332	-0.0518		

Table A.2: Experimental Data (continued)

21: Two Arrays, High Tension, 3 Cylinders per Line, 36 Inches Consecutive Spacing										
Test Number	Tow Speed (ft/sec)	Angle of Attack (deg)	X1 Gauge (lbs)	X2 Gauge (lbs)	Y1 Gauge (lbs)	Y2 Gauge (lbs)	X1 Pre Tension (lbs)	X2 Pre Tension (lbs)	NDP (ft^2)	NLP (ft^2)
429	5.04	30	265.29	-193.94	39.34	-17.26	203.60	-207.90	0.5678	1.9855
430	5.04	50	270.10	-202.19	7.89	-26.52	203.00	-207.40	0.8091	-0.0237
431	5.04	70	262.61	-210.59	-15.48	-31.11	202.90	-207.30	0.9077	0.1242
432	5.04	90	227.11	-226.41	-29.54	-30.19	203.10	-207.50	0.8647	-0.0788

22: One Array, High Tension, 3 Cylinders per Line										
Test Number	Tow Speed (ft/sec)	Angle of Attack (deg)	X1 Gauge (lbs)	X2 Gauge (lbs)	Y1 Gauge (lbs)	Y2 Gauge (lbs)	X1 Pre Tension (lbs)	X2 Pre Tension (lbs)	NDP (ft^2)	NLP (ft^2)
433	5.04	30	242.91	-186.59	39.55	-13.48	192.80	-197.30	0.2664	1.9051
434	5.04	50	244.68	-190.25	13.71	-21.99	193.10	-197.70	0.4746	-0.0952
435	5.04	70	242.00	-194.33	-5.82	-24.07	191.90	-196.60	0.5608	0.1629
436	5.04	90	203.21	-204.36	-21.73	-24.00	191.00	-195.80	0.5804	-0.1083

Table A.2: Experimental Data (continued)

23: One Array, High Tension, 6 Cylinders per Line																
Test Number	Tow Speed (ft/sec)	Angle of Attack (deg)	X1		X2		Y1		Y2		X1		X2		NDP	NLP
			Gauge	(lbs)	Gauge	(lbs)	Gauge	(lbs)	Gauge	(lbs)	Pre Tension (lbs)	Pre Tension (lbs)				
437	5.04	30	251.32	-188.44	40.33	-16.90	194.40	-198.90	0.4086	1.9252						
438	5.04	50	253.61	-193.99	10.88	-23.67	194.30	-198.70	0.6100	-0.0764						
439	5.04	70	248.80	-201.16	-11.46	-27.20	194.70	-199.10	0.7259	0.0970						
440	5.04	90	209.22	-216.65	-27.50	-30.25	199.80	-204.00	0.8245	-0.2480						

24: Two Arrays, High Tension, 6 Cylinders per Line, 24 Inches Consecutive Spacing																
Test Number	Tow Speed (ft/sec)	Angle of Attack (deg)	X1		X2		Y1		Y2		X1		X2		NDP	NLP
			Gauge	(lbs)	Gauge	(lbs)	Gauge	(lbs)	Gauge	(lbs)	Pre Tension (lbs)	Pre Tension (lbs)				
441	5.04	30	263.65	-183.37	35.05	-22.23	196.50	-200.80	0.8190	1.9133						
442	5.04	50	273.44	-195.97	1.81	-34.79	195.60	-199.90	1.1559	-0.0638						
443	5.04	70	261.26	-208.31	-24.79	-40.68	193.90	-198.20	1.2739	0.0089						
444	5.04	90	224.24	-221.35	-39.36	-41.83	192.10	-196.60	1.3007	-0.0323						

Table A.2: Experimental Data (continued)

25: Three Arrays, High Tension, 6 Cylinders per Line, 24 Inches Consecutive Spacing												
Test Number	Tow Speed (ft/sec)	Angle of Attack (deg)	X1 Gauge (lbs)	X2 Gauge (lbs)	Y1 Gauge (lbs)	Y2 Gauge (lbs)	X1 Pre Tension (lbs)	X2 Pre Tension (lbs)	NDP (ft <sup>2</sup> )	NLP (ft <sup>2</sup> )		
445	5.04	30	265.31	-175.03	28.83	-26.48	189.60	-194.30	1.1083	1.8347		
446	5.04	50	288.18	-197.12	-7.76	-42.56	189.10	-193.50	1.6045	-0.0772		
447	5.04	70	281.52	-217.23	-37.55	-51.86	190.00	-193.50	1.8041	0.0438		
448	5.04	90	242.21	-236.72	-51.09	-52.52	193.10	-197.40	1.7561	0.0165		

26: Four Arrays, High Tension, 6 Cylinders per Line, 24 Inches Consecutive Spacing												
Test Number	Tow Speed (ft/sec)	Angle of Attack (deg)	X1 Gauge (lbs)	X2 Gauge (lbs)	Y1 Gauge (lbs)	Y2 Gauge (lbs)	X1 Pre Tension (lbs)	X2 Pre Tension (lbs)	NDP (ft <sup>2</sup> )	NLP (ft <sup>2</sup> )		
449	5.04	30	276.80	-174.40	22.91	-29.30	194.80	-199.10	1.4032	1.8000		
450	5.04	50	307.06	-204.31	-17.20	-52.13	193.90	-198.20	2.0516	-0.1451		
451	5.04	70	299.13	-226.62	-49.22	-63.35	191.00	-195.30	2.3089	0.0550		
452	5.04	90	255.03	-246.35	-62.75	-64.51	187.10	-191.50	2.2365	0.0833		

Table A.2: Experimental Data (continued)

27: One Array, High Tension, 11 Cylinders per Line												
Test Number	Tow Speed (ft/sec)	Angle of Attack (deg)	X1 Gauge (lbs)	X2 Gauge (lbs)	Y1 Gauge (lbs)	Y2 Gauge (lbs)	X1 Pre Tension (lbs)	X2 Pre Tension (lbs)	NDP (ft <sup>2</sup> )	NLP (ft <sup>2</sup> )		
453	5.04	30	247.06	-180.27	35.81	-19.39	185.80	-190.20	0.5469	1.8406		
454	5.04	50	257.76	-188.93	6.30	-27.80	185.10	-189.50	0.8658	-0.0468		
455	5.04	70	256.11	-206.40	-20.82	-35.92	185.50	-189.80	1.0847	0.0077		
456	5.04	90	219.47	-228.83	-39.21	-39.72	192.60	-196.80	1.2548	-0.2872		

28: Two Arrays, High Tension, 11 Cylinders per Line, 12 Inches Consecutive Spacing												
Test Number	Tow Speed (ft/sec)	Angle of Attack (deg)	X1 Gauge (lbs)	X2 Gauge (lbs)	Y1 Gauge (lbs)	Y2 Gauge (lbs)	X1 Pre Tension (lbs)	X2 Pre Tension (lbs)	NDP (ft <sup>2</sup> )	NLP (ft <sup>2</sup> )		
457	5.04	30	266.93	-180.87	28.4	-28.08	192.00	-196.30	1.0476	1.7521		
458	5.04	50	287.08	-198.99	-5.42	-42.4	191.40	-195.70	1.5255	-0.0923		
459	5.04	70	278.58	-217.17	-35.01	-50.48	189.40	-193.80	1.7155	0.0332		
460	5.04	90	231.12	-239.32	-53.42	-55.31	186.70	-190.90	1.8601	-0.2637		

Table A.2: Experimental Data (continued)

29: Three Arrays, High Tension, 11 Cylinders per Line, 12 Inches Consecutive Spacing												
Test Number	Tow Speed (ft/sec)	Angle of Attack (deg)	X1 Gauge (lbs)	X2 Gauge (lbs)	Y1 Gauge (lbs)	Y2 Gauge (lbs)	X1 Pre Tension (lbs)	X2 Pre Tension (lbs)	NDP (ft <sup>2</sup> )	NLP (ft <sup>2</sup> )		
461	5.04	30	278.67	-172.52	23.92	-32.13	185.90	-190.20	1.4877	1.8061		
462	5.04	50	300.92	-199.49	-15.39	-50.43	185.00	-189.40	1.9811	-0.1182		
463	5.04	70	294.46	-224.40	-46.81	-61.02	185.90	-190.30	2.2021	0.0431		
464	5.04	90	248.29	-254.00	-65.54	-66.92	190.80	-195.20	2.3421	-0.2090		

30: Four Arrays, High Tension, 11 Cylinders per Line, 12 Inches Consecutive Spacing												
Test Number	Tow Speed (ft/sec)	Angle of Attack (deg)	X1 Gauge (lbs)	X2 Gauge (lbs)	Y1 Gauge (lbs)	Y2 Gauge (lbs)	X1 Pre Tension (lbs)	X2 Pre Tension (lbs)	NDP (ft <sup>2</sup> )	NLP (ft <sup>2</sup> )		
465	5.04	30	298.69	-175.27	17.53	-37.51	196.30	-200.90	1.9163	1.7750		
466	5.04	50	327.73	-211.64	-29.64	-64.07	196.70	-201.10	2.6065	-0.2543		
467	5.04	70	315.11	-236.25	-61.12	-73.48	192.70	-197.20	2.7749	0.0270		
468	5.04	90	262.80	-263.07	-77.10	-77.24	190.00	-194.40	2.7866	-0.0985		



## Appendix B: Polynomial Fit

As explained in Appendix A, the term Test Set designates all the test runs conducted on a particular towed net configuration. All the data within each Test Set with the same tow speed and force type (NDP or NLP) were plotted together. A polynomial fit curve was computed and drawn with the computer program Mathematica through the data points for each individual plot using the method of least mean squares. Table B.1 contains the polynomial term coefficients for each of these curves. The first three columns identify the specific Test Subset, and the remaining columns list the coefficient terms for the polynomial terms. These terms are identified as  $c1$ ,  $c2$ ,  $c3$ ,  $c4$ ,  $c5$ ,  $c6$ ,  $c7$ , and  $c8$ . This information can be converted into an equation by substituting the coefficients into the following equation:

$$\begin{aligned} NDP [or NLP] = & c1 + c2 \alpha + c3 \alpha^2 + c4 \alpha^3 \\ & + c5 \alpha^4 + c6 \alpha^5 + c7 \alpha^6 + c8 \alpha^7 \end{aligned} \quad (7)$$

Note that  $\alpha$  denotes angle-of-attack. This equation supplies the amount of lift or drag (in normalized form) for a specific net configuration at a specific angle-of-attack. As an example, NDP for Test Set 10 at low speed. The appropriate equation would look like this:

$$NDP = -1.0661 + 0.0273 \alpha + 7.4618 \times 10^{-4} \alpha^2 - 8.8028 \times 10^{-6} \alpha^3 \quad (8)$$

By matching the Reynolds number of the model and the prototype, the equivalent speed of the prototype could be determined. Then, by matching the drag and lift coefficients, the lift and drag forces for the prototype net moving through the air can be determined.

Table B.1: Polynomial Term Coefficients for Normalized Lift and Drag Equations

Test Set	Type	Speed	c1	c2	c3	c4	c5	c6	c7	c8
01	NDP	Low	0.1365	-0.0011	2.3970E-04	4.1284E-07	-1.7119E-08	0	0	0
01	NLP	Low	0.6837	0.1464	-6.2136E-03	7.8261E-05	-3.1684E-07	0	0	0
01	NDP	High	0.0198	0.0039	5.9099E-04	1.2728E-05	1.1682E-07	-4.2123E-10	0	0
01	NLP	High	0.5183	0.0621	-3.3281E-03	5.0055E-05	-2.4179E-07	0	0	0
02	NDP	Low	0.5121	-0.0095	6.7611E-04	-4.8556E-06	0	0	0	0
02	NLP	Low	8.6464	-0.3734	5.4528E-03	-2.7061E-05	0	0	0	0
02	NDP	High	0.7920	-0.0222	1.0203E-03	-1.0359E-05	3.1553E-08	0	0	0
02	NLP	High	-3.0833	0.2695	-8.0801E-03	1.0261E-04	-4.6977E-07	0	0	0
03	NDP	Low	0.6041	-0.0062	1.0129E-03	-8.3694E-06	0	0	0	0
03	NLP	Low	20.7758	-1.0260	1.4562E-02	-6.4414E-05	0	0	0	0
03	NDP	High	-0.4023	0.0598	-3.9321E-04	3.6111E-07	0	0	0	0
03	NLP	High	8.5393	-0.4706	7.0897E-03	-3.2933E-05	0	0	0	0
04	NDP	Low	2.4536	-0.0674	1.9138E-03	-1.2822E-05	0	0	0	0
04	NLP	Low	-10.3997	0.9524	-3.1415E-02	3.9918E-04	-1.7141E-06	0	0	0
04	NDP	High	0.5507	0.0292	8.2738E-05	-1.9639E-06	0	0	0	0
04	NLP	High	-0.1431	-0.0721	1.3586E-03	-9.8255E-06	3.7386E-08	0	0	0
05	NDP	Low	2.1095	-0.0455	1.7203E-03	-1.2511E-05	0	0	0	0
05	NLP	High	9.9349	-0.4334	6.2367E-03	-2.9194E-05	0	0	0	0
06	NDP	Low	-0.6361	0.1164	-7.8474E-04	0	0	0	0	0
06	NLP	Low	19.4722	-0.9064	1.1890E-02	-4.7919E-05	0	0	0	0
07	NDP	Low	0.5102	0.0885	-5.4743E-04	0	0	0	0	0
07	NLP	Low	0.7243	0.1230	-3.9958E-03	2.6997E-05	0	0	0	0
08	NDP	Low	-0.4456	0.1368	-8.9293E-04	0	0	0	0	0
08	NLP	Low	-2.3849	0.7663	-3.3091E-02	4.5651E-04	-2.0112E-06	0	0	0
09	NDP	Low	0.1208	-0.0122	4.8981E-04	-3.1743E-06	0	0	0	0
09	NLP	Low	0.0004	0.0038	2.2512E-02	-1.4946E-03	3.9374E-05	-5.1733E-07	3.3986E-09	-8.9516E-12
09	NDP	High	-0.0543	0.0116	-3.6914E-05	-1.8648E-08	0	0	0	0
09	NLP	High	0.5676	0.0951	-6.7194E-03	1.5394E-04	-1.4890E-06	5.1749E-09	0	0

Table B.1: Polynomial Term Coefficients for Normalized Lift and Drag Equations (continued)

Test Set	Type	Speed	c1	c2	c3	c4	c5	c6	c7	c8
10	NDP	Low	-1.0661	0.0273	7.4618E-04	-8.8028E-06	0	0	0	0
10	NLP	Low	9.7129	-0.4629	5.6161E-03	-1.9300E-05	0	0	0	0
10	NDP	High	-0.4450	0.0626	-7.8510E-04	3.1056E-06	0	0	0	0
10	NLP	High	-0.8657	-0.0293	3.9287E-04	8.6111E-08	0	0	0	0
11	NDP	Low	2.4566	-0.0937	1.7158E-03	-9.4917E-06	0	0	0	0
11	NLP	Low	-5.4877	0.4474	-9.9723E-03	6.6269E-05	0	0	0	0
11	NDP	High	-0.0894	0.0293	-2.6605E-04	8.8889E-07	0	0	0	0
11	NLP	High	5.8816	-0.4982	1.5589E-02	-2.0695E-04	9.8617E-07	0	0	0
12	NDP	Low	-0.0148	0.0128	5.8444E-04	-6.0222E-06	0	0	0	0
12	NLP	Low	17.4832	-0.8172	1.0756E-02	-4.2650E-05	0	0	0	0
12	NDP	High	-0.9528	0.0849	-1.0189E-03	4.1417E-06	0	0	0	0
12	NLP	High	9.6317	-0.5209	7.8401E-03	-3.5544E-05	0	0	0	0
13	NDP	Low	1.7677	-0.0633	1.8404E-03	-1.2475E-05	0	0	0	0
13	NLP	Low	8.8769	-0.3519	4.5491E-03	-1.9208E-05	0	0	0	0
13	NDP	High	0.7622	-0.0074	6.4591E-04	-4.8194E-06	0	0	0	0
13	NLP	High	-1.1523	0.1362	-4.2543E-03	5.2410E-05	-2.2076E-07	0	0	0
14	NDP	Low	0.1579	-0.0049	2.0256E-04	-1.1756E-06	0	0	0	0
14	NLP	Low	0.4877	-0.0234	3.8243E-04	-2.2608E-06	0	0	0	0
14	NDP	High	-0.0543	0.0081	7.0150E-05	-1.5649E-06	5.2034E-09	1.2564E-11	0	0
14	NLP	High	0.6195	-0.0610	1.3287E-03	-8.1384E-06	0	0	0	0
15	NDP	Low	5.1524	-0.2659	4.3802E-03	-2.1900E-05	0	0	0	0
15	NLP	Low	10.1523	-0.3911	4.4697E-03	-1.5828E-05	0	0	0	0
15	NDP	High	0.9800	-0.0506	1.0525E-03	-5.8056E-06	0	0	0	0
15	NLP	High	0.1863	0.0007	-2.4895E-04	3.4543E-06	-1.4659E-08	0	0	0
16	NDP	Low	0.9697	-0.0590	1.4766E-03	-9.4861E-06	0	0	0	0
16	NLP	Low	39.5857	-2.4545	5.2513E-02	-4.6823E-04	1.4812E-06	0	0	0
16	NDP	High	-0.5029	0.0440	-5.2341E-04	2.1194E-06	0	0	0	0

Table B.1: Polynomial Term Coefficients for Normalized Lift and Drag Equations (continued)

Test Set	Type	Speed	c1	c2	c3	c4	c5	c6	c7	c8
16	NLP	High	31.9234	-2.2537	5.4972E-02	-5.6243E-04	2.0697E-06	0	0	0
17	NDP	Low	2.0308	-0.1112	2.4628E-03	-1.5072E-05	0	0	0	0
17	NLP	Low	7.9984	-0.3066	3.8026E-03	-1.5256E-05	0	0	0	0
17	NDP	High	0.1912	0.0084	1.5870E-04	-1.6417E-06	0	0	0	0
17	NLP	High	0.3672	-0.0071	6.9787E-05	0	0	0	0	0
18	NDP	Low	-0.6190	0.0503	-3.1536E-04	0	0	0	0	0
18	NLP	Low	8.0017	-0.3116	3.9589E-03	-1.6331E-05	0	0	0	0
18	NDP	High	-0.2602	0.0415	-3.8575E-04	1.2556E-06	0	0	0	0
18	NLP	High	0.4609	-0.0086	9.6226E-05	-1.8333E-07	0	0	0	0
19	NDP	Low	-0.4852	0.0597	-4.1763E-04	0	0	0	0	0
19	NLP	Low	14.4979	-0.6864	1.0518E-02	-5.1971E-05	0	0	0	0
20	NDP	Low	-0.7384	0.0700	2.6542E-06	0	0	0	0	0
20	NLP	Low	14.9624	-0.7152	1.1011E-02	-5.4650E-05	0	0	0	0
21	NDP	Low	-0.0641	0.0265	-1.8181E-04	2.2917E-08	0	0	0	0
21	NLP	Low	14.5301	-0.6871	1.0534E-02	-5.2250E-05	0	0	0	0
22	NDP	Low	-0.3958	0.0308	-3.2563E-04	1.1542E-06	0	0	0	0
22	NLP	Low	15.2381	-0.7382	1.1535E-01	-5.8077E-05	0	0	0	0
23	NDP	Low	-0.2030	0.0287	-3.2000E-04	1.4208E-06	0	0	0	0
23	NLP	Low	14.8866	-0.7153	1.1122E-02	-5.6031E-05	0	0	0	0
24	NDP	Low	-0.3761	0.0576	-6.7269E-04	2.6604E-06	0	0	0	0
24	NLP	Low	13.4554	-0.6239	9.3238E-03	-4.5077E-05	0	0	0	0
25	NDP	Low	-0.2993	0.0617	-5.2388E-04	1.0208E-06	0	0	0	0
25	NLP	Low	13.2856	-0.6215	9.3574E-03	-4.5442E-05	0	0	0	0
26	NDP	Low	-0.4370	0.0806	-6.8075E-04	1.2792E-06	0	0	0	0
26	NLP	Low	13.8083	-0.6545	9.9221E-03	-4.8271E-05	0	0	0	0
27	NDP	Low	-0.2310	0.0335	-2.8500E-04	1.0667E-06	0	0	0	0
27	NLP	Low	13.3250	-0.6275	9.5877E-03	-4.7735E-05	0	0	0	0

Table B.1: Polynomial Term Coefficients for Normalized Lift and Drag Equations (continued)

Test Set	Type	Speed	c1	c2	c3	c4	c5	c6	c7	c8
28	NDP	Low	-0.7395	0.0886	-1.1177E-03	5.0521E-06	0	0	0	0
28	NLP	Low	13.4454	-0.6431	9.9383E-03	-4.9840E-05	0	0	0	0
29	NDP	Low	-0.1818	0.0802	-9.3863E-04	3.9875E-06	0	0	0	0
29	NLP	Low	14.0696	-0.6744	1.0416E-02	-5.2063E-05	0	0	0	0
30	NDP	Low	-0.8960	0.1407	-1.7932E-03	7.6063E-06	0	0	0	0
30	NLP	Low	15.1120	-0.7352	1.1391E-02	-5.6665E-05	0	0	0	0

### **Appendix C: Alternative Method for Neutralizing Surf Mines**

As stated in the body of the report, it is the opinion of the author that the inherent instability of a net traveling through a fluid precludes its use in military application. Therefore, an alternative method of deploying the cylindrical charges for the purpose of destroying surf zone mines was explored with Midshipman First Class Jason E. Rimmer as part of the capstone senior design project in the mechanical engineering curriculum.

Instead of using a flexible cord to connect the array in a net shape to hold the cylinders together, this alternative concept utilizes rigid rod-like arms arranged like the petals of a flower (see Figures 46a and 46b). Each arm consists of two smaller segments which allow the arm to fold up (see Figure 47), decreasing the amount of space it takes up as it is stored and transported to the delivery point. At each bending joint between the arm segments and between the arm and the central nosepiece is a spring-loaded hinge. The tension in the springs would straighten the arm out and deploy the weapon in the configuration seen in Figures 46a and 46b. To carry the weapon, these arms would be placed in the configuration in Figure 47 and held together by either a hollow cylindrical shell which would fit around the arms or a small tail section which would also fit around the arms.

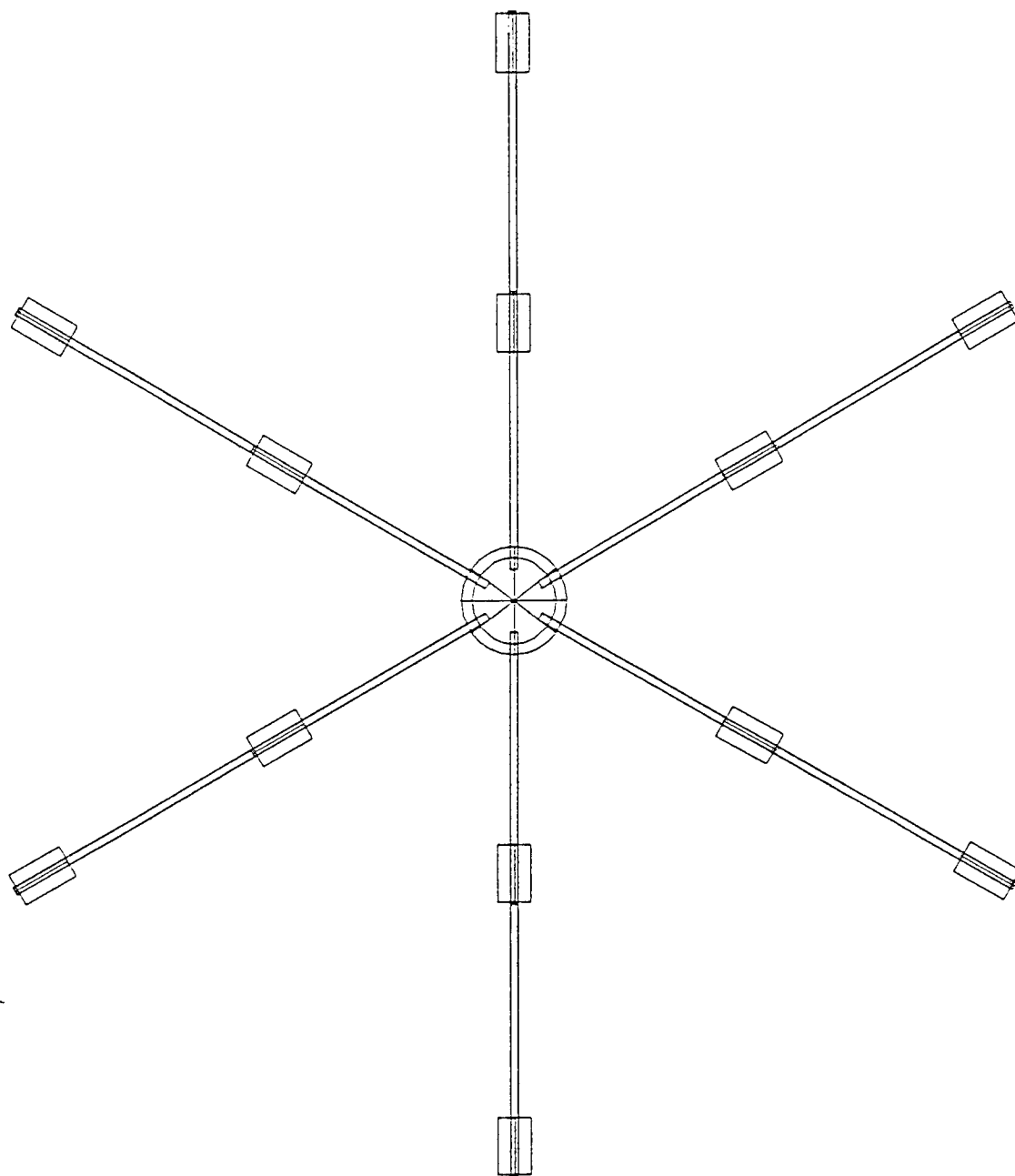


Figure 46a: Deployed Weapon, Top View



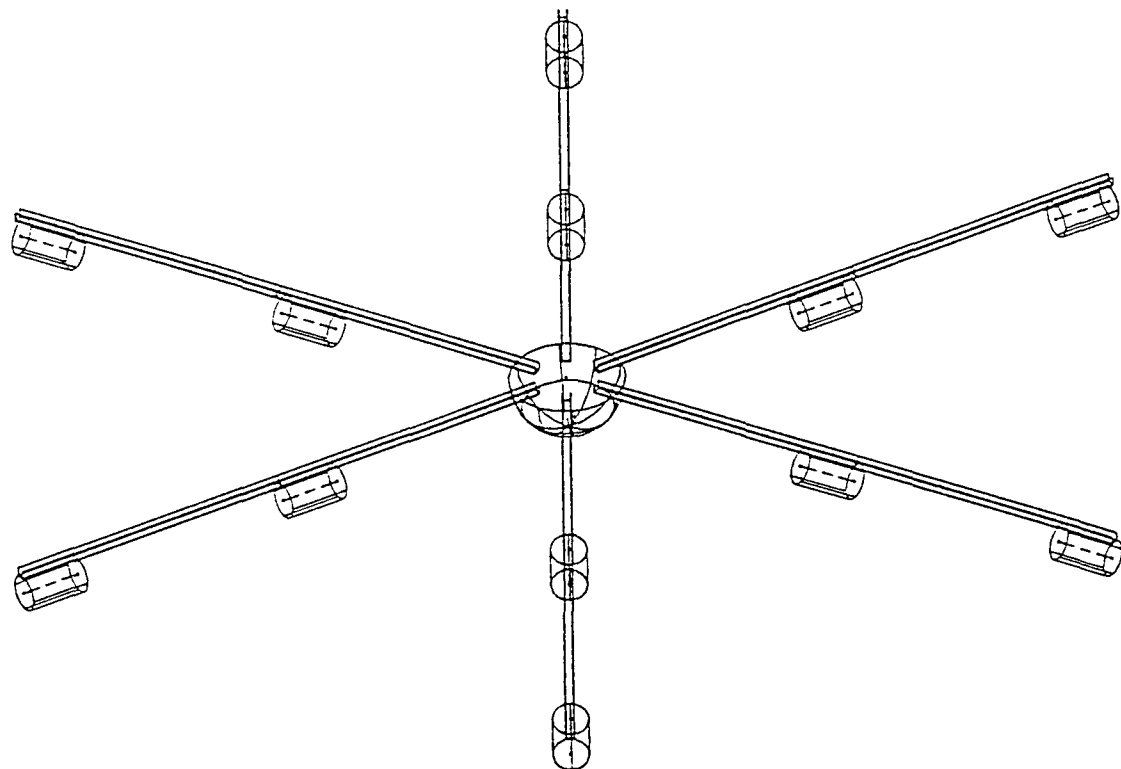
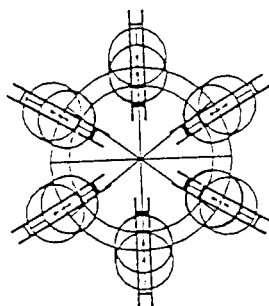
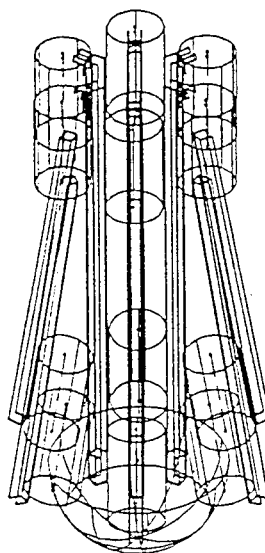


Figure 46b: Deployed Weapon, Perspective View



**Figure 47:** Undeployed Weapon, Perspective View and Top View

This weapon would probably be dropped from a low-altitude, low-speed helicopter in mass quantities to ensure clearance of a desired area. When released, a drogue chute would deploy from the weapon, pulling off the outer shell and allowing the arms to spread out. After impacting the water, it would sink and explode at a predetermined depth, setting off nearby underwater land mines. The central nosecone as well as the cylinders distributed along the arms would contain explosives for this purpose.

A model of the weapon illustrated in Figures 46a, 46b, and 47 was built with the following materials:

- ▶ Nosecone: 16 lb/ft<sup>3</sup> foam cut into a 9.5-inch hemisphere;
- ▶ Cylinders: 16 lb/ft<sup>3</sup> foam cut into cylinders of length 5 inches and diameter 3 inches;
- ▶ Arms: 1/16-inch aluminum sheet bent into channels with three equal sides of length 3/4-inch;
- ▶ Drogue Chutes: Two 24-inch diameter nylon chutes purchased from the Estes Rocket Company;
- ▶ Tail Section: Six-pronged "fork" made of 1/8-inch aluminum sheet which held the arms in the undeployed position.

This model was constructed in the Technical Support Division Shop in the basement of Rickover Hall.

After assembly, the model was dropped off the ten-meter platform at the swimming pool in Lejeune Hall at the United States Naval Academy. It was found that even in this short fall distance, the arms still deployed into their "straight" positions. Additionally, when thrown upside down (nosecone up), the model began to flip itself around before impacting the surface of the water. This suggested an inherent stability to this method of delivering and distributing the explosive charges.